

KATHOLIEKE UNIVERSITEIT
LEUVEN

Arenberg Doctoral School of Science, Engineering & Technology
Faculty of Engineering
Department of Electrical Engineering

Resource Allocation in Modulation and Equalization Procedures in DSL Modems

Prabin Kumar Pandey

Dissertation presented in partial
fulfillment of the requirements for
the degree of Doctor
in Engineering

Month Year

Resource Allocation in Modulation and Equalization Procedures in DSL Modems

Prabin Kumar Pandey

Jury:
Prof. em. dr. ir. Y. Willems, president
Prof. dr. ir. M. Moonen, promotor
Prof. dr. L. Deneire (U. Nice)
Prof. dr. ir. G. Gielen
Prof. dr. ir. I. Verbauwhede
Prof. dr. ir. G. Leus (T.U. Delft)
Prof. dr. ir. J. Louveaux (U.C.L)

Dissertation presented in partial fulfillment of the requirements for the degree of Doctor in Engineering

May 2011

© Katholieke Universiteit Leuven – Faculty of Engineering
Kasteelpark Arenberg 1/2200, B-3001 Leuven (Belgium)

Alle rechten voorbehouden. Niets uit deze uitgave mag worden vermenigvuldigd en/of openbaar gemaakt worden door middel van druk, fotocopie, microfilm, elektronisch of op welke andere wijze ook zonder voorafgaande schriftelijke toestemming van de uitgever.

All rights reserved. No part of the publication may be reproduced in any form by print, photoprint, microfilm or any other means without written permission from the publisher.

Legal depot number
ISBN number

Abstract

Digital subscriber line (DSL) technology is a very popular broadband access technology. It uses the existing telephone infrastructure to provide broadband access. In order to cope with the increased bandwidth demand to support broadband services, such as, Video on Demand (VoD), real time multimedia streaming, it is important to further improve the DSL.

The main performance degradation of the DSL system is caused by channel impairments, such as, crosstalk and inter-symbol interference (ISI). Furthermore, discrete fourier transform (DFT) based discrete multitone (DMT) system has very poor spectral properties, which prohibits the use of tones at the band edges in order to meet the power spectral density (PSD) constraints of the system, thus reducing the achievable bit rate.

In order to mitigate the channel impairments as well as combat the poor spectral properties of the DFT based DMT, sophisticated signal processing techniques are employed both in single user DSL and multi-user DSL scenarios. These signal processing techniques increase the overall run-time complexity of the DSL system, which makes them hard to realize in practice. However, DSL channel is a very slowly time-varying channel, which allows for offline optimization of the signal processing techniques such that the run-time complexity is reduced. This necessitates efficient algorithms to reduce the overall run-time complexity without affecting the system performance significantly.

In this dissertation, various low complexity resource allocation algorithms are investigated in order to reduce the run-time complexity of the signal processing techniques without sacrificing the performance of the system.

In the first part, resource allocation algorithms for the single user DSL scenario are investigated. In particular, the per-tone pulse shaping filter based DMT transmitter and per-tone equalization (MMSE-PTEQ) based DMT receiver will be considered. Owing to various properties of the DSL channel, the use of a constant number of non-zero filter taps in both the pulse shaping filter and the MMSE-PTEQ is seen to unnecessarily increase the run-time complexity. It can

be seen that the filter tap selection problem is a combinatorial problem. In this dissertation, we propose two approaches to simplify this combinatorial complexity: The first approach is based on a contiguous tap selection and the second approach is based on sparse approximation based filter design. It is shown that with both of these methods the number of required non-zero filter taps is reduced significantly. Furthermore, it is shown that the filter tap allocation performs even better when employed in combination with transmit power allocation.

In the second part, resource allocation algorithms for the multi-user DSL scenario are investigated, where crosstalk cancellation is crucial component. In the presence of only additive white Gaussian noise (AWGN), it has been shown that instead of performing a full crosstalk cancellation only few major crosstalkers may be cancelled without significant performance loss. Therefore, an optimum canceler allocation algorithm, known as partial crosstalk cancellation, only cancels the major crosstalkers per line per tone, resulting in a significant reduction in run-time complexity. In this dissertation, we extend this partial crosstalk cancellation concept to the scenario where spatially correlated background noise is present. It is shown that in this scenario, MMSE based cancelers outperform linear ZF cancelers. However, the optimal canceler allocation problem then has a prohibitively high complexity. In this dissertation, we propose two approaches to reduce the complexity: The first approach is based on selection metric, which combines the information of in-domain crosstalk with information of spatially correlated background noise. Based on this selection metric the crosstalkers are ordered and selected to be cancelled. This approach is then extended to include non-linear MMSE cancelers. The second approach, based on sparse approximation, directly chooses the cancelers to be taken into account by first designing a sparse linear MMSE canceler. Both of these approaches reduce the run-time complexity while performing near optimally under the cancellation tap constraint. Furthermore, it is shown that the spectrum balancing, i.e., transmit power optimization, combined with partial crosstalk cancellation further reduces the number of canceler taps required without sacrificing performance.

Glossary

Mathematical notations

x	scalar term
$\mathbf{x}$	vector term
$\mathbf{X}$	matrix term
$\mathbf{x} \star \mathbf{y}$	linear convolution between $\mathbf{x}$ and $\mathbf{y}$
$\mathbf{x}^*$	complex conjugate of the vector $\mathbf{x}$
$\mathbf{X}^T$	transpose of matrix $\mathbf{X}$
$\mathbf{X}^H$	Hermitian transpose of matrix $\mathbf{X}$
$\mathbf{X}^{-1}$	inverse of matrix $\mathbf{X}$
$\|.\|$	absolute value
$\|\|.\|\|$	Euclidean norm
$\|.\|_2$	ℓ_2 norm
$\|.\|_1$	ℓ_1 norm
$\|.\|_0$	ℓ_0 pseudo norm
$[x]^+$	max(0,x)
$x \approx y$	x is approximately equal to y
$\mathbf{x} \geq \mathbf{y}$	componentwise inequality between vectors $\mathbf{x}$ and $\mathbf{y}$
$\mathcal{E}(.)$	expectation operation
$\mathcal{O}(.)$	order
diag($\mathbf{x}$)	diagonal matrix with vector $\mathbf{x}$ as diagonal
diag($\mathbf{X}$)	vector representing diagonal values of $\mathbf{X}$ as its elements

Fixed symbols

$\mathbf{I}_N$	identity matrix of size N
$\mathcal{I}_N$	$N \times N$ inverse discrete Fourier transform
$\mathcal{F}_N$	$N \times N$ discrete Fourier transform
b_k^n	bit loading of user n on tone k

s_k^n	power loading of user n on tone k
$\mathbf{H}_k$	channel matrix for tone k
$h_k^{n,n}$	direct frequency domain channel response of line n on tone k
$h_k^{n,m}$	FEXT from line m on line n
S_{budget}	total available power budget
C_{budget}	total available filter tap budget
Γ	SNR gap
x_k^n	transmitted symbol by transmitter n on tone k
y_k^n	received symbol by receiver n on tone k
$\mathbf{x}_k$	vector containing symbols of all the tranmitters on tone k
$\mathbf{y}_k$	vector containing symbols of all the receivers on tone k
z_k^n	noise signal received by receiver n on tone k
$\mathbf{z}_k$	vector containing all the received noise signal s of all receivers on tone k

Accronyms and Abbreviations

ADC	Analog-to- Digital Converter
ADSL	Asynchronous Digital Subscriber Line
AFE	Analog Front-End
ANSI	American National Standards Institute
AWGN	Additive White Gaussian Noise
BC	Broadcast Channel
BER	Bit Error Rate
BPL	Broadband Power Line
CO	Central Office
CP	Customer Premise
CPE	Customer Premise Equipment
CSA	Carrier Serving Area
DBS	Digital Broadcast Satellite
DFE	Decision Feedback Equalizer
DFT	Discrete Fourier Transform
DMT	Discrete Multi-tone
DS	Downstream
DSL	Digital Subscriber Line
DSM	Dynamic Spectrum Management
e.g.	*exempli gratia*: for example
ETSI	European Telecommunications Standards Institute
FDD	Frequency Division Duplexing
FEQ	Frequency Domain Equalizer
FEXT	Far End Croasstalk
FFT	Fast Fourier Transform

FIR	Finite Impulse Response
FTTB	Fiber to the Box
FTTC	Fiber to the Curb
FTTH	Fiber to the Home
FTTN	Fiber to the Node
GDFE	Generalized Decision Feedback Equalizer
HDTV	High Definition Television
i.e.	*id est*: that is
IC	Interference Channel
ICI	Inter carrier Interference
IDFT	Inverse Discrete Fourier Transform
IFFT	Inverse Fast Fourier Transform
ISDN	Integrated Services Digital Network
ISI	Inter Sysmbol Interference
ISP	Internet Service Provider
kbps	kilo bits per second
kHz	Kilo Hertz
LAN	Local Area Network
LOS	Line of Sight
MAC	Multiple Access Channel
Mbps	Mega bits per second
MC	Multicarrier
MHz	Megahertz
MIMO	Multi Input Multi Output
MMSE	Minimum mean squared error
MMSE-GDFE	Minimum mean squared error generalized decision feeback equalizer
NEXT	Near End crosstalk
NLOS	Non Line of Sight
OFDM	orthogonal frequency division multiplex
OLT	Optical Line termination
OSB	Optimum spectrum balancing
PCC	Partial crosstalk cancellation
PLC	Power line Communication
PSD	Power spectral density
PTEQ	Per-tone equalizer
PTPF	per-tone pulse shaping filter
QAM	Quadrature Amplitude Modulation
QoS	Quality of Service
RFI	Radio Frequency Interference
RT	Remote Terminal
SINR	Signal to interference and noise ratio
SNR	ÃÛ Signal to noise ratio

TEQ	Time domain equalizer
UMTS	Universal Mobile Telecommunications System
US	Upstream
VDSL	Very-high speed digital subscriber line
VoD	Video on Demand
VoIP	Voice over Internet Protocal
WiFi	Wireless Fidelity
WiMAX	Worldwide Interoperability for Microwave Access
WLL	Wireless Local Loop
ZF	Zero Forcing
ZF-GDFE	Zero Forcing Generalized decision feedback equalizer

Contents

Contents vii

List of Figures xiii

List of Tables xvii

1 Introduction 1

1.1 Broadband communication 1

1.1.1 Wireline broadband technology 2

1.1.2 Wireless broadband technology 4

1.2 Digital subscriber line (DSL) 6

1.3 DSL environment 8

1.3.1 Channel impairments 8

1.3.2 Multicarrier modulation 9

1.4 Problem statement 11

1.5 Thesis objective and approach 12

1.6 Thesis overview and contributions 13

2 Preliminaries 17

2.1 Modulation schemes 17

2.1.1 Single carrier modulation 17

2.1.2 Multicarrier modulation 17
2.2 Capacity of a transmission medium 19
2.3 Discrete multitone modulation (DMT) 20
2.4 DMT transmitter 24
2.5 DMT receiver 25
2.6 Bit loading in DSL 26
2.7 Power loading in DSL 26
2.8 Equalization in DSL 27
2.8.1 Time-domain equalization 27
2.8.2 Per-tone equalization 29
2.9 Multi-user DSL 29
2.9.1 Multi-user channel model 31
2.9.2 Dynamic spectrum management (DSM) 32
2.9.3 Crosstalk cancellation 34
2.10 Summary 36

I SINGLE-USER RESOURCE ALLOCATION 39

3 Resource allocation in DMT transmitter with per-tone pulse shaping filters 41

3.1 Introduction 41
3.2 System model 44
3.3 Problem formulation 46
3.3.1 Resource allocation for a fixed power loading 46
3.3.2 Joint pulse shaping filter tap and transmit power allocation 49
3.4 Resource allocation for a fixed power loading 51
3.4.1 Contiguous filter tap selection based resource allocation . . 51
3.4.2 Sparse approximation based resource allocation 52

3.4.3 Computing sparse pulse shaping filters 52
3.4.4 Sparse approximation based pulse shaping filter tap allocation approach 54
3.5 Joint pulse shaping filter tap and transmit power allocation 55
3.5.1 Contiguous tap selection based approach 55
3.5.2 Sparse approximation based approach 56
3.6 Simulation results 58
3.6.1 Resource allocation for a fixed power loading 58
3.6.2 Joint pulse shaping filter tap and transmit power allocation 59
3.7 Conclusion 62

4 Resource allocation in DMT receiver with per-tone equalization 65
4.1 Introduction 65
4.2 Preliminaries 67
4.2.1 Basic Data Model 67
4.2.2 Per-tone Equalization 68
4.2.3 Effect of MMSE-PTEQ length 69
4.3 Problem formulation 70
4.3.1 Resource allocation for a fixed power loading 71
4.3.2 Joint equalizer tap and transmit power allocation 72
4.4 Resource allocation for a fixed power loading 73
4.4.1 Contiguous tap selection resource allocation 73
4.4.2 Sparse approximation based approach 74
4.5 Joint equalizer tap and power allocation 77
4.5.1 Contiguous tap selection based approach 77
4.5.2 Sparse approximation based approach 78
4.5.3 Sparse approximation based resource allocation 78
4.6 Simulation results 80

4.6.1 Resource allocation for a fixed power loading 81
4.6.2 Joint per-tone equalizer tap and transmit power allocation 81
4.7 Conclusion 81

5 Joint resource allocation in DMT transceivers 85
5.1 Introduction 85
5.2 System model 86
5.3 Problem formulation 88
5.3.1 Resource allocation for a fixed power loading 89
5.3.2 Joint filter tap and transmit power allocation 91
5.4 Resource allocation for a fixed power loading 94
5.4.1 Contiguous tap selection based resource allocation 95
5.4.2 Sparse approximation based filte tap allocation under fixed power loading 96
5.5 Joint filter tap and transmit power allocation 98
5.5.1 Contiguous tap selection based joint filter tap and transmit power allocation 99
5.5.2 Sparse approximation based joint filter tap and transmit power allocation 100
5.6 Simulation results 102
5.6.1 Resource allocation for a fixed power loading 102
5.6.2 Joint per-tone equalizer tap and transmit power allocation 103
5.7 Conclusion 105

II MULTI-USER RESOURCE ALLOCATION 109

6 Resource allocation in crosstalk cancellation 111
6.1 Introduction 111
6.2 System model 113

6.3 MMSE-based crosstalk cancellation 115
6.3.1 Linear MMSE canceler 115
6.3.2 Nonlinear MMSE canceler 115
6.3.3 Performance comparison 116
6.4 MMSE-based resource allocation 118
6.4.1 Computation of linear MMSE partial crosstalk canceler coefficients 118
6.4.2 Computation of MMSE-GDFE partial crosstalk canceler coefficients 119
6.5 Problem formulation 120
6.5.1 Partial crosstalk cancellation with a fixed power loading . . 120
6.5.2 Joint partial crosstalk cancellation and spectrum balancing 123
6.6 Resource allocation in MMSE based crosstalk canceler 125
6.6.1 Partial cancellation with a fixed power loading 125
6.6.2 Joint partial crosstalk cancellation and spectrum balancing in MMSE-based DMT receiver 131
6.7 Partial crosstalk cancellation in MMSE-GDFE 135
6.7.1 Partial crosstalk cancellation in MMSE-GDFE under a fixed power loading 135
6.7.2 Joint partial crosstalk cancellation and spectrum balancing in MMSE-based DMT receiver 137
6.8 Simulation results 138
6.9 Conclusion 141

7 Conclusions and Future Works **145**

7.1 Conclusions 145
7.1.1 Conclusions 145
7.2 Future Work 149

Bibliography **151**

Publication List **167**

Curriculum vitae **169**

List of Figures

1.1 Broadband Access Network 2
1.2 Typical DSL access network 7
1.3 Various channel impairments in DSL 10

2.1 Multicarrier modulation 18
2.2 A Multicarrier transceiver 18
2.3 Frequency domain representation of DMT modulation 23
2.4 A DMT transmitter 24
2.5 A DMT receiver 25
2.6 Waterfilling solution 28
2.7 TEQ design 28
2.8 MMSE-GDFE 35
2.9 MMSE-VBLAST structure 35

3.1 Spectrum of two adjacent tones in a DFT based multicarrier system 42
3.2 PSD of a VDSL system without any transmit pulse shaping 44
3.3 PSD of a VDSL system (a) with time domain pulse shaping (b) with per-tone pulse shaping 44
3.4 DMT transmitter with per-tone pulse shaping 45

3.5 Convergence of total number of pulse shaping filter taps using (a) the contiguous tap selection based approach (b) the sparse approximation based approach 59

3.6 Optimum distribution of number of pulse shaping filter taps over tones using (a) the contiguous tap selection based approach (b) the sparse approximation based approach 60

3.7 Transmit PSD for (a) the contiguous tap selection based approach (b) the sparse approximation based approach 60

3.8 Transmit PSD (5000 filter taps) for(a) the contiguous tap selection based approach, (b) the sparse approximation based approach . . . 61

3.9 Pulse shaping filter tap distribution (5000 taps) for (a) the contiguous tap selection based approach, (b) the sparse approximation based approach 62

3.10 Relation of data rate and the total number of available resources . 63

4.1 T-tap per-tone equalizer model [2] 69

4.2 Comparison of signal to interference and noise ratio per tone for different MMSE-PTEQ equalizer lengths for a typical ADSL scenario 70

4.3 Comparison of bit rate versus total number of non-zero MMSE-PTEQ taps for contiguous tap selection based approach, sparse approximation based approach and fixed length MMSE-PTEQ approach 82

4.4 Optimum distribution of number of MMSE-PTEQ taps over tones using (a) the contiguous tap selection based approach (b) the sparse approximation based approach 83

4.5 Comparison of bit rate versus total number of non-zero MMSE-PTEQ taps for contiguous tap selection based approach, sparse approximation based approach and fixed length MMSE-PTEQ approach with and without transmit power loading 84

4.6 Optimum distribution of number of MMSE-PTEQ taps under transmit power loading over tones using (a) the contiguous tap selection based approach(b) the sparse approximation based approach 84

5.1 For a fixed transmit power loading, optimum distribution of (a) pulse shaping filter taps (b) MMSE-PTEQ taps, using contiguous tap selection approach 104

5.2 For a fixed transmit power loading optimum distribution of (a) pulse shaping filter taps (b) MMSE-PTEQ taps, using sparse approximation based approach 105

5.3 For a fixed transmit power loading, transmit PSD for (a) the contiguous tap selection based approach (b) the sparse approximation based approach 105

5.4 Transmit PSD in the case of joint filter tap and transmit power allocation for the tap budget of 5000 taps each in the DMT transmitter and the DMT receiver using (a) the contiguous tap selection based approach, (b) the sparse approximation based approach 106

6.1 A typical VDSL scenario with co-located receivers at the CO (central office) and non co-located transmitters at the CPE (customer-premises equipment) side 113

6.2 Channel characteristics for a 1200m line with 6 in-domain crosstalkers ranging from 600m to 1100m and an alien-crosstalker (dashed line). The solid black rectangular line represents the transmit band for upstream VDSL. 117

6.3 Comparison of the total bit rate achieved with the linear ZF canceler and MMSE-based cancelers when alien crosstalk is (a) not present (b) present. 117

6.4 Performance comparison of the different metrics for partial cancellation using a linear MMSE canceler 140

6.5 Performance comparison of the different metrics for partial cancellation using a linear MMSE canceler 141

6.6 Performance comparison of the different metrics for partial cancellation using a linear MMSE canceler 142

6.7 Comparison between the optimum linear MMSE partial cancellation and the MMSE-GDFE partial cancellation 143

6.8 Comparison between the optimum linear MMSE partial cancellation and the MMSE-GDFE partial cancellation 143

List of Tables

2.1 RLCG parameters 31

3.1 convergence 61

5.1 Number of outer iterations taken to converge to the solution a fixed transmit power loading 103

5.2 Number of outer iterations taken to converge to the solution for a joint filter tap and transmit power allocation 104

5.3 Achievable bit rate in Mbps for various combinations of MMSE-PTEQ filter tap and per-tone pulse shaping (PTPS) filter tap constraint using contiguous tap selection based approach and transmit power allocation 104

5.4 Achievable bit rate in Mbps for various combinations of MMSE-PTEQ filter tap and per-tone pulse shaping (PTPS) filter tap constraint using sparse approximation based approach and transmit power allocation 106

6.1 Simulation Parameters 139

Chapter 1

Introduction

1.1 Broadband communication

Modern human life is increasingly dependent on faster and reliable information access, subsequently to broadband access. The rise in the use of bandwidth intensive applications such as real-time or streaming media, voice-over-internet protocol (VoIP) etc., is fueling the demand for ever increasing data-rate and the quality of service. Furthermore, the broadband providers are trying to provide reliable " Triple Play" service to quell the need for voice, data and video services with a single connection. This has further heated the competition for faster and reliable broadband access technology. For example, to provide HDTV service needs 15-20 Mbps downstream bandwidth even after video compression [114]. This pushes the boundary of the current broadband technologies. In order to provide better broadband services, the broadband access network has been shown to be the bottleneck [116]. There are many broadband access technologies that promise much faster and reliable services if the access network is overhauled. But the cost of the deployment of the new access network has thus far proved to be prohibitive. Therefore, the broadband service providers want to increase the quality of service provided to subscriber but with none or minimum overhaul of the existing access network. Then in time the access network can be gradually replaced such that the cost is spread over time.

There are various competing broadband technologies, e.g. cable modem, DSL, 3G, WiMAX etc. Each technology has its advantages and disadvantages. We can broadly classify the existing broadband technologies into two categories , wireline broadband technology and wireless broadband technology.

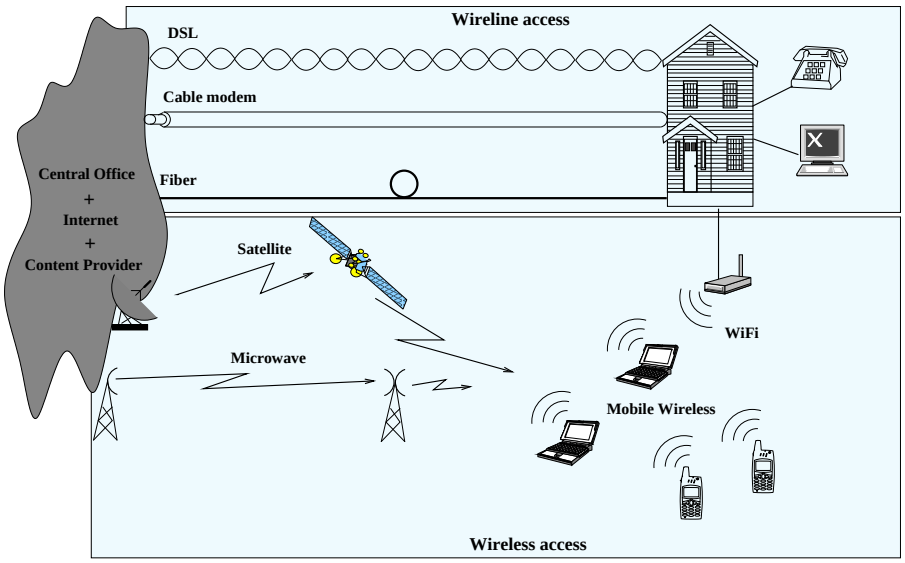

Figure 1.1: Broadband Access Network

1.1.1 Wireline broadband technology

Wireline broadband technology rely on a physical connection to the subscriber's premise. The existing cable TV connection, telephone connection and the power line connection can all be used for this type of broadband technology. The optical fiber connection is also an example of the wireline broadband technology. Optical fiber connection promise tremendous amount of bandwidth but the deployment of optical fiber network in large scale has proven to be very expensive. Below we introduce some of the wireline broadband technologies in more detail.

Hybrid fiber coax (HFC)

HFC uses the coaxial cable TV infrastructure to offer a broadband connection to the subscriber. Since, many subscribers of broadband services already have an existing cable TV connections, it has become popular. The recently proposed HFC standard DOCSIS 3.0 may be able to provide 100 Mbps per channel of 8 MHz [114, 78]. However in cable modem broadband access, the bandwidth is shared because the same cable line connects several subscribers. Therefore, the broadband experience depends on the number of subscribers sharing the same

cable connection. As a consequence, the typical connection speed is around 1 Mbps downstream and 128 kbps upstream [114].

Broadband power line (BPL)

BPL utilizes the existing power lines for high speed data transmission [73]. In a BPL system, data is transmitted as a low voltage high frequency signal coupled with the high voltage low frequency power signal [114]. The subscribers can plug in the modem into an ordinary wall outlet to receive broadband internet access. In practice, it has not seen a large scale deployment because it requires investment to upgrade the power transmission network to support high speed broadband services. Furthermore, the BPL environment is inherently quite noisy and the frequencies used by BPL often interferes with the amateur radio transmission. Nevertheless, BPL remains as a broadband option.

Digital subscriber line (DSL)

DSL technology uses the existing copper telephone network infrastructure to provide broadband connections [19, 44, 142, 63, 62]. This is achieved by splitting the voice and data signal into distinct frequency bands. For example, 0-4 KHz carries the voice signal in traditional telephony and higher frequency is used to carry the data stream. The frequency band carrying data can be further split into two frequency bands, namely, upstream (US) frequency band and downstream (DS) frequency band. DSL using equal band-width for upstream and downstream frequency bands is called symmetric DSL (SDSL). When the DSL uses unequal bandwidth for the upstream and downstream bands, it is known as asymmetric DSL (ADSL). However, DSL has a drawback that its performance is sensitive to the loop length i.e. the broadband connection speed highly depends on the distance between the subscriber and the central office (CO). ADSL can provide maximum DS speed upto 12 Mbps and US speed up to 640 Kbps. The distance limit for ADSL is 5.4 Km, for this distance ADSL can provide approximately 500 Kbps DS speed. In order to provide video on demand (VoD) service, the minimum DS speed required is 15-20 Mbps, which pushes the boundary of the current DSL system. Various types of DSL, e.g., VDSL, VDSL2 etc., has been proposed in order to provide faster and more reliable broadband access. These DSL types increase the speed by both decreasing the loop length and increasing the available bandwidth, e.g. VDSL2 offers the speed of 100-200 Mbps over the distance of 300m [115]. The variety in DSL techniques allows diversity in the service provided and can be deployed as per subscriber demand. The main features of DSL technology and its history and advances will be presented in detail in section 1.2.

Fiber to the curb/home (FTTx)

The term FTTx refers to a set of technologies that bring fiber a step closer to the subscriber [121, 114]. It uses the optical fiber to provide the broadband services. Optical fiber exhibits very low signal attenuation over long distances and does not suffer much from interference. Furthermore, it also provides much larger transmission bandwidth than any other broadband access medium. The fiber to the curb (FTTC), as the name suggests, does not connect individual subscriber to a optical fiber connection but the optical fiber connection is terminated near the subscriber premises. Then the technologies like VDSL, which utilizes the optical fiber connection to provide faster service is used to connect the individual subscribers. The goal is to gradually move toward a fiber to the Home (FTTH) broadband access network, where all subscribers have an individual high speed physical fiber connection. But installing such a fiber access network is difficult, time-consuming, and very cost sensitive. Therefore, existing fiber network is being gradually extended towards the end-users and then the last mile is covered by using other broadband access technologies such as DSL or BPL etc.

1.1.2 Wireless broadband technology

Wireless broadband refers to the use of wireless technologies to transmit broadband signals [114]. It uses very high bandwidth relative to the carrier frequency [100]. The higher frequencies have an advantage over the lower frequencies as more spectrum is available at higher frequencies and smaller antennas can be used. However, at high frequencies signal attenuation is higher, therefore the distance over which a subscriber can be catered is limited.

The wireless technologies can be subdivided into several categories according to the different aspects of transmission. The satellite communication system such as geostationary earth orbit satellite (GEOS), and microwave transmission links require direct line-of-sight (LOS) to be able to operate. Hence, these can be categorized into LOS wireless broadband communication technique. Whereas mobile communication techniques in general do not rely on direct LOS for communication and can be categorized into nonline-of-sight (NLOS) wireless broadband communication technique. Similarly, the wireless communication systems where the transmitter and receiver are fixed (e.g. microwave links) can be categorized as fixed wireless broadband communication technique and when the transmitter and receiver are in relative motion can be categorized as mobile wireless broadband communication technique. This includes WiFi and 3G wireless communication systems.

Satellite communication

Satellite communication entails the use of artificial satellites to provide communication links to connect different geographic locations [124, 114]. This has been primarily used to connect remote and inaccessible landscapes by using small portable terminals, e.g., Very Small Aperture Terminals (VSATs), broadcasting TV signals (Direct Broadcast Satellites (DBS)) etc. The geostationary satellite typically has a 250ms delay, which is unacceptable for the broadband services. However, the lower earth orbit satellites (LEOS) can reduce this delay significantly. But it needs a lot more satellite to offer same coverage.

Microwave links

Microwave links are an example of fixed wireless communication links. It uses two fixed microwave transceivers with direct LOS [126, 114]. These have been used to connect geographically inaccessible areas, where deployment of cables is not possible. These areas can be connected with the microwave link and then the local population can be connected either with a cable network or a wireless local loop (WLL). The major drawback of microwave link is that it relies on direct LOS, which is not always possible.

Wireless fidelity (WiFi) and Worldwide interoperability for microwave access (WiMAX)

WiFi is the wireless communication technique using wireless local area network (WLAN) based on IEEE 802.11x standards [69]. The WiFi enabled devices can connect to the internet when they are within range of a wireless network, known as access point (AP), connected to the internet. WiFi also allows communication directly from one WiFi enabled device to another WiFi enabled device without the involvement of an AP. The main disadvantages of WiFi are that the spectrum assignment are not consistent worldwide and the reach of a WiFi network is limited to 30m to 100m in general.

WiMAX is an IP based wireless broadband access technology. It has similar performance to WiFi but provides the coverage and quality of service (QoS) similar to cellular networks. WiMAX is a wireless digital communications system, also known as IEEE 802.16. It can provide broadband wireless access up to 50 km for fixed stations, and 5 - 15 km for mobile stations. WiMAX operates on both licensed and non-licensed frequencies. WiMAX network operator typically provide a WiMAX subscriber unit, which connects to the WiMAX network and then WiFi can be used to provide the connection within the house or business. The main disadvantages of WiMAX are that LOS is needed for distant connections, bad

weather conditions can affect the performance, and also other wireless equipment can cause interference.

Mobile communication (3G and beyond)

Third generation (3G) and beyond mobile communication technique, such as UMTS, CDMA2000, LTE, features higher speeds for internet access and real-time video [50]. Application services include voice telephony, mobile Internet access, video calls and mobile TV, all in a mobile environment. Recent 3G systems, denoted as 3.5G and 3.75G, also provide mobile broadband access of several Mbit/s to laptop computers and smartphones. Evolved high-speed packet access (HSPA+) can provide peak data rates up to 56 Mbit/s in the downlink in theory (28 Mbit/s in existing services) and 22 Mbit/s in the uplink. The main disadvantage of the wireless mobile communication is that the channel is shared by many users, therefore the QoS depends on the number of active users at a certain time. Furthermore, the scarcity of bandwidth also is a big hindrance.

Currently, the DSL technology remains the most popular broadband access technology. The main reason for the popularity of the DSL is that it can utilize existing telephone networks to provide the broadband access. It is also more cost effective than the other broadband access techniques, such as cable modem, fiber or satellite. Recent survey has shown that digital communication over the twisted pair telephone lines DSL consumer are increasing yearly [161] and it is predicted to rise further in coming years. Considering these trends, DSL broadband access is expected to be an important player in the field of broadband access in the future. However, it is important that the DSL continue to improve in order to remain competitive with the other broadband access techniques.

In this thesis, we focus on resource allocation in DSL system in order to reduce its run-time complexity. In the following section, we will introduce DSL in more detail.

1.2 Digital subscriber line (DSL)

Data communication over the telephone line started with the invention of electric telegraph by Samuel Morse in 1844 [134] and telephone by Alexander Graham Bell [16]. After more than a century of sending data in the voiceband, i.e., 300 Hz to 3.4 kHz, [104] Joseph Lechleider of Bellcore demonstrated that it is possible to transmit the broadband signals over telephone lines in late 1980s.

The integrated services digital networks (ISDN) can be viewed as the first digital subscriber line (DSL) technology, which was able to provide an aggregate bit rate

of 160 kbps using a bandwidth of 80 kHz [117]. But the real broadband service over the telephone line started with the deployment of ADSL in 1995. ADSL is specially suited for applications such as internet access and VoD. The ADSL uses a bandwidth of 1.1 MHz, which is divided into multiple tones (sub-bands) using discrete multitone modulation scheme. The successor of ADSL is VDSL and VDSL2, which uses bandwidth upto 30 MHz to provide higher data rate in order to meet the increasing broadband demands. Figure 1.2 illustrates a typical DSL access network. It consists of a central office (CO), which is connected to the content provider with a optical fiber connection. From the CO twisted pair cables originate to connect to the subscribers. Also, a subscriber can be connected to the CO via remote terminal (RT). An optical network unit (ONU) can be connected to the optical line terminal (OLT) in CO via an optical fiber connection in order to reduce the distance between the CO and the subscriber. ONU can then use the twisted pair cable to deliver VDSL/VDSL2 connection over small distances. A pair of DSL modem is required, one at each side, to set up the DSL connection.

The telephone infrastructure was originally designed to only offer voice telephony, which uses the bandwidth between 0 and 4 kHz. But in order to deliver the broadband connection, higher bandwidth, up to 30 MHz, is used. This results in a DSL environment with many channel impairments. In the following section, we present the various aspects of the DSL environment, which affect its performance.

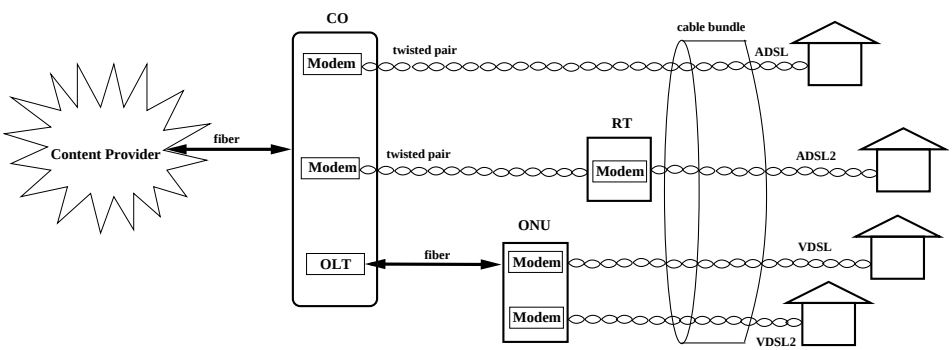

Figure 1.2: Typical DSL access network

1.3 DSL environment

1.3.1 Channel impairments

In this section, we will give an overview of some major transmission impairments in xDSL systems [43, 46, 64, 135] and its effect on the performance of the xDSL system [15, 38, 82, 132, 84].

Transmission channel

Transmission channel causes distortion for any communication system. It also causes the signal to attenuate as a function of the frequency of the transmitted signal and the loop length. This creates problem for subscribers that are far away from the central office and also the limits the use of the higher frequencies. Furthermore, due to the dispersive nature of the channel, which can be typically represented by the impulse response of the channel, the adjacent symbols overlap at the receiver. This is known as intersymbol interference (ISI). The channel dispersion and the attenuation is caused, firstly, by the bridged taps [165, 39, 145], which are unterminated distribution cables. Secondly, use of several wire gauges along a line also causes reflection due to the impedance mismatch at the junction of two line sections with different wire gauges. To mitigate the effect of the channel distortion and attenuation, a channel equalizer is employed [19, 44, 142].

Crosstalk

The twisted pairs in the wired access network are bundled within a large binder groups consisting of 20 to 100 individual pairs per binder. Therefore, the pairs within a binder experience electromagnetic coupling known as crosstalk from each other [56, 57]. There are two types of crosstalks, namely, Near-end crosstalk (NEXT) and Far-end crosstalk (FEXT). NEXT is caused by the a neighboring transmitter on a different pair whereas FEXT is caused by the the signal originating from the remote transmitter in the different pair. Both NEXT and FEXT power increases with the frequency e.g. NEXT $\sim f^{3/2}$ and FEXT $\sim f^2$ [62]. When the transmitters and receivers at both ends of the binder are co-located then the NEXT is much more severe than the FEXT. This is due to the fact that FEXT is attenuated by the channel transfer function. The effect of NEXT can be reduced by using frequency division duplexing (FDD) technique, where the upstream and downstream data occupies different frequency bands [136, 138, 99]. If the FEXT originates from the remote terminal (RT) in the field then the effect might be severe, since it may be near to the receiver. This is known as near far scenario. The effects of FEXT can be mitigated by using power

backoff [79, 169, 160, 131], spectrum coordination [140, 30] or signal coordination [60, 59, 26, 25, 153]. When the interference arises from either a line with different DSL format or from the uncoordinated DSL lines in a vectored DSL, it is known as alien crosstalk [142, 130, 61]. In some cases, it might be the dominating interference in the DSL system. Mitigating the effect of alien crosstalk is much more challenging than mitigating the effect of other interferences such as NEXT, FEXT etc. Some techniques to mitigate the effect of alien crosstalk has been suggested in [175, 159, 61, 153, 20, 164].

Radio frequency interference (RFI)

Every telephone line acts as an antenna that emit and receive radio energy. Radio frequency signals in the same frequency range as xDSL from wireless transmitters impinge on the unshielded telephone line, which results in radio frequency interference (RFI) [143]. Since, VDSL use higher frequency band, the RFI is specially important. There are two types of interference, first *egress* is caused by the xDSL into a radio receiver and second, *ingress* is the interference caused by the radio transmitter into xDSL. Techniques to suppress RFI ingress and egress are presented in [137, 103] and [14, 91, 47, 48] respectively.

Impulse noise

Sudden switching of electronic devices in the vicinity of telephone lines causes impulse noise. These are narrow pulse in time with very high level of noise compared to the received DSL signal level [83, 102, 44, 142]. It is difficult to characterize the impulse noise completely but there has been some effort to measure and model impulse noise [135, 167, 45, 70, 53, 122]. Different techniques to mitigate the impulse noise is presented in [74, 67, 94, 149].

Thermal noise

Due to the thermal agitation of the electron in the copper wire, DSL systems experience a constant background noise known as thermal noise. The thermal noise limit is -173 dBm/Hz at room temperature but due to the quantization noise of analog-to-digital converter (ADC) the limit is set to -140 dBm/Hz [19, 142].

1.3.2 Multicarrier modulation

In order to deal with the frequency selectivity of the transmission channel, the channel can be divided into many sub-channels (tones), each with flat frequency

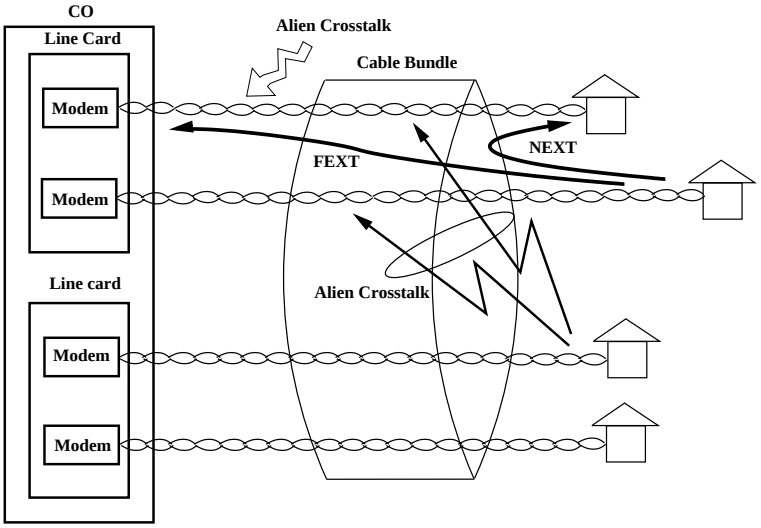

Figure 1.3: Various channel impairments in DSL

response, this is known as multicarrier (MC) modulation [18]. In 1960s, first analog multicarrier systems were implemented [31, 127] with disjoint frequency bands. In [127, 31, 71], it was shown that the spectral overlap may not result in ISI/ICI after reception. Use of discrete Fourier transform (DFT) for MC modulation was first proposed by Weinstein [166, 71, 72]. DFT based MC technique are the basis of popular techniques such as orthogonal frequency division multiplexing (OFDM) [3, 44]. OFDM is used in WLAN, Digital video broadcast (DVB), WiMAX etc. [69, 50, 176]. The performance of the MC system can be further improved by using adaptive bit loading, which allows different number of bits to be transmitted on different tones taking their channel state into account [19, 37, 44, 81, 87]. The bit loading in WLAN/OFDM was proposed in [155]. In order to mitigate the effect of channel distortion and ISI, OFDM system needs equalization at the receiver [19, 44, 119, 8, 2]. However, DFT based MC system has very poor spectral characteristics, requires very stringent synchronization and also exhibit high peak-to-average power ratio (PAPR). In order to overcome these drawbacks of the DFT based MC system, other MC modulation techniques, such as discrete wavelet multitone (DWMT) [4], filtered multitone (FMT) [34, 35, 146, 23], cosine modulated [54] and non-orthogonal pulse based systems [22, 85, 154], have been proposed. However, due to its simple implementation using fast fourier transform (FFT), DFT based MC modulation technique remains very popular.

1.4 Problem statement

Rise in the use of bandwidth intensive broadband applications has increased the demand for faster and more reliable broadband access. In the meantime, rise of various broadband access technologies has increased the competition for the broadband market. To meet the demand, DSL technology also has to improve constantly.

Gradual decrease in the loop length and increased use of optical fiber has enabled DSL to use higher frequencies to provide higher data rate. However, the DSL channel is highly dispersive and hence frequency selective in nature. To overcome the frequency selectivity of the DSL channel, DFT based MC modulation techniques has been proposed. But DFT based MC transmitter has very poor spectral property. The sidelobes are high and they decay very slowly. This causes problem while transmitting under a PSD constraint. Many tones at the band edges cannot be used because the PSD mask constraint will be violated. These tone are known as virtual carriers (VC). In order to improve the poor spectral property, a transmit windowing is used. In [33], it was shown that the per-tone pulse shaping improves the spectral containment of DFT based MC transmitter compared to the time domain transmit windowing. Hence reducing the number of virtual carriers and increasing the achievable data rate.

Due to the dispersive channel, the block transmission based system, such as DFT based MC system, suffers from ISI/ICI. In order to remove ISI, it was shown that a guard time known as cyclic prefix (CP) can be added. This transforms the linear convolution between the channel input and the channel into a cyclic convolution, thus converting the channel matrix into a circulant matrix. A circulant matrix can be diagonalized by applying a DFT and a IDFT matrix. This converts the frequency selective channel into multiple parallel independant AWGN channel. These can be easily equalized by using a 1-tap equalizer. But in order for all this to work, the length of the CP should be greater than the channel length. The dispersive channel such as DSL has very long channel impulse response, therefore equally long CP is required hence decreasing the effective throughput of the system. One way to reduce the CP length is to shorten the effective channel impulse response by using a channel shortening filter at the receiver. In [2], it was shown that a minimum mean squared error per-tone multi-tap equalizer (MMSE-PTEQ) performs much better than the time-domain channel shortening combined with 1-tap frequency domain equalizer (FEQ) without increasing the run-time complexity significantly.

In the multi-user scenario, multiple lines are bundled in the same binder, which causes crosstalk. Crosstalk has been shown to be a major cause of performance degradation in DSL systems. In the literature, various technique to mitigate the effect of crosstalk have been presented. In [60, 59, 26, 25, 30, 153], it has

been shown that the effect of crosstalk can be mitigated using various spectrum coordination and signal coordination techniques for different level of transmit and receive coordination. When the spatially correlated background noise (alien crosstalk) is also present, the crosstalk mitigation becomes much more challenging [61].

The channel impairments mitigation techniques as described above require sophisticated signal processing techniques. These extra signal processing increases the overall run-time computational complexity of the DSL system, which makes it hard to realize in practice.

However, DSL channel is a very slowly time-varying channel. This allows for offline optimization of the signal processing techniques such that the run-time complexity is reduced. This necessiates efficient algorithms to reduce the overall run-time computational complexity without affecting the system performance significantly. This in turn enables the implementation of sophisticated signal processing algorithms to mitigate the crosstalk effect in practice, hence increasing the achievable data rate for the DSL system.

1.5 Thesis objective and approach

The main objective of this dissertation is to provide efficient resource allocation algorithms for the DMT transceivers, which will enable them to operate at much reduced run-time computational complexity without sacrificing the performance.

To this end, at the per-tone pulse shaping based DMT transmitter the effect sparse per-tone filters is investigated. Since the contribution to the stopband energy from a tone depends on its position in the passband, not every pulse shaping filter needs to have same number of non-zero coefficients. This enables us to apply efficient resource allocation algorithms to reduce the overall non-zero coefficients of the pulse shaping filters and hence reduces the run-time computational complexity

Similarly at the per-tone equalization based DMT receiver, it can be shown that due to the frequency selective nature of the DSL channel, use of fixed length non-sparse equalizer wastes resource. This enables us to apply efficient resource allocation algorithms to reduce the number of non-zero MMSE-PTEQ coefficients, hence reducing the run-time computational complexity.

It can also be seen that the per-tone operation based transmitter and receiver affect each other. Hence, the resource allocation algorithms can take this into account to jointly optimize the resource in the DMT receiver and the DMT transmitter. Thus reducing the joint run-time computational complexity.

We then move to the multi-user DSL scenario, where there are multiple lines in

the same binder. In the presence of alien crosstalk, it will be shown that MMSE based receiver performs well. But in order to reduce the run-time computational complexity, we use a technique known as partial crosstalk cancellation. We will show that combining information from the noise correlation matrix and the in-domain crosstalk, efficient algorithm canbe devised, which minimizes the run-time computational complexity without sacrificing the overall bit-rate performance.

1.6 Thesis overview and contributions

In this section, we will provide an overview of the thesis and its contribution.

In **Chapter 2**, the basic concept of DSL transmission is presented in detail. Different modulation schemes for the DSL systems are compared. We will then present the basic structure of DMT transmitter and receiver and outline their main operations. The block transmission scheme of DMT will also be presented in detail and various drawbacks of block transmission over a dispersive channel, such as inter-symbol interference (ISI) and inter-carrier interference (ICI), will also be highlighted. We will then present some well known techniques to mitigate these drawbacks. Multi-user scenario arises in the DSL system when multiple lines in the same binder interfere with each other. In this chapter, a system model of multi-user DSL will be presented. We will then present the multi-user channel modeling methods in detail. We will also explore the effect of crosstalk in such scenario and then present various crosstalk mitigation technique presented in various literatures for different level of line coordination. And finally, some receiver structures to mitigate the crosstalk are presented.

The resource allocation techniques devised to reduce the run-time computational complexity of different signal processing blocks can be applied in both the single-user and the multi-user DSL scenario.

Part I of this dissertation investigates the resource allocation techniques for a single-user DSL scenario. The channel characteristics of the DSL system demands that different sub-channel be treated differently. Therefore, the resource allocation algorithms should try to take advantage of this characteristics to efficiently allocate the available resources such that the system performs optimally with much reduced run-time complexity.

In **Chapter 3**, we will first highlight that DMT transmitter has poor spectral property due to the DFT based windowing. But in applications e.g. in VDSL, the Power Spectral Density (PSD) of the transmitted signal is not allowed to exceed a given PSD mask defining one or more pass bands and stop bands. To meet this constraint, various transmit windowing techniques have been presented in the literature. In this chapter, we will focus on the per-tone based pulse

shaping in DMT transmitter structure presented in [33]. It tries to minimize the spectral leakage by shaping each tone separately by using a constant length non-sparse pulse shaping filter and hence was shown to outperform time-domain based transmit windowing. In [33], per-tone based transmit windowing was shown to significantly reduce the number of virtual carriers, i.e., number of null tones at the band edges. But the contribution to the out of band energy depend on the position of the tone in the band, therefore the design parameter (number of non-zero filter coefficient) to effectively shape each tone also varies. In this chapter, we show that the number of filter taps required to meet the PSD constraint without affecting the performance can then be reduced significantly hence reducing the run-time computational complexity. Efficient resource allocation algorithms are needed in order to allocate the non-zero filter tap. In this chapter, we present efficient algorithms to achieve this goal. First algorithm presented uses only contiguous taps in order to reduce the number of combination of non-zero filter taps, thus reducing a combinatorial search in the number of taps into a linear search in the filter order. This is known as contiguous tap selection (CTS). But restricted sparsity pattern, such as CTS, may not result in the best sparse filters, since the optimal filter sparsity pattern may not be in that search space. To address this problem, we propose a sparse approximation based filter tap allocation algorithm. This ensures that there is no restriction on the sparsity pattern of the filter and hence shown to perform better than the CTS based resource allocation. Furthermore, it is shown that the number of non-zero filter taps can be further reduced when optimal power allocation is performed alongside filter tap allocation.

In **Chapter 4**, we will first highlight that the dispersive nature of DSL channels results in ISI. In order to mitigate ISI, a guard interval known as cyclic prefix is added. But the length of the cyclic prefix depends on the channel impulse response. For the system, which has long channel response, e.g., DSL, channel shortening is also required in order to limit the length of cyclic prefix. To this end, several techniques have been proposed in literatures. In [2], a frequency domain based equalizer, known as MMSE-PTEQ, has been proposed to equalize each tone individually. It uses a constant length non-sparse equalizer on each tone to achieve this. MMSE-PTEQ has been shown to outperform time-domain based channel shortening combined with a 1-tap frequency domain equalizer without increasing the computational complexity significantly. Due to the frequency selective nature of the DSL channel, different tones have different equalization requirement. We show that the number of non-zero equalizer taps required to equalize each tone varies with the tones. Therefore, the number of non-zero equalizer taps required can be reduced without affecting the performance significantly. In this chapter, we propose efficient algorithms to this end. First algorithm is based on selecting only contiguous filter taps in order to reduce the search space which is combinatorial in filter length to linear search space in filter order. We call this algorithm as contiguous tap selection approach. Second algorithm is based on sparse approximation, where the sparsity pattern of MMSE-PTEQ is not restricted. This

is shown to outperform CTS based approach. We also demonstrate that performing optimal transmit power allocation alongside filter tap allocation further reduces the number of non-zero filter taps required.

In **Chapter 5**, we then look into the DMT transceiver with per-tone pulse shaping and per-tone equalization. In chapter 3, we assumed that the channel impulse response fit in the cyclic prefix perfectly and hence ignored the effect of ISI. In this chapter, we will look into the effect of channel impulse response in the received signal-to-noise ratio. Then the effect of channel shortening on the resource allocation in the per-tone based DMT transceiver is investigated. To this end, we will analyze both contiguous tap selection based resource allocation and the sparse approximation based resource allocation. By taking the channel equalization into account we can also compensate for the filtering at the transmitter side. We will then show that we can then minimize over all run-time complexity of the transceiver.

The publications related to the Part I are [107, 106, 113, 105, 112, 109]

Part II of this thesis investigates the multi-user receiver.

In **Chapter 6**, we first present the concept of crosstalk cancellation for upstream VDSL in detail. We will consider the scenario where the receivers are co-located and hence the receiver coordination in possible. In [25], it was shown that due to the columnwise diagonally dominant structure of multi-user DSL channel matrix, a simple linear zero forcing receiver performs optimally in the presence of AWGN background noise. In [27], it was also shown that the majority of the crosstalk originates from the a very small set of lines, hence canceling only these lines would reduce run-time computational complexity without affecting the performance significantly. In the presence of spatially correlated background noise, a prewhitening operation is required, which destroys the CWDD structure of the DSL channel matrix, therefore linear zero-forcing canceler performs poorly. Furthermore, the partial cancellation algorithm presented in [27] also fails to achieve satisfactory results. Hence in this chapter, we will first show that MMSE based cancelers outperform linear zero forcing (ZF) canceler in the presence of spatially correlated background noise. We then extend the concept of partial crosstalk cancellation for MMSE based cancelers. To this end, we propose two efficient algorithms. First algorithm is based on metric selection, which combines the channel crosstalk information and the noise autocorrelation information to efficiently select the crosstalk line to be cancelled. For the linear MMSE canceler, we propose a second algorithm based sparse approximation, which searches for best crosstalk lines to be canceled. It is further shown that use of optimal power allocation along with the partial crosstalk cancellation further improves the performance.

The publication related to part II are [108, 110, 111].

In **Chapter 7**, conclusion are drawn and some direction for future works are discussed.

Chapter 2

Preliminaries

2.1 Modulation schemes

2.1.1 Single carrier modulation

One of the modulation schemes proposed to be used in DSL is carrierless amplitude/phase (CAP) modulation [168, 76, 75]. The CAP modulation is similar to quadrature amplitude modulation (QAM) and performance is same [120]. The key advantage of CAP modulation scheme is its ease of implementation [51]. In order to tackle the problem of dispersive channel, minimum mean squared error decision feedback equalizer (MMSE-DFE) [86, 129] has been suggested. Furthermore, since the DSL channel varies slowly with time, precoding scheme at the transmitters can also be used [148, 68, 55]. Due to the long impulse response of the DSL channel, the equalizer filters have to be very long and are computationally complex [128].

2.1.2 Multicarrier modulation

In the multicarrier modulation scheme, transmission bandwidth is divided into number of smaller parallel orthogonal frequency bands as shown in **Figure 2.1**, also known as subcarriers or tones [18, 31, 32, 127]. The transceiver structure to implement a multicarrier communication scheme is given in **Figure 2.2** [86]. The incoming bit stream acts as an input to the channel encoder. The bit stream is then channel coded in order to protect it from the error introduced by the channel distortion and the noise. The output of the channel encoder is then fed into the interleaver to protect it further from the burst errors e.g., caused by impulse

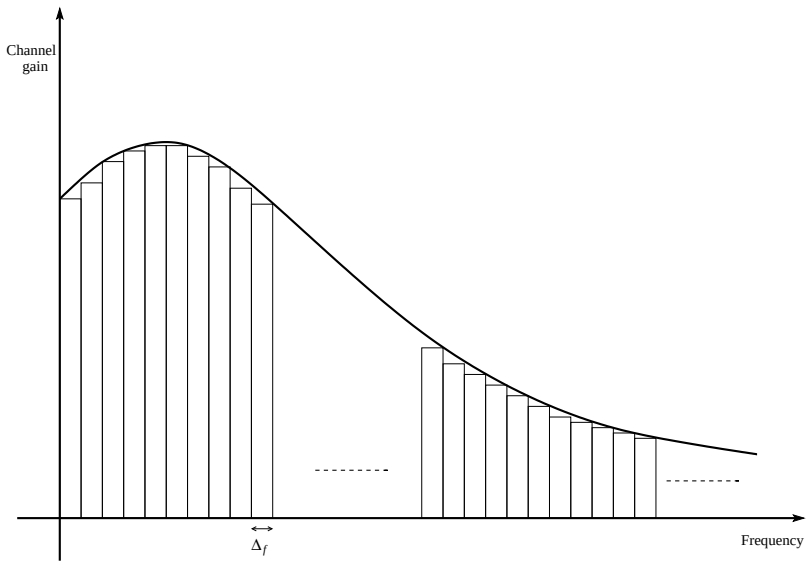

Figure 2.1: Multicarrier modulation

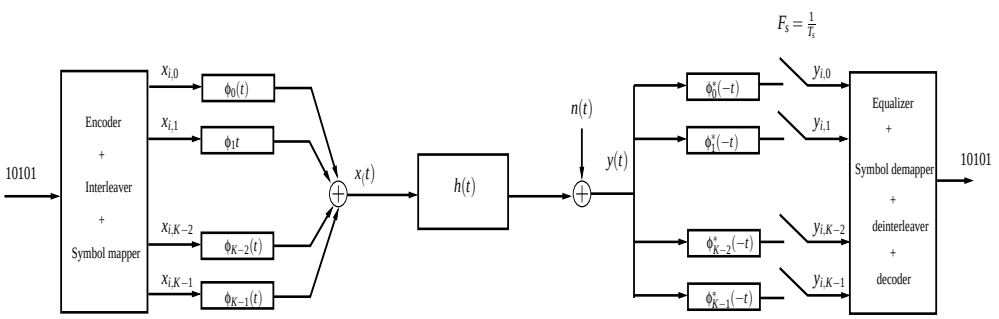

Figure 2.2: A Multicarrier transceiver

noise. The interleaver reorders the bits such that the errors are spread rather than localized hence increasing the chance of error correction. Then, the output of the interleaver is split into K parallel bit streams that are assigned to the K tones. The bit stream is then mapped to a complex-valued transmit symbol corresponding to a point in a M-QAM constellation. The constellation size is related to the number of bits that is represented by a symbol. The output of the multicarrier transmitter at ith symbol period is the superposition of K QAM signals and can be written

as

$$x(t) = \sum_{k=0}^{K-1} x_{i,k}\phi_k(t - iT_s). \tag{2.1}$$

Each term in (2.1) is a output of the orthogonal modulator function $\phi_k(t) = \phi(t)e^{j2\pi f_k t}$. The modulator bank is fed with $K \times 1$ input symbol vectors

$$x_{i,K} = [x_{i,0} \cdots x_{i,K-1}] \tag{2.2}$$

sampled at sampling rate $F_s = \frac{1}{T_s}$ Hz. It can be assumed that the modulator functions use the same prototype pulse shaping filter $\phi(t)$ frquency shifted by f_k. The prototype pulse shaping filter can be written as

$$\phi(t) = \text{sinc}(\frac{\pi t}{T_s}) \tag{2.3}$$

The transmit symbol $x(t)$ is then transmitted over a dispersive channel with impulse response $h(t)$ and corrupted by the additive noise $n(t)$. The received signal can therefore be written as

$$y(t) = h(t) \star x(t) + n(t), \tag{2.4}$$

where $\mathbf{x} \star \mathbf{y}$ represents a linear convolution between the vectors $\mathbf{x}$ and $\mathbf{y}$. At the receiver, demodulation of the received signal is performed by a bank of demodulator functions $\phi_k^*(-t)$, which is matched to the transmit modulator banks. The K outputs of the demodulator are sampled at the sampling frequency F_s. The orthogonality of the used filters guarantees that there is no ICI between the tones. However, the dispersive channel impulse response causes the ISI. If the delay spread of the channel is very small as compared to the symbol time, then the tones can be considered as narrowband i.e., no frequency selectivity within a tone [100]. In this case, the ISI can be ignored and each tone can be assumed as a flat frequency channel. Each tone can be considered as a parallel Gaussian channel. The discrete time data model in this case can be written as

$$y_{i,k} = h_k x_{i,k} + n_{i,k}, \tag{2.5}$$

where $h_k \triangleq h(f_k)$ is the channel frequency response at kth tone. The sampled output of the demodulator is then equalized using a bank of simple complex valued scalars $h_k^{-1}, k \in [0, K-1]$, which are known as frequency domain equalizers.

2.2 Capacity of a transmission medium

The theoretical upper bound on the data rate that can be reliably transmitted over a transmission medium is called capacity of the medium. Claude Shannon

developed a mathematical theory of information that provides with some fundamental boundaries of the performance of a communication system [133, 139]. This states that the maximum number of bits that can be transmitted over a flat AWGN channel can be given by

$$b = \log_2(1 + \mathrm{SNR}), \tag{2.6}$$

where b is the spectral efficiency given as bits per second per Hertz (bps/Hz), and SNR is the signal-to-noise ratio at the receiver. b is the maximum number of bits per transmit symbol that can be transmitted reliably over the given channel. The overall channel capacity can then be written as

$$R = F_s \log_2(1 + \mathrm{SNR}), \tag{2.7}$$

where R is defined as the maximum data rate supported by the channel in bps and it is known as the capacity of the channel, the maximum symbol rate, F_s, is equal to the bandwidth of the channel.

In the case of the frequency selective channel, Shannon suggested to divide the channel into multiple narrowband AWGN subchannels [133], also called tones. The multicarrier system described in Section 2.2 is a possible practical realization of this idea. The capacity of K parallel and independent AWGN channels can be written as

$$R = \sum_{k=0}^{K-1} b_k = \sum_{k=0}^{K-1} F_s \log_2(1 + \mathrm{SNR}_k), \tag{2.8}$$

where b_k is the maximum bits that can be transmitted on kth tone, SNR_k is the signal-to-noise ratio at the receiver on kth tone, and F_s is the symbol rate on each tone. Under the assumption that K is large such that the discrete time model (2.5) is valid, the true SNR_k can be given as

$$\mathrm{SNR}_k = \frac{s_k |h_k|^2}{\sigma_k}, \tag{2.9}$$

where $s_k = \mathcal{E}\{|x_{i,k}|^2\}$ is the transmit power on tone k and $\sigma_k = \mathcal{E}\{|n_{i,k}|^2\}$ is the noise power spectral density (PSD) on tone k.

2.3 Discrete multitone modulation (DMT)

DMT is a multicarrier transmission scheme [81, 36, 125] that employs IDFT to partition the channel bandwidth into parallel subchannels. The use of IDFT and DMT for DSL was originally described in [18, 41]. One of the main advantages of using IDFT to partition the channel bandwidth is the availability of the

efficient computational methods e.g. IFFT. Another advantage of using IDFT for multicarrier modulation is that the basis functions are fixed and channel independant.

Let us consider transmission of a sequence x_i^t sampled at the rate $F_s = 1/T_s$ through the real valued baseband continuous time channel with response $h(t)$. The total channel response typically is the convolution of the transmit filter $h_{tx}(t)$, twisted pair channel response $h_{tp}(t)$ and the receive filter $h_{rx}(t)$ and given as $h_{tx}(t) * h_{tp}(t) * h_{rx}(t)$, where $*$ denotes linear convolution. Then for a synchronized system, the signal at the receiver can be written as

$$y(t) = \sum_{l=-\infty}^{+\infty} x_i^t h(t - lT_s) + n(t), \tag{2.10}$$

where $n(t)$ is the continuous time additive Gaussian noise filtered by the front end filters at the receiver $h_{rx}(t)$. If $y(t)$ is sampled at sample instants $t = iT_s$, then the discrete time samples can be written as

$$y_i^t = \sum_{l=0}^{L} h_l^t x_{i-l}^t + n_i^t, \tag{2.11}$$

where $h_l^t = h(lT_s)$ and the overall channel is modeled as a finite impulse response (FIR) of order L.

Consider a block transmission, where the transmitted block of symbol $\mathbf{x}$ has block length of $\bar{N} \gg L$. Then the ith transmitted symbol can be written as

$$\mathbf{x}_i^t = [x_{i\bar{N}}\ x_{i\bar{N}+1} \cdots x_{(i+1)\bar{N}-1}]^T \tag{2.12}$$

and the corresponding received sequence can be written as

$$\mathbf{y}_i^t = [y_{i\bar{N}}\ y_{i\bar{N}+1} \cdots y_{(i+1)\bar{N}-1}]^T \tag{2.13}$$

From (2.11), we can model this transmission in the matrix form as

$$\mathbf{y}_i^t = \bar{\mathbf{H}}_0 \mathbf{x}_i^t + \mathbf{n}_i^t, \tag{2.14}$$

where $\mathbf{n}_i^t$ is the corresponding noise vector and $\mathbf{H}_0$ is a real toeplitz matrix of size $\bar{N} \times \bar{N}$ and can be written as

$$\bar{\mathbf{H}}_0 = \begin{bmatrix} h_0^t & 0 & \cdots & \cdots & \cdots & 0 \\ h_1^t & h_0^t & 0 & \cdots & \cdots & 0 \\ \vdots & \ddots & \ddots & & & \vdots \\ \vdots & \ddots & \ddots & & & \vdots \\ 0 & \cdots & \cdots & h_L^t & \cdots & h_0^t \end{bmatrix} \tag{2.15}$$

Due to the dispersive nature of the channel, ISI occurs between two successive symbols. To avoid ISI, a cyclic prefix (CP) of length ν is used in each transmitted block [118, 166]. A cyclic preifix is a copy of the last ν data symbol placed at the beginning of the transmitted block. The (2.14) can be rewritten to incorporate the cyclic prefix as

$$\mathbf{y}_i^t = \mathbf{H}_0\mathbf{P}\mathbf{x}_i^t + \mathbf{n}_i^t, \tag{2.16}$$

where

$$\mathbf{P} = \left[\begin{array}{c|c} \mathbf{0} & \mathbf{I}_\nu \\ \hline & \mathbf{I}_N \end{array}\right], \tag{2.17}$$

$\mathbf{I}_x$ is the identity matrix of size x, N is the size of the IDFT, $\mathbf{P} \in \mathbb{R}^{\bar{N}\times N}$, with $\bar{N} = N + \nu$. At the receiver, the first ν samples of $\mathbf{y}_i^t$ is discarded by multiplying the received vector $\mathbf{y}_i^t$ with the matrix $\bar{\mathbf{Q}} = [\mathbf{0}_{N\times\nu}|\mathbf{I}_N]$. The resulting output can be written as

$$\bar{\mathbf{y}}_i^t = \bar{\mathbf{Q}}\mathbf{y}_i^t = \bar{\mathbf{Q}}\mathbf{H}_0\mathbf{P}\mathbf{x}_i^t + \bar{\mathbf{n}}_i^t, \tag{2.18}$$

where $\bar{\mathbf{y}}_i^t \in \mathbb{R}^N$ and noise vector $\bar{\mathbf{n}}_i^t \in \mathbb{R}^N$ with $\bar{\mathbf{n}}_i^t = \bar{\mathbf{Q}}\mathbf{n}_i^t$. $\bar{\mathbf{n}}_i^t$ only retains last N entries of $\mathbf{n}_i^t$.

In the case of $L \leq \nu$, the received signal after the insertion of cyclic prefix of length ν and then discarding the first ν samples at the receiver results in an ISI free system. Here the term $\bar{\mathbf{Q}}\mathbf{H}_0\mathbf{P}$ becomes a circulant matrix. Hence, the linear convolution with the channel is converted into circular convolution. The system can then be written as

$$\bar{\mathbf{y}}_i^t = \mathbf{H}_c\mathbf{x}_i^t + \bar{\mathbf{n}}_i^t, \tag{2.19}$$

where $\mathbf{H}_c = \bar{\mathbf{Q}}\mathbf{H}_0\mathbf{P}$ is circulant matrix and can be written as

$$\mathbf{H}_c = \begin{bmatrix} h_0^t & 0 & \cdots & h_L^t & \cdots & h_1^t \\ h_1^t & h_0^t & \cdots & & \ddots & \vdots \\ \vdots & \ddots & \ddots & & & h_L^t \\ \vdots & & & \ddots & & \vdots \\ 0 & \cdots & h_L^t & \cdots & h_1^t & h_0^t \end{bmatrix}. \tag{2.20}$$

In order to obtain frequency domain signal, we can perform DFT operation on both sides of (2.19). This results in

$$\mathcal{F}_N\bar{\mathbf{y}}_i^t = \mathcal{F}_N\mathbf{H}_c\mathbf{x}_i^t + \mathcal{F}_N\bar{\mathbf{n}}_i^t, \tag{2.21}$$

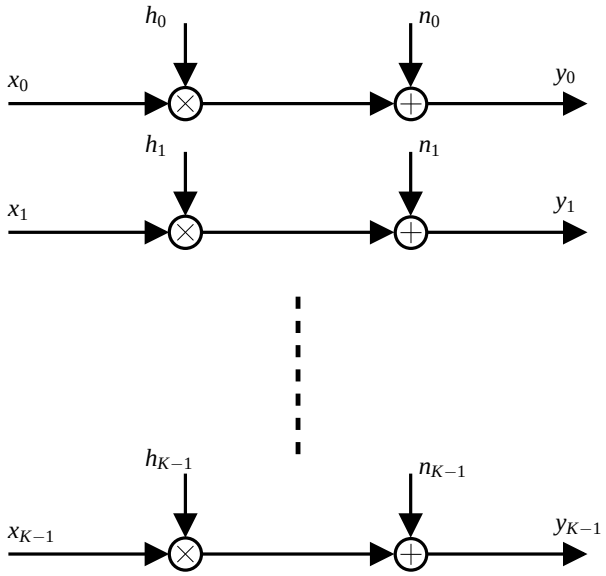

Figure 2.3: Frequency domain representation of DMT modulation

where $\mathcal{F}_N$ is the N-point DFT operation. We know that the time-domain input symbol $\mathbf{x}_i^t$ can be written in terms of frequency domain input symbol as

$$\mathbf{x}_i^t = \mathcal{I}_N \mathbf{x}_i, \tag{2.22}$$

where $\mathcal{I}_N$ is the N-point IDFT operation. Therefore, the frequency domain data model can be written as

$$\mathbf{y}_i = \mathcal{F}_N \mathbf{H}_c \mathcal{I}_N \mathbf{x}_i + \mathbf{n}_i, \tag{2.23}$$

where $\mathbf{y}_i$, $\mathbf{x}_i$ and $\mathbf{n}_i$ are the frequency domain output symbol, frequency domain input symbol and the frequency domain additive noise. The circulant matrix is diagonalized by the IDFT and DFT operation. Therefore, we can write

$$\mathcal{F}_N \mathbf{H}_c \mathcal{I}_N = \mathbf{H}, \tag{2.24}$$

where $\mathbf{H} = diag\{h_{i,0} \cdots h_{i,N}\}$ with the complex valued scalar frequency domain channel response in the diagonal. This can then be written as

$$\mathbf{y}_i = \mathbf{H}\mathbf{x}_i + \mathbf{n}_i. \tag{2.25}$$

Since the channel matrix $\mathbf{H}$ is a diagonal matrix, (2.25) decouples into N parallel Gaussian channel as shown in the **Figure 2.3**.

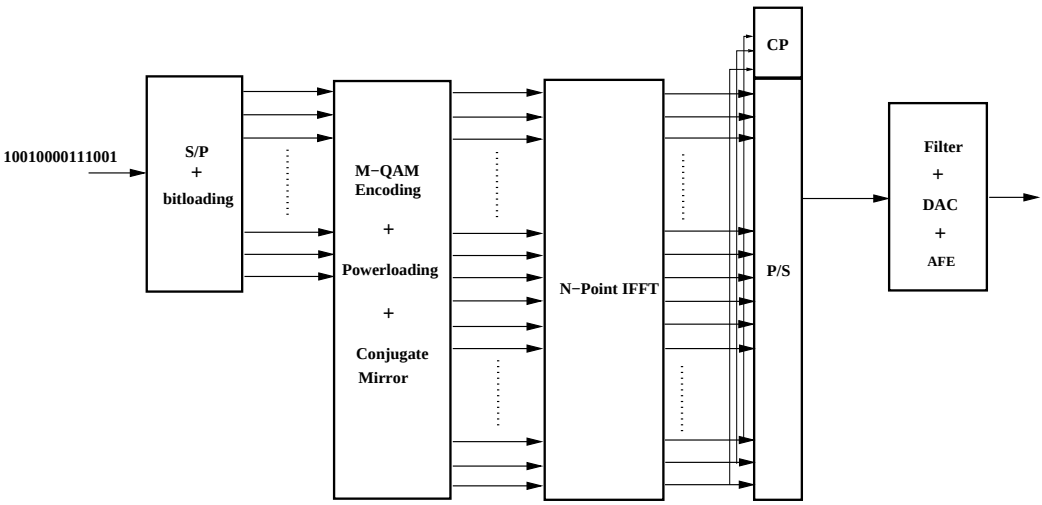

Figure 2.4: A DMT transmitter

2.4 DMT transmitter

Figure 2.4 represents the DMT transmitter. The structure of DMT transmitter is similar to the structure of the multicarrier transmitter in **Figure 2.2**. The DMT transmitter involves following operations

- The incoming bit stream is encoded using a Reed-Solomon (RS) encoder [44] and the output of the encoder is then interleaved and divided into $N/2+1$ parallel stream. Each stream is assigned to a certain tone and mapped on to a complex valued M-QAM signal.
- Then a conjugate mirror operation is performed on these $N/2+1$ M-QAM symbols such that $x^l = x^l_{N-i}$, where l is the symbol index and output block length becomes N symbols.
- The N symbols are then modulated using IDFT resulting in real valued time domain symbol.
- A guard period of ν samples, known as cyclic prefix, is added infront of the block to obtain the effective time-domain signal.
- The resulting time domain symbols is send through the digital front end filters , digital-to-analog converter (DAC) and the analog front end filters before transmission over the DSL channel.

2.5 DMT receiver

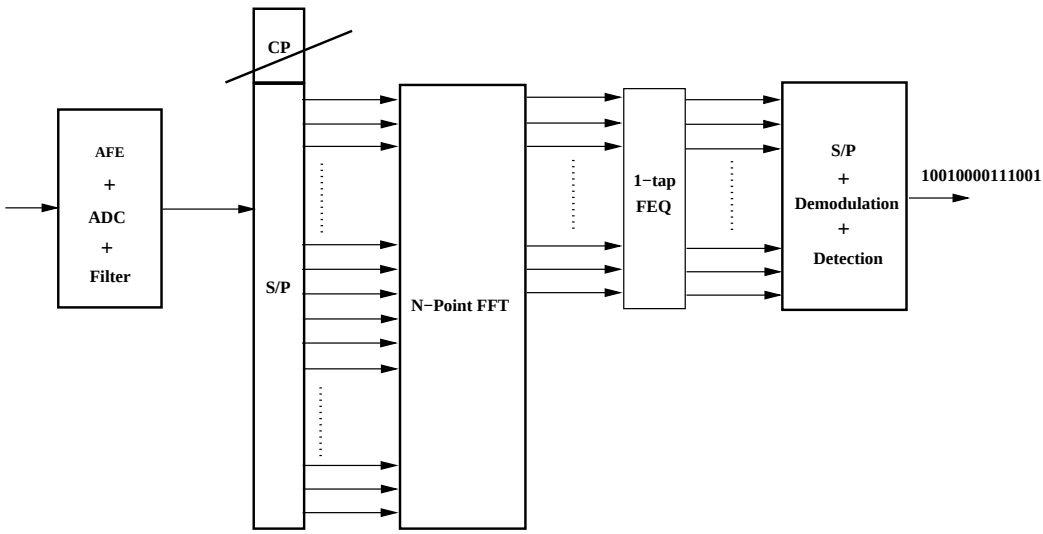

Figure 2.5: A DMT receiver

Figure 2.5 represents a typical DMT receiver structure. The DMT receiver performs following operations

- The received analog signal is first passed through a analog-to-digital converter (ADC) to get a digital output.
- Then it is provided as an input to the time-domain equalizer (TEQ) so that the channel impulse response can be shortened.
- Then the output is serial-to-parallel converted and the CP is discarded
- The N remaining symbols are FFT demodulated.
- Then the frequency domain symbols are equalized using a 1-tap frequency-domain equalizer to correct the channel distortions.
- Then the symbols are demapped, deinterleaved, and decoded to a bit stream.

2.6 Bit loading in DSL

For a noise power on a tone k, $\sigma_k \triangleq \mathcal{E}\{|z_k|^2\}$, and the transmit power on the tone $s_k \triangleq \mathcal{E}\{|x_k|\}$ the theoretical capacity of the DMT is

$$c_k = \Delta_f \log_2(1 + \mathrm{SNR}_k), \tag{2.26}$$

where $\mathcal{E}\{.\}$ denotes the statistical expectation operation, Δ_f denotes the tone-spacing and signal-to-noise ratio (SNR) on tone k, which is defined as

$$\mathrm{SNR}_k = \sigma_k^{-1} |h_k|^2 s_k. \tag{2.27}$$

For most practical coding scheme a SNR-gap (Γ) also have to be considered to account for the fact that the most codes do not provide the theoretical capacity. Γ is a function of the coding gain, desired noise margin and target bit error probability [44, 80]. Therefore, in practice the achievable bit rate is

$$c_k = \Delta_f \log_2(1 + \Gamma^{-1}\mathrm{SNR}_k), \tag{2.28}$$

In DMT based systems, the receiver estimates the SNR on each tone and reports this back to the transmitter. Then the transmitter can adapt the number of bits used on each tone by choosing different constellation size, this is known as bitloading. This allows DMT based systems to achieve high spectral efficiency. The number of bit transmitted on the tone is called bitloading, this can be written as,

$$b_k = \frac{1}{F_s} \Delta_f \log_2(1 + \Gamma^{-1}\mathrm{SNR}_k), \tag{2.29}$$

where F_s denotes the DMT symbol rate. Typically, the sampling rate is equal to the tone-spacing therefore, we can write

$$b_k = \log_2(1 + \Gamma^{-1}\mathrm{SNR}_k). \tag{2.30}$$

The total data rate is then the sum of all the number of bits transmitted in all the tones and can be written as

$$R = F_s \sum_k b_k. \tag{2.31}$$

2.7 Power loading in DSL

DSL systems typically has to conform to a set of spectral masks which ensures that the DSL system is spectrally compatible with other communication systems that may exist in the same binder

$$s_k \leq s_k^{mask} \quad \forall k \tag{2.32}$$

The modems also have the total power constraint due to the limitations on the analog front-end

$$\sum_k s_k \leq P. \tag{2.33}$$

In order to maximize the total data rate, a modem can vary the power allocated to each tone, i.e., s_k subject to the spectral mask and the total power constraints

$$s_k^{opt} = \underset{s_1 \cdots s_K}{\operatorname{argmax}} R_k \tag{2.34}$$

$$\text{subject to } \sum_k s_k \leq P$$

$$s_k \leq s_k^{mask} \; \forall k$$

This adaptive distribution of power over tones is known as the power loading. The objective function of (2.34) is a concave function and the constraints form a convex sets therefore Karush-Kuhn-Tucker (KKT) conditions are sufficient for optimality. This leads to the following solution known as waterfilling [44]

$$s_k^{opt} = \left[\frac{1}{\lambda} - \frac{\Gamma\sigma_k}{|h_k|^2}\right]_0^{s_k^{mask}}, \tag{2.35}$$

where $[x]_a^b \triangleq \max(a, \min(x, b))$. The level $1/\lambda$ is chosen such that the constraints are obeyed. There are efficient algorithms to find the appropriate λ with complexity $\mathcal{O}(K\log K)$ [13]. With a powerful enough error correcting code, the power loading allows DMT based systems to achieve bit rates arbitrarily close to the theoretical channel capacity.

2.8 Equalization in DSL

2.8.1 Time-domain equalization

In order to shorten the effective length of the channel impulse response of a DSL channel, a time domain equalizer (TEQ), $\mathbf{w}$, can be used. The T-taps TEQ is generally designed based on minimum mean square error criterion to shorten the channel impulse response (CIR), $\mathbf{h}^t$, to a $\nu+1$-taps target impulse response (TIR), $\mathbf{b}$. There are a number of techniques to design the TEQ presented in various literatures [7, 5, 6, 97, 158, 157, 98, 156]. One of the important parameter in TEQ design is called decision delay. For a given CIR $\mathbf{h}^t = [h_0^t \cdots h_L]$, it can be shortened to ν coefficients and can be written as $h_0 \cdots h_\nu \; 0 \cdots 0$ for no decision

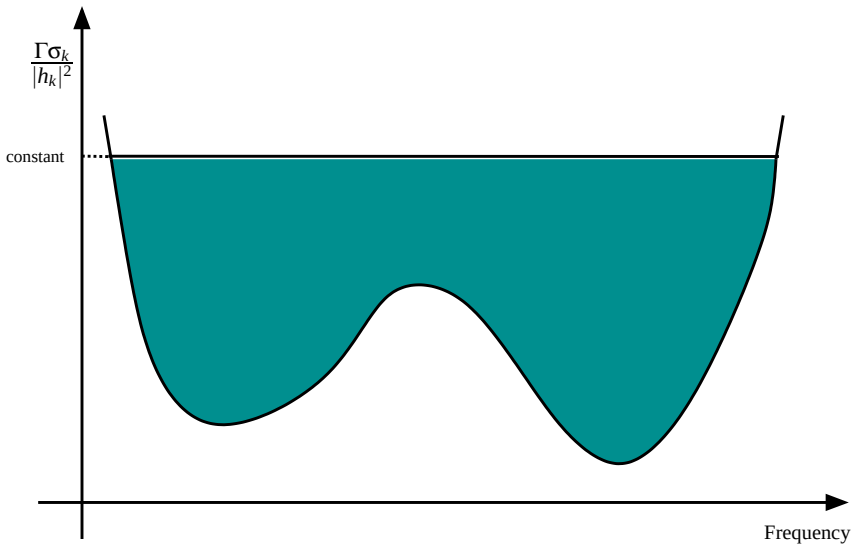

Figure 2.6: Waterfilling solution

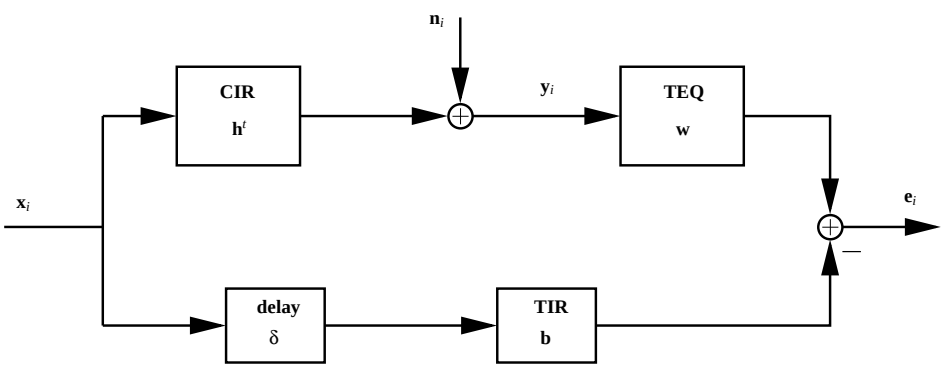

Figure 2.7: TEQ design

delay. With a non-zero decision delay δ, it is given as $[0 \cdots h_\delta \cdots h_{\delta+\nu}\ 0 \cdots 0]$. The MMSE design procedure chooses the optimal decision delay δ as shown in **Figure 2.7** and can be written as

$$\underset{\mathbf{w},\mathbf{b},\delta}{\text{minimize}} \quad J,$$

$$\text{where} \quad J = \mathcal{E}\{\mathbf{e}_i^2\} = \mathcal{E}\left\{\left([x_{i-\delta} \cdots x_{i-\nu-\delta} | y_i \cdots y_{i-T+1}] \begin{bmatrix} -\mathbf{b} \\ \mathbf{w} \end{bmatrix}\right)^2\right\}. \quad (2.36)$$

where x_i and y_i are transmitted and received signal samples and i is the sample index.

There are several disadvantages of the TEQ procedures based on MMSE channel shortening

- The MMSE based TEQ design is not related to the maximum achievable bit rate by the DMT systems.
- The obtained bit rate is a non smooth function of the delay which makes the choice of decision delay difficult.
- All the tones are equalized with the same filter, which limits the performance.
- The bitrate maximizing TEQ are the solution of highly non-linear cost function, which are difficult to optimize [8, 9].

2.8.2 Per-tone equalization

MMSE-PTEQ moves the equalization operation into the frequency domain [2]. In the DMT receiver employing per-tone equalization, each tone has its own multitap equalizer after demodulation. Since each tone can be optimized by formulating a MMSE problem, MMSE-PTEQ provides large improvements with respect to time-domain equalization. The MMSE-PTEQ bit rate is shown to be the upper bound for the TEQ bit rate [2]. It has been shown in [2] that by employing a sliding FFT and difference terms, the run-time complexity of MMSE-PTEQ is comaparable to the run-time complexity of TEQ. The details of MMSE-PTEQ will be presented in chapter 4.

2.9 Multi-user DSL

Thus far, we have only considered a DSL modem in single user scenario. But multiple DSL modem operates and interacts within a binder. This gives rise to the multi-user scenario in DSL system.

Consider multiple modem operating within the same binder. If the modems are synchronized and transmit simultaneously, then the discrete time received signal after sampling at rate F_s at receiver n can be written as

$$y_i^{t,n} = \sum_{l=0}^{L} \left(h_l^{t,n,n} x_{i-l}^{t,n} + \sum_{m \neq n} h_l^{t,n,m} x_{i-l}^{t,m} \right) + z_i^{t,n}, \tag{2.37}$$

where $x_i^{t,n}$ is the time-domain sequence transmitted by modem n. Also $h_l^{t,n,m} \triangleq h^{n,m}(lT_s)$, where $h^{n,m}(t)$ represents the continuous-time CIR from transmitter m to receiver n. When $m = n$ then $h^{n,n}(t)$ is known as the direct channel and when $m \neq n$ then $h^{n,m}(t)$ is known as the crosstalk channel. The $z_i^{t,n}$ denotes the additive Gaussian noise experienced by receiver n and L is the order of the FIR channel response.

In the frequency domain, the channel gain on tone k from transmitter m to receiver n can be written as $h_k^{n,m}$. Since the DMT divides the frequency selective channel into parallel frequency flat subchannels (tones), $h_k^{n,m}$ is just a complex scalar value. The frequency domain channel can be obtained by performing DFT on the time-domain channel impulse response

$$[h_1^{n,m} \cdots h_K^{n,m}]^T = \mathcal{F}_K [h_0^{t,n,m} \; \mathbf{0}_{1\times K-L-1} \; h_L^{t,n,m} \cdots h_1^{t,n,m}]^T, \tag{2.38}$$

where $\mathcal{F}_K$ denotes the K-point DFT operation. The frequency domain signal at the receiver n on tone k can then be written as

$$y_k^n = \sum_{m=1}^{N} h_k^{n,m} x_k^m + z_k^n, \tag{2.39}$$

where N is the number of lines in the binder. (2.39) can be then written in a matrix form as follows

$$\mathbf{y}_k = \mathbf{H}_k \mathbf{x}_k + \mathbf{z}_k, \tag{2.40}$$

where $\mathbf{y}_k \triangleq [y_k^1, \cdots, y_k^N]^T$, $\mathbf{x}_k \triangleq [x_k^1, \cdots, x_k^N]^T$ contains the received and transmitted signal for all the lines on tone k. $\mathbf{z}_k = [z_k^1 \cdots z_k^N]$ contains all the noise signal for all the lines on tone k. The multi-user channel matrix $\mathbf{H}_k$ can be written as

$$\mathbf{H}_k = \begin{bmatrix} h_k^{1,1} & h_k^{1,2} & \cdots & h_k^{1,N} \\ h_k^{2,1} & h_k^{2,2} & \ddots & \vdots \\ \vdots & \ddots & \ddots & \vdots \\ h_k^{N,1} & \cdots & \cdots & h_k^{N,N} \end{bmatrix}, \tag{2.41}$$

where the diagonal elements of $\mathbf{H}_k$ contains the direct channel and the off-diagonal elements contain the crosstalk channels.

Cable Type	TP1	TP2
diameter(mm)	0.4	0.5
$r_{0c}(\Omega/\text{km})$	286.176	174.559
a_c	0.1476962	0.0530735
$l_0(\mu\text{H/km})$	675.369	617.295
$l_\infty(\mu$ H/km)	488.952	478.971
b	0.929	1.152
f_m(kHz)	806.339	553.760
c_∞(nF/km)	49	50
g_0(n℧/km)	43	0.00023487476
g_e	0.7	1.38

Table 2.1: RLCG parameters

2.9.1 Multi-user channel model

The direct channel of a twisted pair cable can be modeled by using an incremental RLCG model. The RLCG model defines the resistance (R), inductance (L), capacitance (C) and the conductance (G) of the twisted pair cable per kilometer. The R, L, C, and G of a twisted pair cable can be written as follows

$$R_k = (r_{0c}^4 + a_c f_k^2)^{1/4}$$

$$L_k = (l_0 + l_\infty (f_k/f_m)^b)(1 + (f_k/f_m)^b)^{-1}$$

$$C_k = c_\infty$$

$$G_k = g_0 (f_k)^{g_e},$$

where $f_k \triangleq \Delta_k.k$ is the frequency on the tone k in Hz [11]. These models are frequency dependant and the parameters r_{0c}, a_c, l_0, l_{infty}, f_m, b, c_∞, g_0, and g_e depend on the materials and the diameter of the twisted pair cable. The typical values of these parameters are given in **Table 2.1**

The direct channel transfer function of a twisted pair cable of length d km can be written as

$$h_k(d) = \frac{Z_L + Z_S}{Z_L \cosh(\gamma_k d) + Z_{0,k} \sinh(\gamma_k d) + Z_S Z_L Z_{0,k}^{-1} \sinh(\gamma_k d) + Z_S \cosh(\gamma_k d)}, \tag{2.42}$$

where γ_k is the propagation constant per unit length for the twisted pair cable at tone k and it is given as

$$\gamma_k = \sqrt{(R_k + j2\pi f_k L_k)(G_k + j2\pi f_k C_k)},$$

$Z_{0,k}$ is defined as the characteristic impedance of the line on tone k and can be given as

$$Z_{0,k} \triangleq \sqrt{\frac{R_k + j2\pi f_k L_k}{G_k + j2\pi f_k L_k}},$$

Z_S is known as the source impedance of the transmitting modem and Z_L is the load impedance of the receiving modem.

Similarly, the crosstalk channels can also be modeled based on 1% worst-case analysis. This model provides the crosstalk model such that in 99% of cases the crosstalk is less severe than the value suggested by the model. These models ensure that the DSL modems operate for the majority of the customers. In this model, the crosstalk channel gain between two lines is given as

$$h_k^{n,m} = \alpha_{k,n,m} |h_k(d^{n,m})| \tag{2.43}$$

where

$$\alpha_{k,n,m} \triangleq K_{xf} \frac{f_k}{f_0} \sqrt{d^{n,m}_{\text{coupling}}}, \tag{2.44}$$

$f_0 = 1$ MHz and $K_{xf} = 0.0056$ [52]. If $d_{\text{coupling}^{n,m}}$ is the length of the binder segment over which coupling between the line m and line n, then we can write

$$d_{\text{coupling}^{n,m}} \leq \min(d_m, d_n), \tag{2.45}$$

where d_n is the length of the line n in kilometers.The distance from the crosstalk source m to the crosstalk victim n is denoted as $d^{n,m}$ and the channel transfer function of $d^{n,m}$ can be given as (2.42).

The 1% worst-case model cannot be used to assess the possible gains for any particular crosstalk mitigation techniques, since the gains would only be applicable to 1% of the lines. This would be a overestimation of the performance gains. To counter this problem, full statistical models have been proposed in [90, 141]. These models could provide more realistic impact of the crosstalk mitigation techniques in practical DSL systems.

2.9.2 Dynamic spectrum management (DSM)

The techniques to optimize the transmission for a bundle of twisted pairs is known as dynamic spectrum management (DSM). The optimization depends on the different level of coordination between the lines in the bundle. The resources and different parameters of the DSL modems are then optimized by taking the interference of the particular DSL scenario into account. A DSL DSM

infrastructure may consist of a central office (CO) and a spectrum management center (SMC). The SMC is responsible for the DSM. It collects the data from the modems e.g. line margins, transmit spectra, channel charecteristics etc. After processing the collected data, the SMC then optimizes the DSL parameters e.g. transmit spectra, data rates, forward error correcting (FEC) codes etc., such that the quality of service for the users is maintained. This optimization can be performed on a regular basis or multiple times per day [42].

The DSM techniques can be classified into following levels based on the level of coordination between the lines in the binder [42].

DSM level-0

DSM level 0 corresponds to no DSM coordination. No specific optimization is performed.

DSM level-1

DSM level-1 corresponds to the management of each twisted pair transmission based on estimated characteristics of the cable. Spectrum of each line is optimized independently.

DSM level-2

DSM level 2 corresponds to the the joint coordination of the parameters of multiple DSL line with full knowledge of direct and the crosstalk channel. It is often termed as multi-user spectrum coordination.

DSM level-3

DSM level 3 corresponds to the multi-user signal coordination e.g. precoding, cancellation, such that the crosstalk is cancelled. It is also refered as vectored DSL.

2.9.3 Crosstalk cancellation

Linear zero forcing (ZF) crosstalk cancellation

The linear ZF canceler output can be written as [163]

$$\hat{\mathbf{x}}_k = decision\left(\mathbf{W}_{k,ZF}\mathbf{y}_k\right), \tag{2.46}$$

where

$$\mathbf{W}_{k,ZF} = \mathbf{H}_k^{-1} \tag{2.47}$$

is the $N \times N$ linear zero-forcing canceler matrix. The ZF canceler does not take background noise into account. Therefore, if the channel is not well conditioned, it can amplify the background noise and degrade the overall performance.

Linear MMSE crosstalk canceler

The linear MMSE canceler output can be written as [163]

$$\hat{\mathbf{x}}_k = decision\left(\mathbf{W}_k\mathbf{y}_k\right), \tag{2.48}$$

where

$$\mathbf{W}_k = \mathbf{S}_k\mathbf{H}_k^H(\mathbf{H}_k\mathbf{S}_k\mathbf{H}_k^H + \mathbf{R}_{z,k})^{-1} \tag{2.49}$$

is the $N \times N$ linear MMSE canceler matrix. Unlike the zero-forcing canceler, the linear MMSE canceler takes the noise correlation matrix into account. This enables the linear MMSE canceler to cancel the alien crosstalk much more efficiently than the zero-forcing canceler. In a high signal-to-noise ratio (SNR) AWGN scenario, the linear MMSE canceler approaches the zero-forcing canceler.

Nonlinear MMSE crosstalk cancellation

The linear MMSE canceler in general performs suboptimally. A non-linear MMSE canceler such as the MMSE-GDFE [142, 60, 173, 162] and the MMSE-VBLAST [170] achieves optimal performance by feeding back the already detected symbols to remove the corresponding interference.

MMSE-GDFE

Figure 2.8 shows the MMSE-GDFE structure described in [142, 60, 173]. The feedforward filter $\mathbf{W}_f^k$ of the MMSE-GDFE can be written as

$$\mathbf{W}_{k,f} = (\mathbf{Q}_k)^{-1}(\mathbf{G}_k)^{-H}\mathbf{H}_k^H \tag{2.50}$$

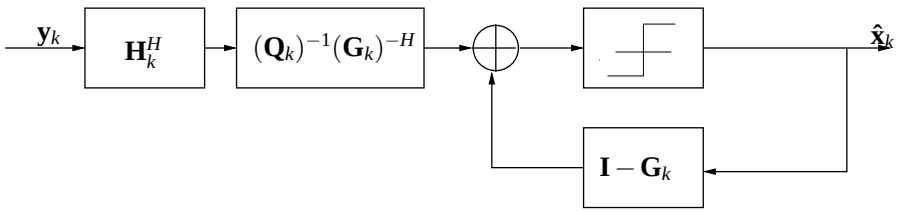

Figure 2.8: MMSE-GDFE

where $\mathbf{Q}_k$ is a diagonal matrix and $\mathbf{G}_k$ is a monic lower triangular matrix. Here $\mathbf{Q}_k$ and $\mathbf{G}_k$ can be obtained from the Cholesky factorization of

$$(\bar{\mathbf{R}}_k)^{-1} = ((\mathbf{S}_k)^{-1} + \mathbf{H}_k^H(\mathbf{R}_{z,k})^{-1}\mathbf{H}_k) \tag{2.51}$$

i.e.

$$(\bar{\mathbf{R}}_k)^{-1} = \mathbf{G}_k\mathbf{Q}_k\mathbf{G}_k^H. \tag{2.52}$$

The lower triangular structure of $\mathbf{G}_k$ defines a detection order (line 1 is detected first, line N is detected last). When different lines have different priorities, the highest priority line should be detected last [153]. In [60, 173], it was shown that the MMSE-GDFE performs optimally in the spatially correlated noise scenario.

MMSE-VBLAST

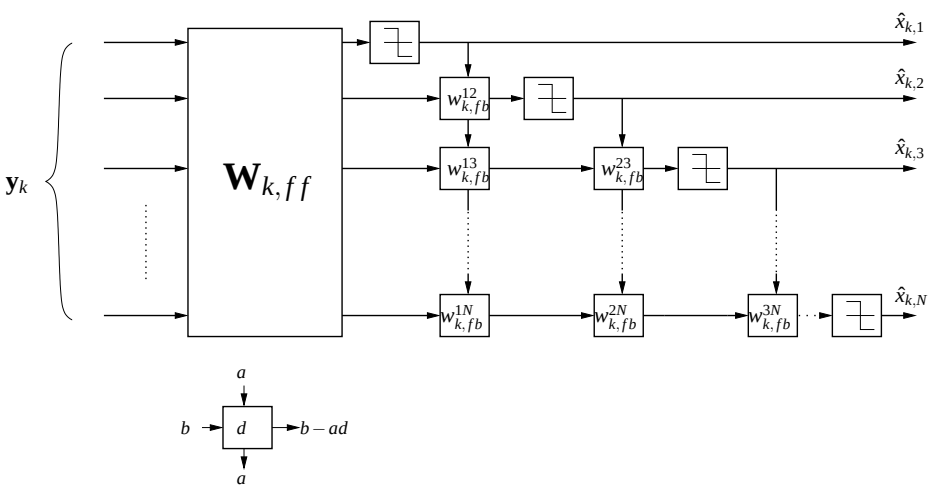

Figure 2.9: MMSE-VBLAST structure

In the MMSE-VBLAST [170], the interference from the already detected lines is subtracted from the received vector and then a MMSE linear canceler is applied to reduce the interference from the yet undetected lines. Let us define the channel $\mathbf{H}_k = [\mathbf{h}_{1,k} \cdots \mathbf{h}_{N,k}]$. The MMSE-VBLAST detection algorithm is given as,

$$\text{For } n = 1 \cdots N$$

$$\hat{x}_k^n := decision \left(\mathbf{w}_{ff,k}^n (\mathbf{y}_k - \sum_{l=1}^{n-1} \mathbf{h}_{l,k} \hat{x}_{l,k}) \right) \tag{2.53}$$

The feedforward filter is

$$\mathbf{w}_{ff,k}^n = s_k^n \mathbf{h}_k^{nH} ([\mathbf{h}_k^n \cdots \mathbf{h}_k^N] \mathbf{S}_k^{N-n} [\mathbf{h}_k^n \cdots \mathbf{h}_k^N]^H + \mathbf{R}_{z,k})^{-1}, \tag{2.54}$$

where s_k^n is the n-th diagonal element of matrix $\mathbf{S}_k$, $\mathbf{S}_k^{N-n}$ is an $(N-n) \times (N-n)$ diagonal matrix containing the power transmitted on lines n to line N and $\hat{x}_k^n$ is the estimate of x_k^n.

$$\text{For } n = 1 \cdots N$$

$$\hat{x}_k^n := decision \left(\mathbf{w}_{ff,k}^n \, \mathbf{y}_k - \sum_{l=1}^{n-1} \underbrace{\mathbf{w}_{ff,k}^n \mathbf{h}_{l,k}}_{\triangleq \mathrm{w}_{fb,k}^{ln}} \hat{x}_k l \right), \tag{2.55}$$

where the decision feedback operation is again applied at the end as indicated in the Figure 2.9. In [58], the MMSE-GDFE and the MMSE-VBLAST were shown to be equivalent.

2.10 Summary

In this chapter, we provided introduction to various aspects of a DSL system. This comprises the important building block of a DSL transceiver. A brief overview of the different modulation schemes considered for the DSL system is introduced and the motivation toward using the multicarrier modulation is then presented. A mathematical model of a DMT based system is also introduced and DMT transmitter and receiver structures are then described. Various techniques in order to increase the capacity of the DMT system, such as bitloading and power loading is also discussed in detail. Furthermore, some techniques, to mitigate the effect of channel impairments, such as time domain equalization and per-tone based equalization is also introduced.

In the multi-user DSL scenario, the effect of crosstalk on the system performance is discussed and then a simple multi-user channel modelling technique is also presented. Various technique to optimize the transmission in this scenario is also discussed in order to either avoid the crosstalk or cancel it. Finally, various receiver structures to cancel the effect of crosstalk are presented.

In the following chapters, we will develop various efficient algorithms to reduce the run-time complexity of the signal processing blocks used to mitigate numerous channel impairments discussed in this chapter.

Part I

SINGLE-USER RESOURCE ALLOCATION

Chapter 3

Resource allocation in DMT transmitter with per-tone pulse shaping filters

3.1 Introduction

VDSL modems use DMT modulation [44]. DMT divides the available spectrum into smaller parallel sub-bands or tones. Each tone corresponds to an orthogonal carrier. The input bit-stream is divided into independent parallel streams, which then QAM-modulate the different carriers. These QAM modulations are implemented based on an IDFT [18]. A cyclic prefix is added to each resulting time domain symbol before transmission, which allows for an easy channel equalization at the receiver. However, if the cyclic prefix is too short, i.e. shorter than the channel impulse response, then this results in ISI and ICI. Highly dispersive channels such as the VDSL channel have a very long channel impulse response, hence to mitigate ISI/ICI a very long cyclic prefix is needed.

The IDFT filters used to implement the DMT have a poor frequency response as shown in Figure 3.1. Firstly, their first side lobe is only 13 dB below the main lobe and secondly, the rate of decay of the side lobe energy is only inversely proportional to frequency. In some applications e.g. in VDSL, the Power Spectral Density (PSD) of the transmitted signal is not allowed to exceed a given PSD mask defining one or more pass bands and stop bands. To satisfy this constraint, many tones near the band edges cannot be used, which are known as virtual carriers (VC). This significantly reduces the available bandwidth for data transmission. An example

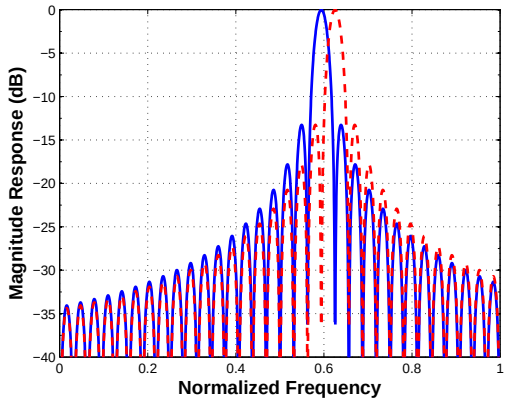

Figure 3.1: Spectrum of two adjacent tones in a DFT based multicarrier system

of the effect of not using enough VC is shown in Figure 3.2. One of the attempted approaches to improve the spectral characteristics of the transmit signal is to use alternative transmit and receive filters instead of the DFT filters [154, 22, 85], but this is found to make the equalization at the receiver more complicated. Another approach is to use time domain windowing of the transmit signal [10] either with or without extending the cyclic prefix and possibly an additional cyclic suffix [40]. Inter-symbol windowing, in which only the cyclic prefix and cyclic suffix is multiplied with the window function to preserve the orthogonality was presented in [93]. Similarly, intra-symbol windowing where the window function is applied to the transmit block was proposed in [89, 47, 92]. However, this approach destroys the orthogonality and needs a post processing at the receiver. The idea of spectral compensation was considered in [17, 14, 91]. Theoretically, one of the simplest approaches is to filter the transmit signal [100]. A per-tone pulse shaping procedure to reduce the energy in the stop bands was proposed in [33]. It uses a filter to shape the spectrum for each tone separately. These filters can be designed using many techniques [95, 123, 147]. In [33], a simple filter design procedure was proposed, where a pulse shaping filter is designed for each tone such that its stop band energy contribution is minimized. The method allows for asymmetric filters which helps to reduce the stop band energy contribution of the tones at the band edges. This in turn helps to increase the number of tones that can be used for data transmission without violating the PSD mask constraint compared to a time domain windowing as shown in Figure 3.3. The resulting transmitter structure was derived in [33] and shown to be a dual of the per-tone equalization structure proposed in [2]. It is noted that the transmit signal filtering has the same effect as the time dispersive channel and therefore the cyclic prefix length has to be increased accordingly in order to mitigate the ISI/ICI [91, 100].

In the DMT transmitter using per-tone pulse shaping as described in [33], every tone is shaped using a constant length non-sparse pulse shaping filter and each tone has the same transmit power, i.e., no specific power loading scheme used. However for a given per-tone transmit power, tones in the middle of a pass band contribute less to the overall stop band energy. Therefore, a sparse pulse shaping filter, i.e., with fewer non-zero filter taps and hence lower runtime complexity, may be used for such tones without affecting the overall performance significantly. A better alternative is thus to consider variably sparse pulse shaping filters, where each tone can use a pulse shaping filter with a different degree of sparsity. Furthermore, the number of used tones can also be increased by using a lower transmit power at the band edges. Using a lower transmit power on a larger number of tones may help to increase the achievable data rate without violating the PSD mask constraint. In conclusion, there is a need for efficients method to optimally allocate the non-zero filter taps as well as transmit power over tones, such that a maximum data rate is achieved with the available resources, i.e., for a given power budget and filter tap (run-time complexity) budget, and without violating the PSD mask constraint.

The Lagrange multipliers method is often used to convert a constrained optimization problem into a dual unconstrained problem [101, 24]. In this chapter, we propose two algorithms to optimally allocate the non-zero filter taps and transmit power over tones by solving the dual problem. The first approach is based on exhaustive search over all the pulse shaping filter order and is called contiguous tap selection based approach. The second approach uses sparse approximation to compute the sparse pulse shaping filters, hence we call it sparse approximation based approach.

The chapter is organized as follows: In **section 3.2**, the filter design criteria for a per-tone pulse shaping filter is presented. Additionally, an efficient DMT transmitter structure to incorporate the effect of per-tone pulse shaping filter is also given.

In **section 3.3**, optimization problem to allocate pulse shaping filter taps for a constant power loading scenario as well as joint pulse shaping filter tap and transmit power allocation scenario is formulated. In each case, it is shown that the dual problem formulation decouples the optimization problem in tones, hence reducing the computational complexity of the solution of the optimization problem.

In **section 3.4**, we then present algorithms to further reduce the computational complexity of the optimization problem derived in section 3.3. The first algorithm is based on restricting the sparsity pattern of the pulse shaping filter to allow only certain patterns, and it is called contiguous tap selection based approach. The second algorithm is based on sparse approximation based filter design and is called sparse approximation based approach.

In **section 3.5**, the two algorithm presented in section 3.4 is extended to include both filter tap and transmit power allocation problem formulated in section 3.3.

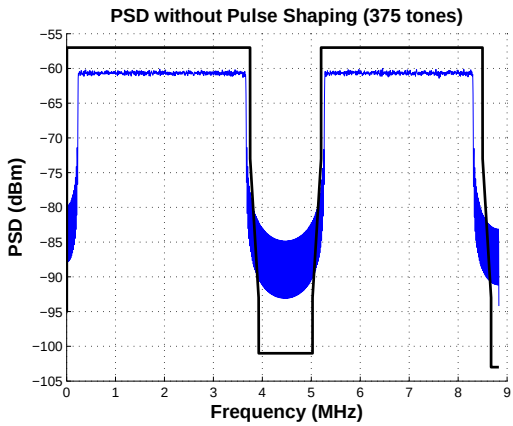

Figure 3.2: PSD of a VDSL system without any transmit pulse shaping

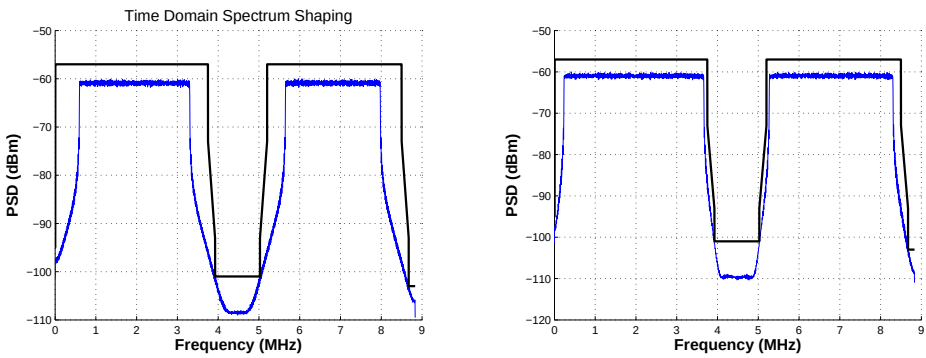

(a) (b)

Figure 3.3: PSD of a VDSL system (a) with time domain pulse shaping (b) with per-tone pulse shaping

In **section 3.6**, the simulation results are shown and conclusions are drawn in **section 3.7**.

3.2 System model

The following notation is adopted in the description of the DMT system. N is the IDFT-size and i denotes the tone index. C_{max} is the order of the pulse shaping

filters, ν is the cyclic prefix length. $\mathbf{x}_l$ is the output of the transmitter i.e. a vector of length $K = N + C_{max} + \nu$, corresponding to one transmitted symbol at time l.

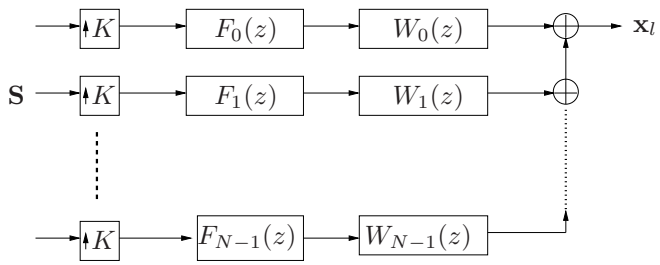

Figure 3.4: DMT transmitter with per-tone pulse shaping

Figure 3.4 shows the DMT transmitter structure with the per-tone pulse shaping as derived in [33]. The filters $F_i(z)$ are the DFT filters defined as

$$F_i(z) = \mathbf{e}^H(z)\mathbf{f}_i, \tag{3.1}$$

where $\mathbf{e}^H(z) = [1\ z^{-1} \cdots z^{N+\eta-1}]$, $\mathbf{f}_i = [f_i^0 \cdots f_i^{N+\eta-1}]$ and $f_i^l = e^{-j\frac{2\pi i}{N}(\eta-l)}$ for $l = 0 \cdots (N+\eta-1)$. The pulse shaping filters, $W_i(z)$, are designed using a minimum stop band energy criterion. For simplicity we will use FIR per-tone pulse shaping filters and adopt the following design criterion, presented in [33], for every filter $W_i(z)$:

$$\begin{aligned} &\underset{\mathbf{w}_i}{\text{minimize}} \quad (1-\beta)\int_{\omega\in\Omega_1} |F_i(e^{j\omega})W_i(e^{j\omega})|^2 d\omega + \beta\int_{\omega\in\Omega_2} |F_i(e^{j\omega})W_i(e^{j\omega})|^2 d\omega \\ &\text{subject to} \qquad W_i(e^{j\omega_i}) = 1 \end{aligned} \tag{3.2}$$

where Ω_1 represents the stop band frequencies, Ω_2 represents the pass band frequencies as defined by the PSD mask, $W_i(z) = \hat{\mathbf{e}}^H(z)\mathbf{w}_i$, $\hat{\mathbf{e}}^H(z) = \left[1\ z^{-1} \cdots z^{-C_{max}}\right]$, $\mathbf{w}_i = [w_i^0\ w_i^1\ \cdots\ w_i^{C_{max}}]^T$, $F_i(e^{j\omega})$ is the frequency response of the DFT filter $F_i(z)$ at frequency ω, $W_i(e^{j\omega})$ is the frequency response of the per-tone pulse shaping filter $W_i(z)$ at frequency ω_i, $\omega_i = \frac{2\pi i}{N}$ and β is a small constant $0 < \beta \ll 1$. The pass band term is included as a regularization term[33]. The design criterion can be restated as

$$\min_{\mathbf{w}_i} \quad \mathbf{w}_i^H \mathbf{Q}_i \mathbf{w}_i \quad \text{subject to} \quad W_i(e^{j\omega_i}) = 1 \tag{3.3}$$

where,

$$\mathbf{Q}_i = (1-\beta)\int_{\omega\in\Omega_1} |F_i(e^{j\omega})|^2 \hat{\mathbf{e}}(e^{j\omega})\hat{\mathbf{e}}^H(e^{j\omega})\ dz + \beta\int_{\omega\in\Omega_2} |F_i(e^{j\omega})|^2 \hat{\mathbf{e}}(e^{j\omega})\hat{\mathbf{e}}^H(e^{j\omega})\ dz$$

with $\hat{\mathbf{e}}^H(\omega) = [1\ e^{-j\omega} \cdots\ e^{-jC_{max}\omega}]$.

We will designpulse shaping filter under additional sparsity constraints, i.e, we will complement (3.2) or (3.3) with constraints

$$w_i^j = 0 \quad \text{if} \quad c_{ij} = 0 \quad \text{for } j = 0 \cdots C_{max}, \tag{3.4}$$

where the c_{ij}'s define the sparsity pattern, see section 3.3. The filter design problem given by (3.2) or (3.3) and (3.4) corresponds to a linearly constrained least squares problem, which is easily solved.

From **Figure 3.4** we can see that the transmitter output is

$$\mathbf{x}_l = \sum_i x_i \mathbf{f}_i \star \mathbf{w}_i \tag{3.5}$$

where, $\star$ denotes the convolution operation and s_i is the input symbol for tone i. In [33] it has been shown that this transmitter output can be generated cheaply based on

$$\mathbf{x}_l = \begin{pmatrix} \mathbf{0} & \mathbf{I}_\nu \\ \mathbf{I}_N & \\ \mathbf{0}_{C_{max} \times N} & \end{pmatrix} \mathbf{\Phi}^H \mathbf{D} \mathbf{x} + \sum_{i=0}^{N-1} \begin{pmatrix} -\alpha^{i(\nu+1)} \bar{\mathbf{v}}_i \\ \mathbf{0}_{(N+\nu-C_{max}) \times 1} \\ \alpha^i \bar{\mathbf{v}}_i \end{pmatrix} x_i. \tag{3.6}$$

Here $\mathbf{I}_k$ is the k by k identity matrix, $\mathbf{\Phi}^H$ is the IDFT matrix, $\mathbf{x} = [x_0 \cdots x_{N-1}]^T$ is the input symbol vector, $\alpha = e^{-j2\pi/N}$, $\mathbf{v}_i = \mathbf{U}_i \mathbf{w}_i$ and can be written as $[v_{i,0}\ \bar{\mathbf{v}}_i^T]^T$, $\mathbf{U}_i$ is an $(C_{max}+1)$ by $(C_{max}+1)$ upper triangular Toeplitz matrix whose first row is $[1\ \alpha^i \cdots \alpha^{iC_{max}}]$, $\mathbf{D}$ is a diagonal matrix with diagonal elements $[v_{0,0}\ v_{1,0} \cdots v_{N-1,0}]$ consisting of the first element of $\mathbf{v}_i$ for each i.

3.3 Problem formulation

In section 3.3.1, we first consider the problem of pulse shaping filter tap allocation under fixed power loading. In Section 3.3.2, we then consider the problem of joint pulse shaping filter tap allocation and power loading, to maximize the data rate under the PSD mask constraints.

3.3.1 Resource allocation for a fixed power loading

When the collection of tones to be used for transmission and the powers are fixed, the tap allocation in the pulse shaping filters does not affect the achievable bit-rate (cfr. the constraint in problem (3.2) and (3.3)). Hence, in this case we only need a procedure to optimally allocate the filter taps, such that the PSD mask constraints are fulfilled. For a given tap budget C_{budget}, we can write the resource allocation

problem as

$$\begin{aligned} \max_{\mathbf{C}} \quad & 0 \\ \text{subject to} \quad & \sum_{i\in\mathcal{I}}\sum_{j=0}^{C_{max}} C_{ij} \leq C_{budget} \\ & \mathbf{T}_{spec} \leq \mathbf{T}_{mask} \end{aligned} \tag{3.7}$$

where $\mathcal{I}$ is the set containing the indices of the used tones, $C_{ij} \in \{0,1\}$ defines the tap allocation i.e. C_{ij} is 1 if jth tap of the pulse shaping filter for tone i is selected and 0 otherwise, $\mathbf{c}_i = [C_{i0} \cdots C_{iC_{max}}]$ is the vector that represents the position of the non-zero pulse shaping filter taps for tone i and is referred to as the sparsity pattern of the pulse shaping filter, $\mathbf{C}$ is a matrix that has $\mathbf{c}_i$ as its ith row, C_{budget} is the predefined maximum total number of non-zero pulse shaping filter taps for all used tones, $\mathbf{t}_{mask}$ is the vector containing $\bar{M}$ sample points of the PSD mask at different frequencies and $\mathbf{t}_{spec}$ is the vector containing the similarly sampled PSD of the transmitter output. It is seen that (3.7) merely checks if the PSD mask constraint can be met with the given filter tap budget. This type of problem is known as a feasibility problem, which tests whether the constraints are mutually exclusive. Problem (3.7), amounts to a combinatorial selection and therefore is a non-convex problem. This problem is further complicated by the fact that the second constraint is coupled over tones. In order to simplify the optimization problem presented in (3.7) let us write it as the following equivalent constrained optimization problem

$$\boxed{\begin{aligned} \max_{\mathbf{C}} \quad & -\sum_{i\in\mathcal{I}}\sum_{j=0}^{C_{max}} C_{ij} \\ & \text{subject to} \quad \mathbf{t}_{spec} \leq \mathbf{t}_{mask} \end{aligned}} \tag{3.8}$$

If $\sum_{i\in\mathcal{I}}\sum_{j=0}^{C_{max}} C_{ij}$ is larger than C_{budget} after the maximization then the problem is considered infeasible. This optimization problem is still combinatorial and the constraint is still coupled over tones. The computational complexity of (3.8) is $\mathcal{O}(2^{M(C_{max}+1)})$, where M is the cardinality of the set $\mathcal{I}$ and denotes the total number of used tones. This is intractable even for moderate M and C_{max}. In order to solve this problem let us write the dual of the problem in 3.8 as

$$\min_{\lambda_1\cdots\lambda_{\bar{M}}} \left\{ \max_{\mathbf{C}} \left(\hat{\Psi} \right) \right\} \quad \text{subject to } \lambda_m \geq 0 \quad \text{for} \quad m = 1 \cdots \bar{M}, \tag{3.9}$$

where

$$\hat{\Psi} = -\sum_{i\in\mathcal{I}}\sum_{j=0}^{C_{max}} C_{ij} - \sum_{m=1}^{\bar{M}} \lambda_m (t_{mask,m} - t_{spec,m}). \tag{3.10}$$

Here, m is the index for the frequency samples, i.e. $t_{mask,m}$ and $t_{spec,m}$ correspond to the PSD samples at frequency ω_m.

With,

$$\begin{aligned} t_{spec,m} &= \sum_{i\in\mathcal{I}} s_i |F_i(e^{j\omega_m}) W_i(e^{j\omega_m)})|^2 \\ &= \sum_{i\in\mathcal{I}} s_i |F_i(e^{j\omega_m}) \hat{\mathbf{e}}^H(e^{j\omega_m}) \mathbf{w}_i|^2, \end{aligned} \tag{3.11}$$

where $s_i = E\{|x_i|^2\}$, and $\mathbf{w}_i$ is computed from the sparsity pattern $\mathbf{c}_i$ based on (3.3) and (3.4), we can rewrite equation (3.10) as,

$$\hat{\Psi} = -\sum_{i\in\mathcal{I}} \sum_{j=0}^{C_{max}} C_{ij} + \sum_{m=1}^{\bar{M}} \lambda_m \sum_{i\in\mathcal{I}} s_i |F_i(e^{j\omega_m}) \hat{\mathbf{e}}^H(e^{j\omega_m}) \mathbf{w}_i|^2 + \sum_{m=1}^{\bar{M}} \lambda_m t_{mask,m} \tag{3.12}$$

which is equivalent to

$$\hat{\Psi} = \sum_{i\in\mathcal{I}} \left\{ -\sum_{j=0}^{C_{max}} C_{ij} + \sum_{m=1}^{\bar{M}} \lambda_m s_i |F_i(e^{j\omega_m}) \hat{\mathbf{e}}^H(e^{j\omega_m}) \mathbf{w}_i|^2 \right\} + \underbrace{\sum_{m=1}^{\bar{M}} \lambda_m t_{mask,m}}_{\text{constant for a given } \lambda_m} \tag{3.13}$$

For a fixed Lagrange multipliers λ_m, the term $\sum_{m=1}^{\bar{M}} \lambda_m T_{mask,m}$ is constant and therefore the optimization problem is effectively decoupled over tones, and can be written for each tone as,

$$\boxed{\max_{\mathbf{c}_i} \quad \hat{\psi}_i(\Lambda)}$$

$$\hat{\psi}_i(\Lambda) = -\sum_{j=0}^{C_{max}} C_{ij} + \sum_{m=1}^{\bar{M}} \lambda_m s_i |F_i(e^{j\omega_m}) \hat{\mathbf{e}}^H(e^{j\omega_m}) \mathbf{w}_i|^2 \tag{3.14}$$

where Λ is a vector containing all $\lambda'_m s$. This per-tone optimization problem can be solved by exhaustively searching over all possible $\mathbf{c}_i$'s. The Lagrange multipliers can then be updated until all the PSD constraints are met. Even though the problem is now decoupled over tones, it is still combinatorial for each tone. The computational complexity now is $\mathcal{O}(M2^{(C_{max}+1)})$ per update of the Lagrange multipliers, which is still very high for practical values of C_{max}. In section 3.4, we will present efficient algorithms to reduce this complexity.

In the following section, optimal transmit power allocation will also be considered along with the pulse shaping filter tap allocation.

3.3.2 Joint pulse shaping filter tap and transmit power allocation

To maximize the data rate of a single-user DMT system under a total power constraint, the optimal per-tone transmit power can be calculated by using the water filling procedure [40]. With additional PSD constraints this is no longer applicable. In the previous section, the pulse shaping filter tap allocation problem was formulated when the collection of used tones and their transmit powers are known was formulated for a system with PSD constraints. However, the number of used tones can possibly be increased if a lower transmit power at the band edges is used. Therefore by also allocating the appropriate amount of transmit power for each tone the total achievable data rate can be maximized for a given total transmit power budget. This then requires a procedure to allocate the available resources, i.e., transmit power and pulse shaping filter tap, efficiently over tones such that the achievable bit-rate is maximized and the PSD mask constraints are met. The corresponding constrained optimization problem can be written as

$$\begin{aligned} \underset{\mathbf{C},\mathbf{S}}{\text{maximum}} \quad & \sum_{i\in\mathcal{I}} R_i \\ \text{subject to} \quad & \mathbf{t}_{spec} \leq \mathbf{t}_{mask} \\ & \sum_{i\in\mathcal{I}} \sum_{j=0}^{C_{max}} C_{ij} \leq C_{budget} \\ & \sum_{i\in\mathcal{I}} s_i \leq S_{budget} \\ & 0 \leq s_i \leq S_{max,i} \end{aligned} \tag{3.15}$$

where R_i is the achieved bit rate for tone i which is given as

$$R_i = log_2(1 + \frac{SNR_i}{\Gamma}),$$

SNR_i is the signal-to-noise ratio of tone i, Γ is the SNR gap, $\mathbf{S}$ is the matrix containing all the possible transmit power allocation, S_{budget} is the total transmit power budget, $s_i \in \mathcal{S}$ is the transmit power allocated to tone i, $\mathcal{S}$ is the set containing all the allowed discrete power levels, $S_{max,i}$ is the maximum transmit power allowed for tone i. All the other quantities are as in section 3.3.1. Optimization problem (3.15) is coupled over tones and is a combinatorial problem. It has a computational complexity of $\mathcal{O}(\tilde{L}^M 2^{M(C_{max}+1)})$, where $\tilde{L}$ is the cardinality of set $\mathcal{S}$ and M is the cardinality of set $\mathcal{I}$. This is intractable even for moderate $M, \tilde{L}$ and C_{max}. In the previous section, it was shown that the dual problem formulation possibly leads to the decoupling of the problems over tones.

Therefore, in order to reduce the computational complexity, we will also formulate a dual problem of (3.15). The dual optimization problem can be written as

$$\min_{\gamma,\alpha,\Lambda}\left\{\max_{\mathbf{C},\mathbf{S}}(\Psi)\right\}$$

where,

$$\Psi = \sum_{i\in\mathcal{I}} R_i + \gamma\left(C_{budget} - \sum_{i\in\mathcal{I}}\sum_{j=0}^{C_{max}} C_{ij}\right) + \alpha\left(S_{budget} - \sum_{i\in\mathcal{I}} s_i\right) + \sum_{m=1}^{\bar{M}} \lambda_m(t_{mask,m} - t_{spec,m})$$

$$\text{and} \qquad \alpha,\gamma,\lambda_j > 0 \tag{3.16}$$

The last constraint in (3.15) may be excluded from the dual formula since it can be implicitly imposed by reducing $\mathcal{S}$ in each per-tone minimization problem, as defined next.

For fixed Lagrange multipliers the optimization problem is again decoupled over tones, and by substituting (3.11), can be written for each tone as,

$$\max_{\mathbf{c}_i,s_i} \quad \psi_i(\gamma,\alpha,\Lambda),$$

where

$$\psi_i(\gamma,\alpha,\Lambda) = R_i - \gamma\sum_{j=0}^{C_{max}} C_{ij} - \alpha s_i - \sum_{m=1}^{\bar{M}} \lambda_j s_i |F_i(e^{j\omega_m})\hat{\mathbf{e}}^H(e^{j\omega_m})\mathbf{w}_i|^2 \tag{3.17}$$

The computational complexity now reduces to $\mathcal{O}(M\tilde{L}_s 2^{(C_{max}+1)})$ per update of the Lagrange parameters which is still very high for practical values of C_{max}.

In section 3.5, we will present efficient algorithms to reduce this complexity.

3.4 Resource allocation for a fixed power loading

3.4.1 Contiguous filter tap selection based resource allocation

Here we present an approach that is based on (3.14) to further reduce the computational complexity. Let us restate (3.14) again for convenience as

$$\boxed{\max_{\mathbf{c}_i} \quad \hat{\psi}_i(\Lambda)}$$

$$\hat{\psi}_i(\Lambda) = -\sum_{j=0}^{C_{max}} C_{ij} + \sum_{m=1}^{\bar{M}} \lambda_m s_i |F_i(e^{j\omega_m})\hat{\mathbf{e}}^H(e^{j\omega_m})\mathbf{w}_i|^2 \tag{3.18}$$

The computational complexity of the (3.18) is $\mathcal{O}(M2^{C_{max}+1})$. The computational complexity can be reduced by restricting the sparsity pattern of the pulse shaping filter such that only contiguous taps can be non-zero. We will call this *contiguous tap selection* (CTS) approach. Thus the combinatorial search over all the sparsity patterns is reduced to the linear search in the filter order. This can be written as

$$\boxed{\max_{L_i} \quad \hat{\psi}_i(\Lambda)} \tag{3.19}$$

$$\hat{\psi}_i(\Lambda) = -L_i - \sum_j \lambda_j s_i |F_i(e^{j\omega_j})\mathbf{e}^H(\omega_j)\mathbf{w}_i|^2, \tag{3.20}$$

where L_i is the filter order on tone i. The values of Lagrange multipliers can then be updated until all the PSD constraints are met.

An algorithm description is given below. The computational complexity is thus reduced to $\mathcal{O}(M(C_{max}+1))$ from $\mathcal{O}(M2^{C_{max}+1})$. The Lagrange multipliers, λ_j are updated based on the difference between the PSD mask and the output PSD, i.e.

$$\lambda_j^{t+1} = \lambda_j^t - \mu_j(T_{mask,j} - T_{spec,j}) \tag{3.21}$$

where μ_j is the step size for the update which is always positive. The μ_j can be varied in order to drop the energy at a frequency point quickly if the output spectrum at that frequency exceeds the PSD mask and to cautiously increase it

if the output spectrum is under the PSD mask. A typical initialization value for $\mathbf{\Lambda} = \{\lambda_j\}$ is $\mathbf{0}$ and then $\mu = \{\mu_j\}$ can be initialized with a value generally much larger than 1 as we need to establish a very high value for $\mathbf{\Lambda}$ in order to make the $\sum_j \lambda_j s_i |F_i(\omega_j)\mathbf{e}^H(\omega_j)\mathbf{w}_i|^2$ comparable to the value L_i. The algorithm stops when the number of taps stops updating.

Algorithm 3.1 Optimization of pulse shaping filter lengths

1: Initialize $\mathbf{\Lambda}$,μ
2: **repeat**
3: **for** tone $i \in \mathcal{I}$ **do**
4: **for** filter order $L_i = 0 \cdots L_{max}$ **do**
5: compute $\mathbf{w}_i$ (equation 1)
6: $\hat{\psi}_i \underset{\text{argmax}}{\Leftarrow} \{-L_i - \sum_j \lambda_j s_i |F_i(\omega_j)\mathbf{w}_i(\omega_j)|^2\}$
7: **end for**
8: **end for**
9: compute $\mathbf{T}_{spec}$
10: **for** $j = 1 \cdots M$ **do**
11: $\lambda_j^{t+1} = \lambda_j^t - \mu_j(T_{mask,j} - T_{spec,j})$
12: **if** $\lambda_j^{t+1} < 0$ **then**
13: $\lambda_j^{t+1} = 0$
14: **end if**
15: **end for**
16: **until** (change in filter taps)

It is important to note that an analytical expression for the duality gap will be difficult to obtain. Therefore, it should be noted that the solution obtained from the dual problem formulation after the constraint relaxation may not be the globally optimal solution of the primal problem but nevertheless the procedure is found to provide practically relevant solutions (see section 3.6).

3.4.2 Sparse approximation based resource allocation

3.4.3 Computing sparse pulse shaping filters

From the previous section, it is clear that if we can somehow control the possible sparsity patterns of the pulse shaping filters, the computational complexity of the per-tone optimization problem will be reduced significantly. In section 3.4.1, the sparsity pattern of the pulse shaping filter was restricted to combinations where only contiguous taps can be non-zero thus reducing the computational complexity from the combinatorial search to a linear search in the filter orders. However, restricting the sparsity pattern may not be the best approach. Since, the best

sparsity pattern may not be on the restricted search space. In order to find a better way to control the sparsity pattern, let us write the problem of designing a pulse shaping filter (3.3) as a sparse approximation problem[150], i.e.

$$\min_{\mathbf{w}_i} \quad \mathbf{w}_i^H \mathbf{Q}_i \mathbf{w}_i + \tau \left\|\mathbf{w}_i\right\|_0 \quad \text{subject to} \quad W_i(e^{j\omega_i}) = 1, \tag{3.22}$$

where

$$\mathbf{Q}_i = (1-\beta) \sum_{\omega \in \Omega_1} |F_i(e^{j\omega})|^2 \hat{\mathbf{e}}(\omega)\hat{\mathbf{e}}^H(\omega)\lambda_\omega + \beta \sum_{\omega \in \Omega_2} |F_i(e^{j\omega})|^2 \hat{\mathbf{e}}(\omega)\hat{\mathbf{e}}^H(\omega)\lambda_\omega$$

Here $\|.\|_0$ is known as the ℓ_0 quasi-norm, which basically counts the number of non-zero elements of the vector in the argument, λ_ω is the Lagrange multiplier corresponding to frequency sample ω, ω_i is the frequency sample at the i-th tone and τ controls the trade off between the sparsity and the quadratic term. Note that the integral in (3.3) have been replaced by summations over the frequency samples ω, and that the Lagrange parameters have been introduced as additional weight factor. Problem (3.22) is however known to be a NP hard in general. To simplify (3.22) the non-convex ℓ_0 quasi-norm is often replaced by the convex ℓ_1 norm [150]. This can be written as

$$\min_{\mathbf{w}_i} \quad \mathbf{w}_i^H \mathbf{Q}_i \mathbf{w}_i + \bar{\tau} \left\|\mathbf{w}_i\right\|_1 \quad \text{subject to} \quad W_i(e^{j\omega_i}) = 1, \tag{3.23}$$

where now $\bar{\tau}$ controls the trade off between the sparsity and the quadratic term. (3.23) is a convex problem and can be solved using any generic solver in polynomial time [24]. If the underlying system admits a sparse solution, it has been shown that solving (3.23) is equivalent to solving (3.22) [150]. In our case, the underlying system does not necessarily admit sparse solution, therefore we can not obtain a sparse pulse shaping filter by just solving (3.23). One way to obtain a sparse pulse shaping filter is to adopt a two steps procedure. Firstly, we use (3.23) for a given $\bar{\tau}$ to obtain a nearly-sparse pulse shaping filter and then force the coefficients below a certain threshold level ρ_i to zero. Secondly, we use the sparsity pattern obtained after applying the threshold and we compute the pulse shaping filter using (3.3) and (3.4). It is clear that the choice of the trade off parameter $\bar{\tau}$ and the threshold ρ_i is important for the algorithm to work properly. An efficient update rule for these parameter is based on the difference between the total available system resources and the used system resources for the current value of $\bar{\tau}$. This can be written as

$$\bar{\tau}^{t+1} = \left[\bar{\tau}^t - \mu(C_{\text{budget}} - \sum_{i \in \mathcal{I}} \left\|\mathbf{w}_i\right\|_0)\right]^+, \tag{3.24}$$

where $\bar{\tau}^c$ is the value of $\bar{\tau}$ at cth iteration, μ is a step size parameter and $[a]^+$ is max(0,a). We can either use a fixed threshold or we can also update the threshold

in order to speed up the algorithm. The update formula for the threshold can be written as

$$\rho_i^{t+1} = \left[\rho_i^t - \bar{\mu}(C_{\text{budget}} - \sum_{i \in \mathcal{I}} \|\mathbf{w}_i\|_0)\varepsilon_i^{-1} \right]^+, \tag{3.25}$$

where ε_i is a normalization and is equal to $\mathbf{w}_i^H \mathbf{Q}_i \mathbf{w}_i$.

3.4.4 Sparse approximation based pulse shaping filter tap allocation approach

Let us rewrite the per-tone dual optimization problem under the fixed power loading (3.14) as

$$\hat{\psi}_i(\Lambda) = -\|\mathbf{w}_i\|_0 + \sum_{m=1}^{\bar{M}} \lambda_m s_i |F_i(e^{j\omega_m}) \hat{\mathbf{e}}^H(e^{j\omega_m}) \mathbf{w}_i|^2, \tag{3.26}$$

where $\|\mathbf{w}_i\|_0 = \sum_{j=0}^{C_{max}} C_{ij}$. Since we compute the sparsity pattern $\mathbf{c}_i$ directly using (3.23) and then applying the threshold, there is no need to maximize the objective function given in (3.26). For given λ_m, $\bar{\tau}$ and ρ_i, the problem reduces to computing $\mathbf{w}_i$ for different $i \in \mathcal{I}$ and then checking if the PSD mask constraints and the filter tap budget constraint are met. An algorithm description is given in **Alg. 1**. The complexity of the proposed algorithm is then $O(M * \kappa)$ per update of Lagrange multipliers, where κ is the cost associated with computing the nearly-sparse filter and then a sparse filter for one tone. For large C_{max}, $\kappa \approx C_{max}$, therefore the computational complexity for sparse approximation based pulse shaping filter tap allocation under fixed power loading is similar to the exhaustive search based contiguous tap selection approach in section 3.4.1. The Lagrange multipliers, λ_j are updated based on the difference between the PSD mask and the output PSD, i.e.

$$\lambda_m^{t+1} = \left[\lambda_m^t - \hat{\mu}_m (T_{mask,m} - T_{spec,m}) \right]^+ \tag{3.27}$$

where $\hat{\mu}_m$ is the step size parameter for the update, which is always positive. The $\hat{\mu}_m$ can be varied in order to speed up the algorithm. A typical initialization value for $\mathbf{\Lambda} = \{\lambda_m\}$ is $\mathbf{0}$ and then $\hat{\mu} = \{\hat{\mu}_m\}$ can be initialized with a value generally much larger than 1. The algorithm stops when the number of taps stops updating.

In the next section, the algorithms discussed in this section will be extended in order to jointly allocate the pulse shaping filter tap and transmit power.

Algorithm 3.2 Sparse approximation based per-tone pulse shaping filter taps with fixed power loading

Initialize $\mathbf{\Lambda}$, $\bar{\tau}$, ρ, $\hat{\mu}$, μ, $\bar{\mu}$
repeat
  for tone $i \in \mathcal{I}$ **do**
    compute nearly-sparse $\mathbf{w}_i$ solving (3.23)
    apply threshold ρ_i and obtain sparsity pattern $\mathbf{c}_i$
    compute sparse $\mathbf{w}_i$ solving (3.3) for the given sparsity pattern $\mathbf{c}_i$
  end for
  compute $\mathbf{T}_{spec}$
  update Λ using (3.21)
  update $\bar{\tau}$ using (3.24)
  update ρ_i using (3.25)
until (change in filter taps)

3.5 Joint pulse shaping filter tap and transmit power allocation

3.5.1 Contiguous tap selection based approach

Here, we present an approach that is based on a dual problem formulation presented in (3.16). For convenience, let us rewrite the dual problem below

$$\min_{\gamma,\alpha,\Lambda} \left\{ \max_{\mathbf{C},\mathbf{S}} (\Psi) \right\}$$

where,

$$\Psi = \sum_{i\in\mathcal{I}} R_i + \gamma \left(C_{budget} - \sum_{i\in\mathcal{I}} \sum_{j=0}^{C_{max}} C_{ij} \right) + \alpha \left(S_{budget} - \sum_{i\in\mathcal{I}} s_i \right)$$

$$+ \sum_{m=1}^{\bar{M}} \lambda_m (t_{mask,m} - t_{spec,m})$$

$$\text{and} \qquad \alpha, \gamma, \lambda_j > 0 \tag{3.28}$$

we can restrict the sparsity pattern of the pulse shaping filter as suggested for contiguous tap selection in previous section. Therefore, we can rewrite (3.28) as

$$\boxed{\max_{L_i, s_i} \quad \psi_i(\gamma, \alpha, \Lambda)} \tag{3.29}$$

$$\psi_i(\gamma, \alpha, \Lambda) = R_i - \gamma L_i - \alpha s_i - \sum_j \lambda_j s_i |F_i(e^{j\omega_j}) \mathbf{e}^H(\omega_j) \mathbf{W}_i|^2 \tag{3.30}$$

This per-tone optimization problem can be solved (for fixed Lagrange multiplier) by exhaustively searching over all values of s_i (i.e. from -140dBm to s_{max}(-60dBm) in discrete steps)and all the other quantities are as defined in section 3.4. The values of the Lagrange multipliers can then be updated until all the constraints are met. An algorithm description is given below. The complexity of the proposed algorithm is $O(N * \tilde{L} * C_{max})$.

The Lagrange multipliers (γ, α and λ) are updated based on the difference between the obtained values for the corresponding resources and their target values, i.e.

$$\lambda_j^{t+1} = \lambda_j^t - \mu_j (t_{mask,j} - t_{spec,j})$$

$$\gamma_i^{t+1} = \gamma_i^t - \hat{\mu} (C_{budget} - \sum_i L_i)$$

$$\alpha_i^{t+1} = \alpha_i^t - \bar{\mu} (S_{budget} - \sum_i s_i)$$

where μ_j, $\hat{\mu}$ and $\bar{\mu}$ are the step sizes for the updates which are always positive.

3.5.2 Sparse approximation based approach

We can rewrite the per-tone optimization problem for the joint per-tone pulse shaping filter tap allocation and power loading given in (3.17) as

$$\psi_i(\alpha, \Lambda) = R_i - ||\mathbf{w_i}||_0 - \alpha s_i - s_i \underbrace{\sum_{m=1}^{\bar{M}} \lambda_m |F_i(e^{j\omega_m}) \mathbf{e}^H(\omega_m) \mathbf{w}_i|^2}_{a} \tag{3.31}$$

Since, we fix the sparsity pattern of $\mathbf{w}_i$ using (3.23) and then applying the threshold, for a fixed Lagrange multipliers Λ, α and γ, the per-tone optimization problem (3.31) can be solved by exhaustively searching over only all possible discrete power levels s_i. Since the minimization of the weighted energy of the filter (a in (3.31)) is not power dependent, i.e. the minimization can be performed on a normalized filter and then multiplied by the power, we need to compute the

Algorithm 3.3 Joint resource allocation algorithm

λ, α, γ, $\mu_{\mathbf{j}}$, $\bar{\mu}$, $\hat{\mu}$
repeat
  for tone $i \in \mathcal{I}$ **do**
    for filter order $L_i = 0 \cdots L_{max}$ **do**
      compute W_i (equation 1)
      for power level $s_i = 0 \cdots s_{max}$ **do**
        $\psi_i \underset{\text{argmax}}{\Leftarrow} \{R_i - \gamma L_i - \alpha s_i - \sum_j \lambda_j s_i |F_i(\omega_j)\mathbf{e}^H(\omega_j)\mathbf{w}_i|^2\}$
      end for
    end for
  end for
  compute $\mathbf{T}_{spec}$
  for $j = 1 \cdots M$ **do**
    $\lambda_j^{t+1} = \lambda_j^t - \mu_j(T_{mask,j} - T_{spec,j})$
  end for
  $\gamma^{t+1} = \gamma^t - \hat{\mu}(L_{max} - \sum_i L_i)$
  $\alpha^{t+1} = \alpha^t - \bar{\mu}(s_{max} - \sum_i P_i)$
until (change in filter taps and used power)

sparse filter only once at the beginning. The per-tone objective function in (3.31) for a given sparse per-tone pulse shaping filter can be rewritten as

$$\psi_i(\alpha, \Lambda) = R_i - s_i(\alpha + a). \tag{3.32}$$

Here $\|\mathbf{w}_i\|_0$ is a constant, hence it can be removed from the optimization problem. By fixing the sparsity pattern using the sparse approximation technique, the total computational complexity is $\mathcal{O}(M\tilde{L} + \kappa)$ per Lagrange multiplier iteration in contrast to $\mathcal{O}(M\tilde{L}(C_{max} + 1))$ per Lagrange multiplier iteration. For large C_{max} this is a significant reduction in computational complexity. The values of the Lagrange multipliers can then be updated until all the constraints are met. An algorithm description is given below in **Alg. 2**. The Lagrange multiplier λ_m could be updated using (3.21) and Lagrange multiplier α can be updated based on the difference between the obtained values for the corresponding resources and their target values, i.e.

$$\alpha_i^{t+1} = \left[\alpha_i^t - \tilde{\mu}(S_{budget} - \sum_{i \in \mathcal{I}} s_i)\right]^+ \tag{3.33}$$

where $\tilde{\mu}$ is a positive step size.

Algorithm 3.4 Sparse approximation based joint resource allocation algorithm

Initialize $\mathbf{\Lambda}$, α, $\bar{\tau}$, ρ $\bar{\mu}$, $\hat{\mu}$, $\tilde{\mu}$
repeat
  for tone $i \in \mathcal{I}$ **do**
    compute a sparse $\mathbf{w}_i$ using (3.23), ρ_i, and (3.3)
    compute a using (3.31)
    for power level $s_i = 0 \cdots s_{max,i}$ **do**
      $P_{opt,i} \underset{\text{argmax}}{\Leftarrow} \{R_i - s_i(\alpha + a)\}$
    end for
  end for
  compute $\mathbf{t}_{spec}$ using $S_{opt,i}$
  update $\mathbf{\Lambda}$ using (3.21)
  update α using (3.33)
  update $\bar{\tau}$ using (3.24)
  update ρ using (3.25)
until (change in filter taps and used power)

3.6 Simulation results

In our simulations, we consider VDSL downstream transmission with a PSD mask corresponding to the FTTCab M1 deployment scenario [10]. The size of the IDFT is 1024, the cyclic prefix length plus the overhead due to the maximum pulse shaping filter order per tone C_{max} is 80 samples and the SNR gap $\Gamma = 9.8$ dB. We use $C_{max} = 17$ to be able to compare our results to [33]. The initial values are $\lambda_j = 0$, $\alpha = 0$, $\hat{\mu}_m = 1e8$, $\bar{\mu} = 1$ and $\hat{\mu} = 1e-7$, $\bar{\tau} = 0$ and $\rho_i = 0$.

3.6.1 Resource allocation for a fixed power loading

In the first simulation, the channel under consideration here is a 400m twisted pair cable in a bundle of 8 with an interference channel of 400m. We fix the tones used for transmission as suggested in [33], i.e., 375 predefined tones. **Figure 3.6(a)** shows the pulse shape filter tap distribution by using contiguous tap selection based approach. It can be seen that the tones at the band edges uses filters with higher order than the tones at the middle of the band. **Figure 3.5(a)** shows that the total number of pulse shaping filter taps can be reduced significantly without violating the PSD mask constraint by using the contiguous tap selection based pulse shaping filter tap allocation. The total required number of pulse shaping filter taps reduces from 6735 (17*375) taps to 3787 taps,i.e., 40% reduction. In **Figure 3.5(b)**, it is seen that the pulse shaping filter taps can be further reduced by using the sparse approximation based approach to 3509 taps. From **Figure 3.5(a)** and **b**, it can be seen that sparse approximation based approach aslo converges faster than the

contiguous tap selection based approach. Therefore, we can conclude that sparse approximation based approach provides a better solution at a lower computational complexity. The sparse approximation problem as formulated in (3.23) is solved using the `CVX` software for solving convex programs [66]. The distribution of pulse shaping filter taps over the 375 used tones for both algorithms is shown in **Figure 3.6(b)**. It is observed that the total number of taps is significantly smaller than 6375(=17*375), when a fixed pulse shaping filter of length 17 is used for all 375 tones as in [33]. **Figure 3.7** show the corresponding transmit PSD and the PSD mask.

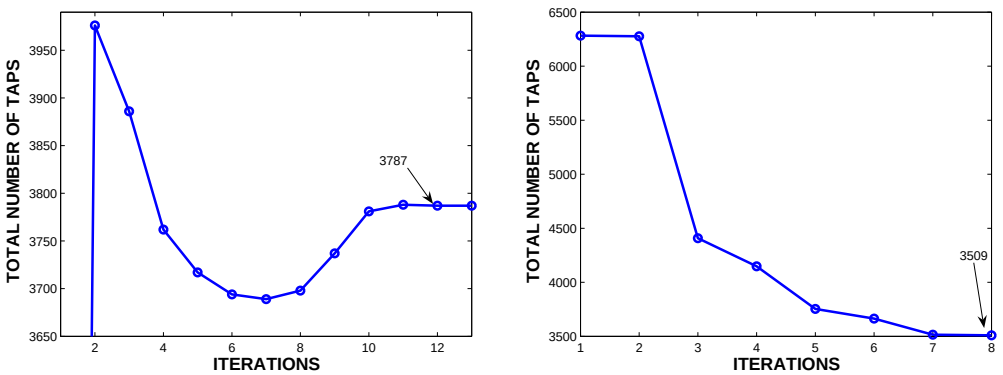

(a) (b)

Figure 3.5: Convergence of total number of pulse shaping filter taps using (a) the contiguous tap selection based approach (b) the sparse approximation based approach

3.6.2 Joint pulse shaping filter tap and transmit power allocation

The channel under consideration is identical to the fixed powerloading scenario. However, we now make all 428 tones available for transmission (instead of only 375 tones). The total available power is 11.5 dBm [10], which is greater than the total power needed to transmit maximum power −60 dBm/Hz on all tones, i.e., 8.682 dBm. **Figure 3.8** shows the observed transmit PSD for the case of 5000 pulse shaping filter taps for a contiguous tap selection based approach and sparse approximation based approach. It can be seen that both the contiguous tap selection based approach and the sparse approximation based approach can use the tones at the band edges more efficiently. But sparse approximation based approach outperforms the contiguous tap selection based approach. The tap distribution over tones for both approaches is presented in **Figure 3.9** for both the approaches. **Table 3.1** shows that the number of iterations taken for the algorithm to converge

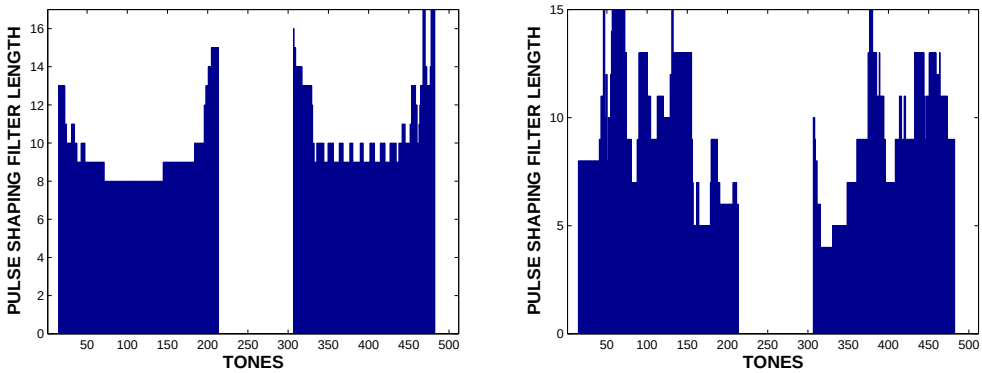

(a) (b)

Figure 3.6: Optimum distribution of number of pulse shaping filter taps over tones using (a) the contiguous tap selection based approach (b) the sparse approximation based approach

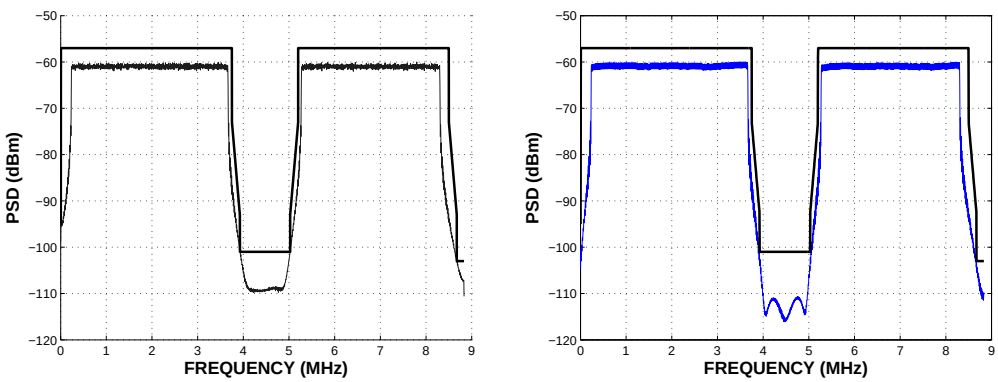

(a) (b)

Figure 3.7: Transmit PSD for (a) the contiguous tap selection based approach (b) the sparse approximation based approach

for the different pulse shaping filter tap budgets are similar for both approaches. Hence we can conclude that the over all complexity for the sparse approximation based approach is smaller than for the contiguous tap selection based approach. It is obvious that if the resources are scarce, the algorithm requires a larger number of iterations, as it is then harder to distribute the resources optimally.

In **Figure 3.10** we compare the achieved bit-rates. Since the total available

Total filter taps	CTS based approach	SA based approach
5000	12	10
1000	20	21

Table 3.1: Number of outer iterations taken to converge to the solution

transmit power is always larger than the total transmit power needed, we compare our results only for different total pulse shaping filter taps constraints. We can see that the sparse approximation based approach performs better than the contiguous tap selection based approach. It can be seen that the sparse approximation based approach utilizes the tones at the band edges more efficiently and hence the overall performance is increased. We also compare our results with two extreme cases. The first case is when there are no resource constraints (i.e. maximum allowed transmit power and maximum pulse shaping filter taps on all 428 used tones), which results in the dotted line in the **Figure 3.10**. The second case is when only 375 tones are used and maximum transmit power is used for all these tones as in [33] (dashed line with + marker in the **Figure 3.10**). It can also be seen that the achieved rate for the sparse approximation based approach is consistently larger than for the contiguous tap selection based approach. Furthermore, the sparse approximation based approach achieves the performance of case 2 [33] with much less (3000 vs 37*17=6325 taps) resources.

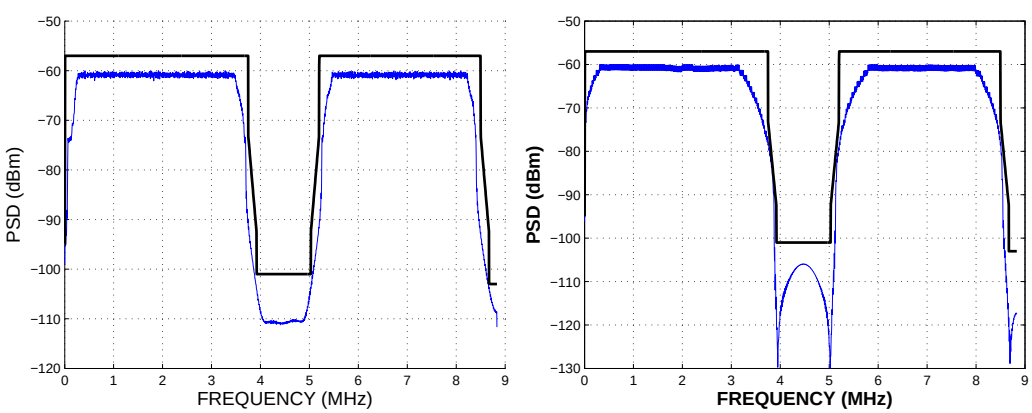

(a) (b)

Figure 3.8: Transmit PSD (5000 filter taps) for(a) the contiguous tap selection based approach, (b) the sparse approximation based approach

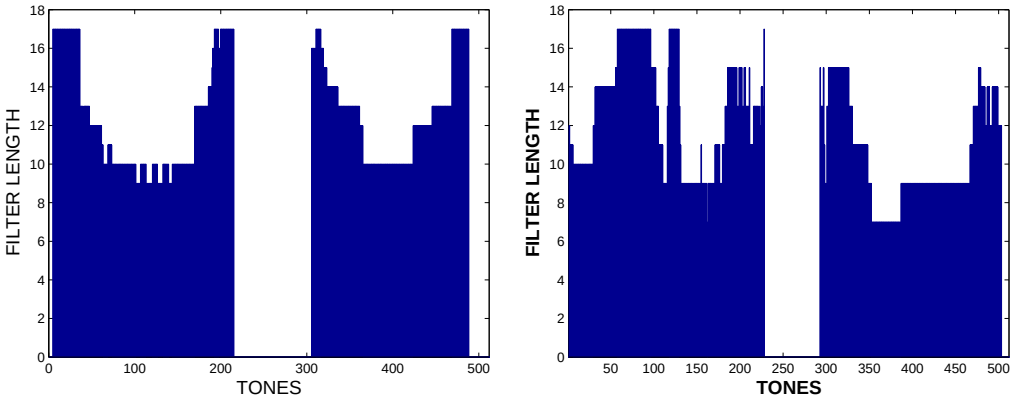

(a) (b)

Figure 3.9: Pulse shaping filter tap distribution (5000 taps) for (a) the contiguous tap selection based approach, (b) the sparse approximation based approach

3.7 Conclusion

In this chapter, it was shown that the use of per-tone pulse shaping decreases the number of virtual carriers on the band edges, thus increasing the achievable bit rate of the DMT system. Furthermore, it was also shown that using a constant length non-sparse pulse shaping filter on every tone unnecessarily increases the run-time complexity of the system. Therefore, using variably sparse pulse shaping filter on each tone reduces the run-time complexity without affecting the performance significantly.

To this end, we have proposed efficient resource allocation algorithms to distribute the available resources (total transmit power budget and total per-tone pulse shaping filter tap budget) over tones in a DMT transmitter with per-tone pulse shaping. We have shown that a dual problem formulation leads to an unconstrained optimization problem that is decoupled over tones but due to the combinatorial nature of the filter tap allocation the resulting optimization problem is still NP hard.

We proposed two approaches to further simplify the problem. First, by restricting the filter sparsity pattern such that only contiguous taps is allowed to be non-zero hence the combinatorial search in the sparsity pattern is reduced to the linear search in filter order. Second, by using sparse approximation technique to design the sparse pulse shaping filter directly. Using convex relaxation of the sparsity constraints, the sparse filter design problem can be written as convex problem and solved efficiently. Furthermore, the techniques were also extended to jointly

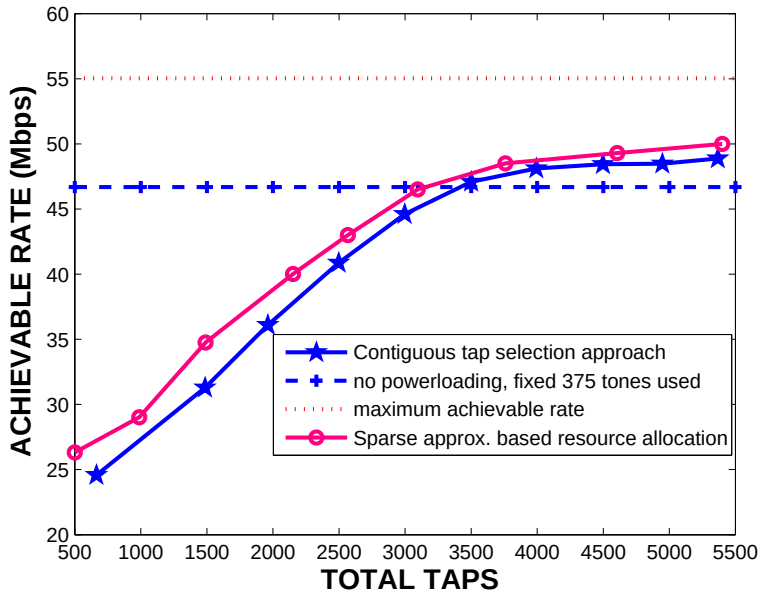

Figure 3.10: Relation of data rate and the total number of available resources

allocate pulse shaping filter taps and the transmit power.

A VDSL simulation demonstrates that under a fixed power loading, the number of pulse shaping filter taps can be reduced to approximately 40% compared to the fixed length non-sparse case without sacrificing performance. Furthermore, we also showed that the sparse approximation based per-tone pulse shaping filter tap allocation approach performs better than the contiguous tap selection based approach. When combined with an transmit power loading algorithm these approaches can further reduce the number of per-tone pulse shaping filter taps needed to achieve the same bit-rate performance.

Chapter 4

Resource allocation in DMT receiver with per-tone equalization

4.1 Introduction

Dispersive channel such as DSL channel results in ISI. In order to remove ISI a guard period is inserted between two DMT symbols known as cyclic prefix (CP). CP allows for an easy channel equalization at the DMT receiver. However, if the CP is shorter than the CIR then this results in ISI and ICI. Highly dispersive channels such as DSL channel have a very long CIR, hence to mitigate ISI/ICI a very long CP is needed. As a long CP results in a large transmission overhead, channel equalization is used to shorten the effective length of the CIR [44] [18]. The usual time domain equalization (TEQ) [8] then corresponds to a joint equalization of all the tones and hence cannot optimize the performance in each and every tone. An alternative frequency domain equalization technique, known as per-tone equalization (MMSE-PTEQ), was proposed in [2] in order to equalize each tone separately. It is then possible to optimize the bit rate performance of the receiver using a suitable multitap equalizer for every tone, even without increasing the overall run-time computational complexity. For a detailed comparison of several equalizer architectures, we refer to [97, 96].

In a per-tone equalization based DSL system, typically every tone is equalized using a constant length non-sparse equalizer. However the DSL channel is frequency selective, therefore the channel gain varies for different tones, and so

for a tone with low channel gain using a long equalizer does not improve its bit rate performance significantly. Furthermore, due to the presence of transmit and receiver filtering effect, the tones at the band edges require longer equalizers [1]. Therefore, using a constant length non-sparse equalizer for all tones may correspond to a increase in run-time complexity without much performance improvement. A better approach is then to consider variably sparse MMSE-PTEQ filter, where each tone employs a MMSE-PTEQ filter with different degree of sparsity, on each tone. One of the main challenges then is to allocate the non-zero MMSE-PTEQ filter taps for each tone without affecting the overall performance. In [171, 172], the order of the equalizer is determined by minimizing the MSE (Mean Squared Error) of the equalizer outputs. While the method tries to minimize the MSE for every tone, it does not provide a way to incorporate global resource constraints in the algorithm. Hence an alternative method to distribute the non-zero equalizer taps which incorporates global resource constraints in the optimization problem is needed.

For a given constraint (total number of equalizer taps and total power), the overall bit rate optimization problem can be written as a dual problem using Lagrange multipliers. In this chapter, we will propose two algorithms to determine the optimal equalizer taps and transmit power allocation over the tones by solving this dual problem. The first approach is based on exhaustive search over all the MMSE-PTEQ filter order and is called contiguous tap selection based approach. The second approach is based on sparse approximation and is called sparse approximation based approach.

The chapter is organized as follows: In **section 4.2**, a basic data model of the received DMT signal is described and per-tone equalization in DSL is reviewed.

In section **4.3**, optimization problem for allocating the resources under a global resource constraint (total number of equalizer taps) is formulated for both constant power loading scenario and the with the optimal power loading. It is then shown that the original optimization problem can be decoupled into per-tone optimization problem using dual problem formulation.

In **section 4.4**, the algorithm to solve the the per-tone dual optimization problem is presented. We present two different approach to solve the per-tone dual problem, the first approach is the exhaustive search over the MMSE-PTEQ filter order and we will refer to it as contiguous tap selection (CTS) approach. The second approach uses sparse approximation to compute the sparse MMSE-PTEQ filters, we will refer to this as sparse approximation based (SAB) approach.

In **section 4.6** the simulation results is presented. Finally conclusions are drawn in section **4.7**.

4.2 Preliminaries

4.2.1 Basic Data Model

The following notation is adopted in the description of the DMT system. N is the size of the (I)DFT and ν represents the length of the cyclic prefix, $s = N + \nu$. i, k denote the tone index and DMT symbol index respectively. $\mathcal{F}_N$ and $\mathcal{I}_N$ are the N-point DFT and IDFT matrices where $\mathcal{F}_N(i,:)$ is the ith row of $\mathcal{F}_N$. T is the length of the MMSE-PTEQ filter and the equalizer coefficients vector for tone i is $\mathbf{v}_i$. $\mathbf{I}_Q$ and $\mathbf{0}_Q$ are the $Q \times Q$ identity and zero matrix respectively. $x_i^{(k)}$ is a complex subsymbol on tone i ($i = 1 \cdots N$ in k. $\mathbf{x}_N^{(k)} = [x_1^{(k)} \cdots x_N^{(k)}]^T$. $y_{\tilde{k}}$ represents the received signal and $n_{\tilde{k}}$ represents the additive noise at time $\tilde{k}$, $\mathbf{h} = [h_L \cdots h_0 \cdots h_{-K}]$ is the channel impulse response in reverse order, $\{.\}^T$ denotes the transpose, $\{.\}^*$ denotes the conjugate.

The received signal can be modeled as

$$
\begin{aligned}
&\overbrace{\begin{bmatrix} y_{k.s+\nu-T+2+\delta} \\ \ddots \\ y_{(k+1).s+\delta} \end{bmatrix}}^{\mathbf{y}} \Big\updownarrow N+T-1 \\
&= \left[\begin{array}{c|ccc|c} & \mathbf{h} & 0 & \dots & \\ \mathbf{0} & \ddots & \ddots & \ddots & \mathbf{0} \\ & 0 & \dots & \mathbf{h} & \end{array}\right] . \begin{bmatrix} \mathbf{P} & \mathbf{0} & \mathbf{0} \\ \mathbf{0} & \mathbf{P} & \mathbf{0} \\ \mathbf{0} & \mathbf{0} & \mathbf{P} \end{bmatrix} \\
&\quad . \begin{bmatrix} \mathcal{I}_N & \mathbf{0} & \mathbf{0} \\ \mathbf{0} & \mathcal{I}_N & \mathbf{0} \\ \mathbf{0} & \mathbf{0} & \mathcal{I}_N \end{bmatrix} . \overbrace{\begin{bmatrix} \mathbf{x}_N^{(k-1)} \\ \mathbf{x}_N^{(k)} \\ \mathbf{x}_N^{(k+1)} \end{bmatrix}}^{\mathbf{x}} \\
&\quad + \overbrace{\begin{bmatrix} n_{k.s+\nu-T+2+\delta} \\ \vdots \\ n_{(k+1).s+\delta} \end{bmatrix}}^{\mathbf{n}} \\
&= \mathbf{H}.\mathbf{X} + \mathbf{n}
\end{aligned}
\tag{4.1}
$$

δ is the synchronization delay and is a design parameter. Matrix $\mathbf{P}$ adds the cyclic prefix and is given as

$$
\mathbf{P} = \left[\begin{array}{c|c} \mathbf{0} & \mathbf{I}_\nu \\ \hline \multicolumn{2}{c}{\mathbf{I}_N} \end{array}\right]
$$

In (4.1), the kth symbol is the symbol of interest, the $(k-1)$th and the $(k+1)$th symbol have been used to fully describe the ISI. $\mathbf{y}$ is the input at the front end of the receiver. For further details on the used data model we refer to [2].

4.2.2 Per-tone Equalization

MMSE-PTEQ moves the equalization operation into the frequency domain and can be written as follows [2]

$$Z_i^{(k)} = \mathrm{row}_i \underbrace{(\mathcal{F}_N.\mathbf{Y})}_{\text{T FFTs}}. \underbrace{\mathbf{w}.D_i}_{\text{T-tap FEQ}} \quad . \tag{4.2}$$

where $\mathbf{w}$ is the vector representing the T-tap time domain equalizer (TEQ) and D_i is the single tap frequency domain equalizer coefficient for tone i, $Z_i^{(k)}$ is the equalizer output for tone i at time k. $\mathbf{Y}$ is the $N \times T$ Toeplitz matrix given as

$$\mathbf{Y} = \begin{bmatrix} y_{k.s+\nu+1} & y_{k.s+\nu} & \cdots & y_{k.s+\nu-T+2} \\ y_{k.s+\nu+2} & y_{k.s+\nu+1} & \cdots & y_{k.s+\nu-T+3} \\ \ddots & \ddots & \ddots & \ddots \\ y_{(k+1).s} & y_{(k+1).s-1} & \cdots & y_{(k+1).s+\nu-T+1} \end{bmatrix},$$

where we have set $\delta = 0$ for conciseness.

In (4.2), it can be seen that T FFT operations are needed to calculate one output symbol compared to one FFT operation per output symbol when time domain equalization is used. However it was shown in [2] that (4.2) can first be written in terms of a sliding FFT and then eventually only one FFT and T-1 difference terms are needed to calculate the one output symbol, as shown in (4.3) and (4.4).

$$\tilde{y}_i^{(k)} = \underbrace{\mathbf{w}^T.D_i}_{\mathbf{v}_i^T}. \begin{bmatrix} \mathcal{F}_N(i,:) & 0 & \cdots \\ \vdots & \ddots & \vdots \\ 0 & \cdots & \mathcal{F}_N(i,:) \end{bmatrix} .\mathbf{y} \tag{4.3}$$

$$\tilde{y}_i^{(k)} = \mathbf{v}_i^T. \underbrace{\left[\begin{array}{ccc} \mathbf{I}_{T-1} & |\mathbf{0} & | -\mathbf{I}_{T-1} \\ \hline \mathbf{0} & |\mathcal{F}_N(i,:) & \end{array}\right]}_{\mathbf{F}_i} .\mathbf{y} \tag{4.4}$$

The first block row in matrix $\mathbf{F}_i$ in (4.4) extracts the difference terms, while the last row corresponds to the single FFT. **Figure 4.1** shows a general structure for a per-tone equalizer as given by (4.4).

For each used tone a MMSE-PTEQ can be found by minimizing the cost function $J(\mathbf{v}_i)$ in (4.5). This MMSE-PTEQ optimizes the SNR for each tone separately.

$$\begin{aligned}
\underset{\mathbf{v}_i}{\text{minimize}} \;\; J(\mathbf{v}_i) &= \underset{\mathbf{v}_i}{\text{minimize}}\; \mathcal{E}\left\{\left|\mathbf{v}_i^T.\mathbf{F}_i.\mathbf{y} - X_i^{(k)}\right|^2\right\} \\
&= \underset{\mathbf{v}_i}{\text{minimize}} \left\| \underbrace{\begin{bmatrix} {\mathbf{R_x}}^{1/2}\mathbf{H}^H\mathbf{F}_i^H \\ {\mathbf{R_n}}^{1/2}\mathbf{F}_i^H \end{bmatrix}}_{\mathbf{A}_i} \mathbf{v}_i^* - \underbrace{\begin{bmatrix} {\mathbf{R_x}}^{1/2}\mathbf{e}_i^{(k)H} \\ \mathbf{0} \end{bmatrix}}_{\mathbf{b}_i} \right\|_2^2 \\
&= \underset{\mathbf{v}_i}{\text{minimize}} \;\; \|\mathbf{A}_i\mathbf{v}_i^* - \mathbf{b}_i\|_2^2 ,
\end{aligned} \tag{4.5}$$

where $\mathcal{E}(.)$ is the expectation operation, $\mathbf{R_x} = \mathcal{E}(\mathbf{x}\mathbf{x}^H)$ and $\mathbf{R_n} = \mathcal{E}(\mathbf{n}\mathbf{n}^H)$ and $\mathbf{e}_i^{(k)H}$ is a column vector with 1 as the i-th position and 0s elsewhere.

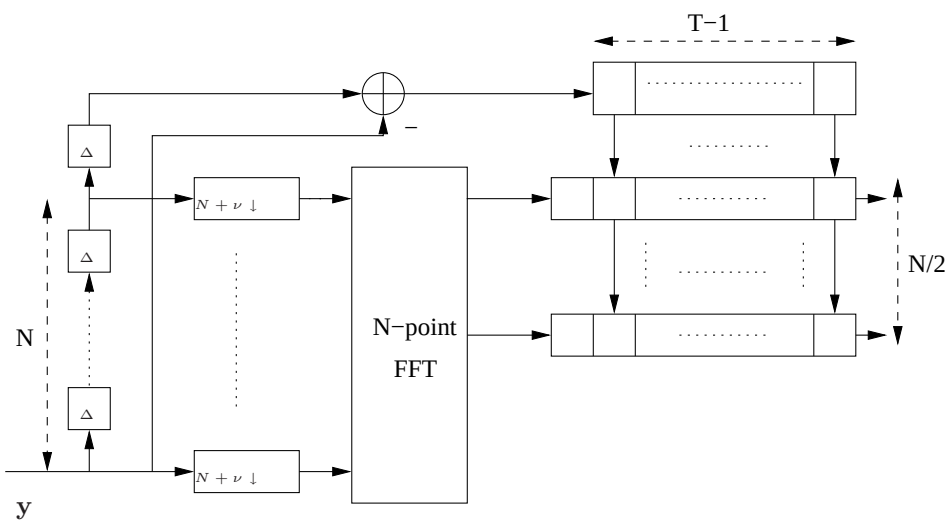

Figure 4.1: T-tap per-tone equalizer model [2]

4.2.3 Effect of MMSE-PTEQ length

The general per-tone equalizer structure uses a constant length non-sparse of equalizer for all the tones. The higher frequency part in the DSL spectrum has

lower channel gains, therefore using longer equalizers does not result in a significant performance gain at these high frequencies. This is shown in **Figure 4.2**. In most of the tones a shorter equalizer can achieve almost the same performance as a longer equalizer. This highlights that a significant portion of the system resources is wasted without any performance gain.

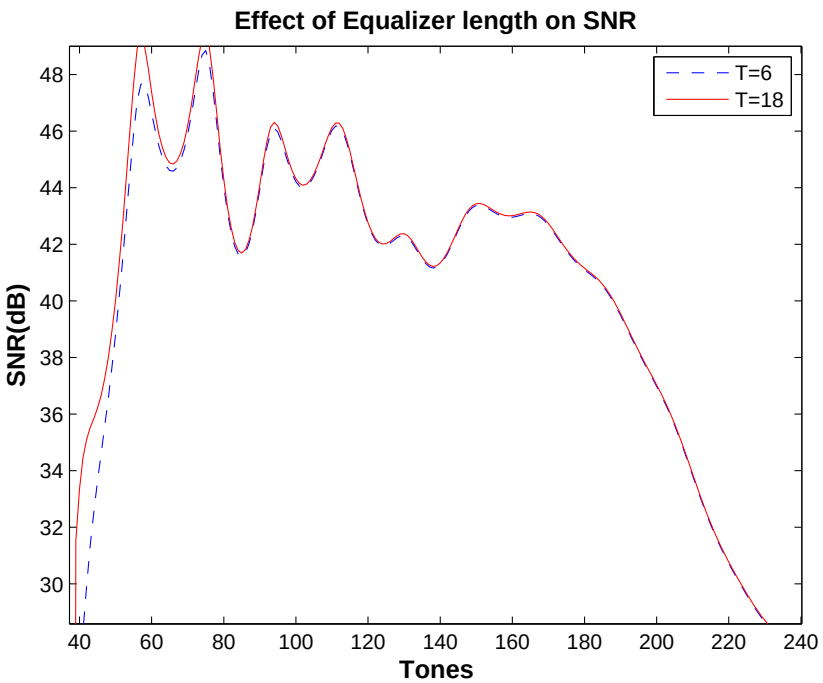

Figure 4.2: Comparison of signal to interference and noise ratio per tone for different MMSE-PTEQ equalizer lengths for a typical ADSL scenario

4.3 Problem formulation

In section 4.3.1, an optimization problem for the MMSE-PTEQ tap allocation for a constant power loading is formulated. In section 4.3.2, we then extend the problem formulation to accommodate the joint MMSE-PTEQ tap and transmit power allocation.

4.3.1 Resource allocation for a fixed power loading

In the previous section, the motivation for the use of variably sparse MMSE-PTEQ equalizer without affecting the overall performance was presented. The main challenge then is to allocate the non-zero equalizer taps over tones such that the performance is optimal.

For a given equalizer tap budget, we can write this as an optimization problem as follows

$$\begin{array}{ll} \max\limits_{\mathbf{C}} & \sum_{i\in\mathcal{I}} R_i \\ \text{subject to} & \sum_{i\in\mathcal{I}} \sum_{j=1}^{T} C_{ij} < C_{\text{budget}} \end{array} \tag{4.6}$$

where,

$$R_i = F_s \log_2 \left(1 + \tfrac{\text{SNR}_i}{\Gamma}\right)$$

where $\mathcal{I}$ is the set containing the indices of the used tones, R_i is the total bitrate on tone i, F_s is the sampling frequency, Γ is SNR gap, $C_{ij} \in \{0, 1\}$. C_{ij} is 1 if the equalizer tap is selected and 0 otherwise, C_{budget} is the predefined maximum total number of equalizer taps, $\mathbf{c}_i = [C_{i1} \cdots C_{iT}]$ is the vector, which represents the position of the used equalizer taps on i-th tone, $\mathbf{C}$ is a matrix which has $\mathbf{c}_i^T$ as its column. SNR_i is the SNR obtained for tone i, as a function of its equalizer with sparsity pattern $\mathbf{c}_i$, based on (4.5).

Constraint in (4.6) is coupled in tone and furthermore it is also a combinatorial problem. One possibility to solve (4.6) is to perform an exhaustive search for all the tones over all possible sparsity pattern of the equalizer. This method has a prohibitively high complexity of $\mathcal{O}(2^{MT})$. In order to simplify the (4.6), it can be posed as an unconstrained optimization problem using dual formulation as

$$\max_{\mathbf{C}}(\mathcal{L}) \quad \text{where } \mathcal{L} = \sum_i R_i + \lambda(C_{\text{budget}} - \sum_{i\in\mathcal{I}} \sum_{j=1}^{T} C_{ij}) \tag{4.7}$$

where λ is known as the Lagrange multiplier and $\mathcal{L}$ is the Lagrangian.

As C_{budget} is a predefined constant, for a fixed λ, the term $\lambda C_{\text{budget}}$ does not have any impact on the optimization procedure, hence it can be removed from (4.7). It is seen that for a given value of λ, the optimization (4.7) decouples over tones and can be written as

$$\max_{C_i}(\mathcal{L}_i) \quad \text{where } \mathcal{L}_i = R_i - \lambda \sum_{j=1}^{T} C_{ij} \tag{4.8}$$

where $\mathcal{L}_i$ is the per-tone Lagrangian, and $\lambda \sum_{j=1}^{T} C_{ij}$ represents the penalty for increasing the number of non-zero equalizer taps for tone i. This per-tone optimization problem (for given λ) can be readily solved by exhaustively searching over all possible sparsity pattern $\mathbf{c}_i$. The value of λ can be updated in order to achieve a balance between overall bitrate performance and total system resources and can be adjusted until $\sum_{i\in\mathcal{I}} \sum_{j=1}^{T} c_{ij}$ matches C_{budget}. The dual problem is still combinatorial and has the complexity of $\mathcal{O}(M2^T)$. In section 4.4, we will present algorithms to further reduce the computational complexity.

4.3.2 Joint equalizer tap and transmit power allocation

In the previous section, MMSE-PTEQ tap allocation problem in the case of constant power loading was presented. The frequency selective nature of the DSL channel also calls for a different transmit power allocation over different tones to achieve a maximum overall bit rate. Therefore, for a given resource constraints (total number of non-zero equalizer taps and total power), an efficient algorithm to allocate the resources over all the tones is needed. The resource allocation problem can be posed as an optimization problem as follows

$$\begin{aligned} \max_{\mathbf{C}} \quad & \sum_{i\in\mathcal{I}} R_i \\ \text{subject to} \quad & \sum_{i\in\mathcal{I}} \sum_{j=1}^{T} C_{ij} \leq C_{\text{budget}} \\ & \sum_{i\in\mathcal{I}} s_i \leq S_{tot} \\ & 0 \leq s_i \leq s_{i,max}, \end{aligned} \tag{4.9}$$

where $s_i \in \mathcal{S}$ is the power on tone i, $\mathcal{S}$ is the set containing all the possible discrete power levels, S_{tot} is the total power constraint, $s_{i,max}$ is the maximum power allowed on the tone i and other quantities as defined in section 4.3.1. This primal optimization problem given by (4.9) is coupled over tones and is a combinatorial problem. It has computational complexity of $\mathcal{O}(\tilde{L}^M 2^{MT})$, where $\tilde{L}$ is the cardinality of the set $\mathcal{S}$ and gives the number of total discrete power levels and M is the cardinality of set $\mathcal{I}$ and gives the total number of used tones. This is intractable even for moderate number of tones, discrete power levels and equalizer taps. In the previous section, it was shown that for a fixed power (4.6) decouples over tones if formulated as a dual problem, thus reducing the

computational complexity. The dual problem formulation of (4.9) can be written as

$$\max_{\mathbf{C}} \quad (\mathcal{L}) \qquad \text{where } \mathcal{L} = \sum_{i\in\mathcal{I}} b_i + \lambda \left(C_{\text{budget}} - \sum_{i\in\mathcal{I}} \sum_{j=1}^{T} C_{ij} \right) + \gamma \left(S_{tot} - \sum_{i\in\mathcal{I}} s_i \right), \tag{4.10}$$

where λ and γ are known as the Lagrange multipliers and $\mathcal{L}$ is the Lagrangian. Since C_{budget} and S_{tot} are predefined constants, it does not have any impact on the overall optimization procedure, hence they can be removed from equation (4.10). It is seen that for given value of λ and γ the optimization (4.10) is equivalent to

$$\max_{\mathbf{c}_i} (\tilde{\mathcal{L}}_i) \quad \text{where } \tilde{\mathcal{L}}_i = R_i - \lambda \sum_{j=1}^{T} C_{ij} - \gamma s_i, \tag{4.11}$$

where $\mathcal{L}_i$ is the per-tone Lagrangian. Eventhough (4.11) is decoupled over tones, we still have to perform exhaustive search over all possible discrete values of s_i and all the combinations of $\mathbf{c}_i$. The search over all combination of $\mathbf{c}_i$ is still combinatorial problem and incurs exponential complexity in T. From (4.5), it can be seen that to compute every $\mathbf{v}_i$ we need full $\mathbf{R}_x$. Therefore computing the power on tone i and then computing the per-tone equalizer $\mathbf{v}_{i+1}$ for tone $i+1$ using the new power on i-th tone is equivalent to solving the power loading problem iteratively for each tone. For given λ and γ, the computational complexity is $\mathcal{O}(ML2^T)$, which is still quite high for large T (e.g. for $T = 20$ it is $\mathcal{O}(2^{20})$ per tone). It can be seen that if we can somehow restrict the number of ways the equalizer taps can combine then the combinatorial search is avoided and the exponential complexity reduces to linear complexity in T. In section 4.4, we will present algorithms to further reduce this complexity.

4.4 Resource allocation for a fixed power loading

4.4.1 Contiguous tap selection resource allocation

Here we present an approach that is based on (4.8) to further reduce the computational complexity. Let us restate (4.8) again for convenience as

$$\max_{C_i} (\mathcal{L}_i) \quad \text{where } \mathcal{L}_i = R_i - \lambda \sum_{j=1}^{T} C_{ij} \tag{4.12}$$

he computational complexity of the (4.12) is $\mathcal{O}(M2^T)$. The computational complexity can be reduced by restricting the sparsity pattern of the pulse shaping

filter such that only contiguous taps can be non-zero. We will call this *contiguous tap selection* (CTS) approach. Thus the combinatorial search over all the sparsity patterns is reduced to the linear search in the filter order. This can be written as

$$\max_{C_i}(\mathcal{L}_i) \quad \text{where } \mathcal{L}_i = R_i - \lambda L_i \tag{4.13}$$

where L_i is the filter order on tone i. This reduced the total number of combination from 2^T to T. This makes the overall computational complexity, $\mathcal{O}(MT)$, linear in the number of tones and the number of taps. The values of Lagrange multipliers can then be updated until all the PSD constraints are met.

In (4.13), increasing the λ increases the penalty for increasing the equalizer length. Hence the value of λ is quite important in obtaining the optimal solution. There are many ways to update the value of λ such as the bisection method, the gradient descent method etc. [29] [152]. In [152], the update of λ is based on the difference between the total available system resources and the used system resources for the current value of λ. For our problem this can be written as,

$$\lambda^{t+1} = \lambda^t - \mu(C_{\text{budget}} - \sum_{i\in\mathcal{I}}\sum_{j=1}^{T} c_{ij}) \tag{4.14}$$

where λ^c is the value of λ at cth iteration, μ is a scaling factor, whose value can be changed in order to obtain a faster convergence to the solution. For simplicity, in our simulations μ is taken as a fixed arbitrary value close to zero. For further details of the algorithm we refer to [152].

In the presented algorithm a search over the equalizer length for a particular tone and for a fixed λ is terminated when either the maximum number of taps that can be allocated is reached or when the cost function for a particular equalizer length is lower than that for the previous length. This follows from the fact that the bitrate is a monotonically increasing function of the equalizer length and hence that L_i is a concave function.

4.4.2 Sparse approximation based approach

From the previous section, it is clear that if we can somehow control the possible sparsity patterns of the pulse shaping filters the computational complexity of the per-tone optimization problem will be reduced significantly. The sparsity pattern was restricted to combinations where only contiguous taps can be non-zero thus reducing the computational complexity from the combinatorial search to linear search in the MMSE-PTEQ filter orders. However restricting the sparsity pattern may not be the best approach, since the best sparsity pattern may not be on the restricted search space. In following section we will use sparse approximation based approach to design a sparse MMSE-PTEQ filter.

Algorithm 4.1 Contiguous taps selection based MMSE-PTEQ tap allocation under constant power loading

initialize λ, μ
repeat
  for tones $i \in \mathcal{I}$ **do**
    initialize $\mathcal{L}_i = 0$
    $L_i = 0$
    for filter order $l = 0 \cdots T-1$ **do**
      if $L_i > R_{i,l} - \lambda l$ **then**
        $L_i = l + 1$
        Break;
      end if
      $\mathcal{L}_i = R_{i,l} - \lambda T$
      $L_i = l$
    end for
  end for
  $C_{total} = \sum_i L_i$
  $\lambda = \lambda - \mu(C_{\text{budget}} - C_{total})$
until $C_{total} \neq C_{budget}$

Sparse approximation based equalizer design

In order to find a better way to control the sparsity pattern, let us write the problem of designing a MMSE-PTEQ filter (4.5) as a sparse approximation problem [150, 151, 49]

$$\underset{\mathbf{v}_i}{\text{minimize}} \quad \|\mathbf{A}_i\mathbf{v}_i^* - \mathbf{b}_i\|_2^2 + \tau \|\mathbf{v}_i\|_0 , \tag{4.15}$$

where $\|.\|_0$ is a ℓ_0 quasi-norm of the vector in the argument; it just counts the number of non-zero elements of the vector in the argument, τ controls the trade off between the sparsity and the quadratic term. Problem (4.15) is however a known to be a NP hard in general [150]. To simplify (4.15) the non-convex ℓ_0 quasi-norm is often replaced by the convex ℓ_1 norm [150, 151, 49]. This can be written as

$$\boxed{\underset{\mathbf{v}_i}{\text{minimize}} \quad \|\mathbf{A}_i\mathbf{v}_i^* - \mathbf{b}_i\|_2^2 + \beta \|\mathbf{v}_i\|_1 ,} \tag{4.16}$$

where β controls the trade off between the sparsity and the quadratic term. (4.16) is a convex problem and can be solved using any generic solver in polynomial time [24]. If the underlying system admits a sparse solution, it has been shown that

solving (4.16) is equivalent to solving (4.15) [151, 49]. In our case, the underlying system does not necessarily admit sparse solution, therefore we can not obtain a sparse MMSE-PTEQ filter by just solving (4.16). One way to obtain a sparse MMSE-PTEQ filter is to adopt a two steps procedure. Firstly, we use (4.16), for a given β, to obtain a nearly-sparse MMSE-PTEQ and then force the coefficients below a certain threshold level ζ to zero to obtain the sparsity pattern $\mathbf{c}_i$. Secondly, we use sparsity pattern $\mathbf{c}_i$ to compute a sparse MMSE-PTEQ filter using modified (4.5) as follows

$$\begin{aligned} &\min_{\mathbf{v}_i} \quad \|\mathbf{A}_i\mathbf{v}_i^* - \mathbf{b}_i\|_2^2 \\ \text{subject to} \quad v_{ij} = 0 \quad &\text{if} \quad c_i j = 0 \qquad \text{for} \quad j = 1 \cdots T \end{aligned} \tag{4.17}$$

It is clear that the choice of the trade off parameter β and ζ is important for the algorithm to work properly. An efficient update rule for these parameter is based on the difference between the total available system resources and the used system resources for the current value of β . This can be written as

$$\beta^{t+1} = \left[\beta^t - \mu(C_{\text{budget}} - \sum_{i\in\mathcal{I}} \|\mathbf{v}_i\|_0)\right]^+ \tag{4.18}$$

where β^c is the value of β at c-th iteration, μ is a scaling factor, and [a]+ is max(0,a). For simplicity, in our simulations μ is taken as a fixed arbitrary value close to zero. Furthermore we can penalize the equalizers with low approximation error. This criteria can also be incorporated in (4.18) and can be rewritten as

$$\beta^{t+1} = \left[\beta^t - \mu(C_{\text{budget}} - \sum_{i\in\mathcal{I}} \|\mathbf{v}_i\|_0)\varepsilon_i^{-1}\right]^+, \tag{4.19}$$

where ε_i.

The threshold level can be fixed to a constant level and the coefficients smaller than the threshold value can be set to zero. But we can also update threshold level to speed up the convergence. It is obvious that if the threshold level is set to a higher value, the probability of a sparser equalizer becomes higher. The update formula for the threshold level can be written as

$$\zeta^{t+1} = \left[\zeta^t - \sigma(C_{\text{budget}} - \sum_{i\in\mathcal{I}} \|\mathbf{v}_i\|_0)\varepsilon_i^{-1}\right]^+, \tag{4.20}$$

where σ is an arbitrarily small scaling factor.

Sparse approximation based MMSE-PTEQ tap allocation

Based on section 4.4.2, we are now ready to describe the full convex relaxation based resource allocation. From definition we can see that $\|\mathbf{v}_i\|_0 = \sum_{j=1}^{T} C_{ij}$ therefore we can also write (4.8) as

$$\max_{\mathbf{v}_i} \quad b_i - \lambda \|\mathbf{v}_i\|_0 , \tag{4.21}$$

Even though the equalizer coefficient needs to be computed twice, for a large T it has similar computational complexity to the contiguous tap selection based approach of section 4.4.2.

Furthermore the Lagrange multiplier λ to enforce the total tap constraint has to be updated. The Lagrange multiplier only depends on the difference between the current total number of allocated and the equalizer tap budget and hence can be written as

$$\lambda^{t+1} = \left[\lambda^t - \theta(C_{\text{budget}} - \sum_{i \in \mathcal{I}} \|\mathbf{v}_i\|_0) \right]^+ , \tag{4.22}$$

where θ is an arbitrarily small step size.

An algorithm to allocate the non-zero equalizer taps for given resource constraints in the case of a constant power loading is given in **Alg.** 4.2.

4.5 Joint equalizer tap and power allocation

4.5.1 Contiguous tap selection based approach

Here, we present an approach that is based on a dual problem formulation presented in (4.11). For convenience, let us rewrite the dual problem below

$$\max_{\mathbf{c}_i} (\tilde{\mathcal{L}}_i) \quad \text{where } \tilde{\mathcal{L}}_i = R_i - \lambda \sum_{j=1}^{T} C_{ij} - \gamma s_i, \tag{4.23}$$

we can restrict the sparsity pattern of the MMSE-PTEQ as suggested for contiguous tap selection in previous section. Therefore we can rewrite

$$\max_{\mathbf{c}_i} (\tilde{\mathcal{L}}_i) \quad \text{where } \tilde{\mathcal{L}}_i = R_i - \lambda L_i - \gamma s_i, \tag{4.24}$$

where L_i is the MMSE-PTEQ filter order. This per-tone optimization problem can be solved (for fixed Lagrange multiplier) by exhaustively searching over all values

Algorithm 4.2 Sparse approximation based MMSE-PTEQ tap allocation

1: Initialize parameters β and threshold ζ
2: Initialize step sizes μ and σ
3: **repeat**
4: **for** tone $i \in \mathcal{I}$ **do**
5: Compute nearly sparse MMSE-PTEQ $\tilde{\mathbf{v}}_i$ using

$$\underset{\mathbf{v}_i}{\text{minimize}} \quad \|\mathbf{A}_i\mathbf{v}_i^* - \mathbf{b}_i\|_2^2 + \beta\|\mathbf{v}_i\|_1$$

6: Apply threshold ζ on $\tilde{\mathbf{v}}$ to compute sparsity pattern $\mathbf{c}_i$
7: compute sparse MMSE-PTEQ $\mathbf{v}_i$ using

$$\mathbf{v}_{i,opt} \Leftarrow \underset{\mathbf{v}_i}{\text{argmin}} \|\mathbf{A}_i\mathbf{v}_i^* - \mathbf{b}_i\|_2^2$$

$$\text{subject to} \quad v_{ij} = 0 \quad \text{if} \quad c_i j = 0 \qquad \text{for} \quad j = 1 \cdots T$$

8: **end for**
9: compute $C = \sum_{i\in\mathcal{I}} \|\mathbf{v}_i\|_0$
10: update $\beta = \left[\beta - \mu(C_{\text{budget}} - C)\varepsilon_i^{-1}\right]^+$
11: update $\zeta = \left[\zeta - \sigma(C_{\text{budget}} - C)\varepsilon_i^{-1}\right]^+$
12: **until** $(C_{budget} - C \leq \text{tolerance})$

of s_i (i.e. from -140dBm to s_{max}(-60dBm) in discrete steps)and all the other quantities are as defined in section 4.3.1. The values of the Lagrange multipliers can then be updated until all the constraints are met. An algorithm description is given below. The complexity of the proposed algorithm is $O(N * \tilde{L} * T)$.

4.5.2 Sparse approximation based approach

4.5.3 Sparse approximation based resource allocation

Based on section (4.4.2), we are now ready to describe the full convex relaxation based resource allocation. From definition we can see that $\|\mathbf{v}_i\|_0 = \sum_{j=1}^{T} C_{ij}$, therefore we can also write (4.8) as

$$\max_{\mathbf{v}_i} \quad b_i - \lambda\|\mathbf{v}_i\|_0 - \gamma s_i, \tag{4.25}$$

Now for each discrete power level, we can compute sparse $\mathbf{v}_i$ using method described above. This results in solving (4.16) and (4.15) once for each power level. Even though the equalizer coefficient needs to be computed twice, for a large T it has similar computational complexity to the contiguous tap selection

Algorithm 4.3 Contiguous tap selection based joint MMSE-PTEQ tap and transmit power allocation

Initialize vector containing transmitted power $\mathbf{s} = [s_{max}]_{1\times M}$, $s_i^{opt} = s_{max}$, $L_i^{opt} = T$
Initialize Lagrange multipliers λ and γ
Initialize step sizes θ and η
repeat
  for tone $i \in \mathcal{I}$ **do**
    Initialize $\mathcal{L}_i^{opt} = 0$
    for power level $s_i \in \mathcal{S}$ **do**
      for Filter order $l = 0 \cdots T-1$ **do**
        Compute $\mathbf{v}_i$ of order l using $\mathbf{s}$
        Compute $\mathcal{L}_i \Leftarrow R_i - \lambda l - \gamma s_i$
        if $\mathcal{L}_i \geq \mathcal{L}_i^{opt}$ **then**
          $L_i^{opt} \Leftarrow l$
          $s_i^{opt} \Leftarrow s_i$
        end if
      end for
    end for
    $\mathbf{s}_{i,:} \Leftarrow s_i^{opt}$
  end for
  Compute $C = \sum_{i\in\mathcal{I}} L_i^{opt}$
  Compute $S = \sum_{i\in\mathcal{I}} s_i^{opt}$
  Update $\lambda^{t+1} = [\lambda^t - \theta(C_{budget} - C)]^+$
  Update $\gamma^{t+1} = [\gamma^t - \eta(S_{budget} - S)]^+$
until ($s_{budget} - S \leq$ tolerance & $C_{budget} - S \leq$ tolerance)

based approach of [105], which requires solving (4.15) T times for each power level. The computational complexity can be further reduced by solving (4.16) only once for the initial power level and then using same sparsity pattern for all the other power levels.

Furthermore the Lagrange multiplier γ, which enforces the power constraint also has to be updated. The Lagrange multiplier only depends on the difference between the current total power and the total power budget and hence can be written as

$$\gamma^{t+1} = \left[\gamma^t - \eta(S_{\text{tot}} - \sum_{i\in\mathcal{I}} s_i)\right]^+, \tag{4.26}$$

where η is an arbitrarily small scaling factor. Similarly, to enforce the total tap constraint in the outer loop we can use similar formulation and can be written as

$$\lambda^{t+1} = \left[\lambda^t - \theta(C_{\text{budget}} - \sum_{i\in\mathcal{I}} \|\mathbf{v}_i\|_0)\right]^+, \tag{4.27}$$

where θ is an arbitrarily small step size.

An algorithm to allocate the resources, i.e. number of equalizer taps and the power, for given resource constraints is given in **Alg.** 4.4.

Algorithm 4.4 Sparse approximation based joint MMSE-PTEQ tap and transmit power allocation

Initialize vector containing transmitted power $\mathbf{s} = [s_{max}]_{1\times M}$, $s_i^{opt} = s_{max}$
Initialize Lagrange multipliers β, λ and γ
Initialize step sizes μ, σ and η and threshold ζ
repeat
  for tone $i \in \mathcal{I}$ **do**
    Compute $\mathbf{v}_i$ using (4.16) and $\mathbf{s}$
    Find the sparsity pattern $\mathbf{c}_i$ by applying the threshold to $\mathbf{v}_i$
    Initialize $\mathcal{L}_i^{old} = 0$
    for power level $s_i \in \mathcal{S}$ **do**
      Compute sparse $\mathbf{v}_i$ using (4.5)
      Compute the objective function $\mathcal{L}_i$ using (4.8)
      if $\mathcal{L}_i \geq \mathcal{L}_i^{old}$ **then**
        $s_i^{opt} \Leftarrow s_i$
        $\mathcal{L}_i^{old} \Leftarrow \mathcal{L}_i$
      end if
    end for
    Replace transmitted power tone i in $\mathbf{s}$ with s_i^{opt}
    $\mathbf{v}_i^{opt} \Leftarrow \mathbf{v}_i$
  end for
  Update all Lagrange multipliers β, γ and λ using (4.19), (4.26) and (4.27)
  Update threshold ζ (4.20)
until ($s_{tot} - \sum_i s_i \leq$ tolerance & $C_{budget} - \sum_i \|\mathbf{v}_i\|_0 \leq$ tolerance)

4.6 Simulation results

The channel under consideration here is a 400m twisted pair cable in a bundle of 8 with an interference channel of 400m.. We use the same setting as in [105] in order to compare the results. In these simulations, the synchronization delay δ

has not been considered. The bit error rate probability has been fixed to 10^{-7}, the coding gain and the noise margin are 3 dB and 6 dB respectively. The signal and noise PSD (power spectral density) levels are -60dB and -140 dB respectively and total power budget is 11.5 dBm [10]. Three consecutive symbols are considered to account for the ISI. The channel is assumed to be known perfectly at the receiver. We fix the tones used for transmission as suggested in [33], i.e., 375 predefined tones, to be consistent with previous chapter. For the variable length per-tone equalizer the maximum number of equalizer taps per tone is 20.

4.6.1 Resource allocation for a fixed power loading

In the first scenario, the transmit power on tones are assumed to be fixed and only MMSE-PTEQ filter tap optimization is performed. **Figure 4.3** compares the bit rates for contiguous tap selection based approach, sparse approximation based approach and fixed length MMSE-PTEQ for a given per-tone equalizer tap constraint. To compute the sparsity pattern using (4.16), we can use any available numerical solvers e.g. CVX [66, 65], and apply the threshold. Then we can compute the required sparse equalizer simply using a least squares method. From **Figure 4.3**, it can be clearly seen that for a given bit rate the sparse approximation based equalizer tap allocation approach performs better than the contiguous tap selection based equalizer tap allocation. Therefore, we can conclude that for similar computational complexity we can always get better performance using sparse approximation based equalizer tap allocation.

4.6.2 Joint per-tone equalizer tap and transmit power allocation

In the second scenario, we also perform transmit power loading. The total power constraint is 11dBm. In our case we have 375 used tones and -60 dBm maximum PSD. Therefore, the available power budget is larger than the required power budget and the power constraint is not active. But, it can still be seen from **Figure 4.5** that transmit power loading improves the MMSE-PTEQ tap distribution.

4.7 Conclusion

In this chapter, it was shown that the use of MMSE-PTEQ increasing the achievable bit rate of the DMT system. Furthermore, it was also shown that using a constant length non-sparse MMSE-PTEQ filter on every tone unnecessarily increases the run-time complexity of the DMT system. Therefore, using variably sparse MMSE-PTEQ filter on each tone reduces the run-time complexity without affecting the performance significantly.

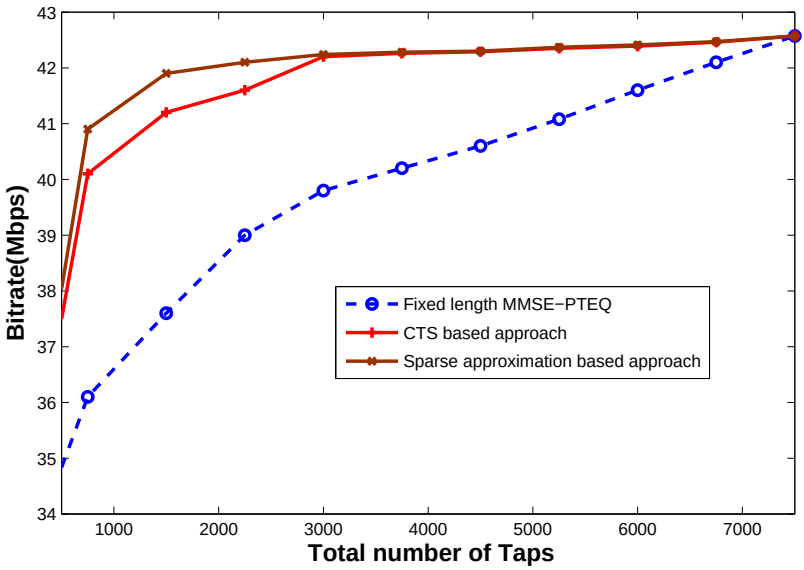

Figure 4.3: Comparison of bit rate versus total number of non-zero MMSE-PTEQ taps for contiguous tap selection based approach, sparse approximation based approach and fixed length MMSE-PTEQ approach

To this end, we have proposed efficient resource allocation algorithms to distribute the available resources (total transmit power budget and total MMSE-PTEQ filter tap budget) over tones in a DMT receiver with per-tone equalization. We have shown that a dual problem formulation leads to an unconstrained optimization problem that is decoupled over tones but due to the combinatorial nature of the filter tap allocation the resulting optimization problem is still NP hard.

We proposed two approaches to further simplify the problem. First, by restricting the sparsity pattern of the MMSE-PTEQ such that only contiguous MMSE-PTEQ taps are allowed to be non-zero, hence the combinatorial search in the sparsity pattern is reduced to the linear search in filter order. Second, by using sparse approximation technique to design the sparse MMSE-PTEQ filter directly. Using convex relaxation of the sparsity constraints, the sparse filter design problem can be written as convex problem and solved efficiently. Furthermore, the techniques were also extended to jointly allocate MMSE-PTEQ filter taps and the transmit power.

A VDSL simulation demonstrates that under a fixed power loading, the number of

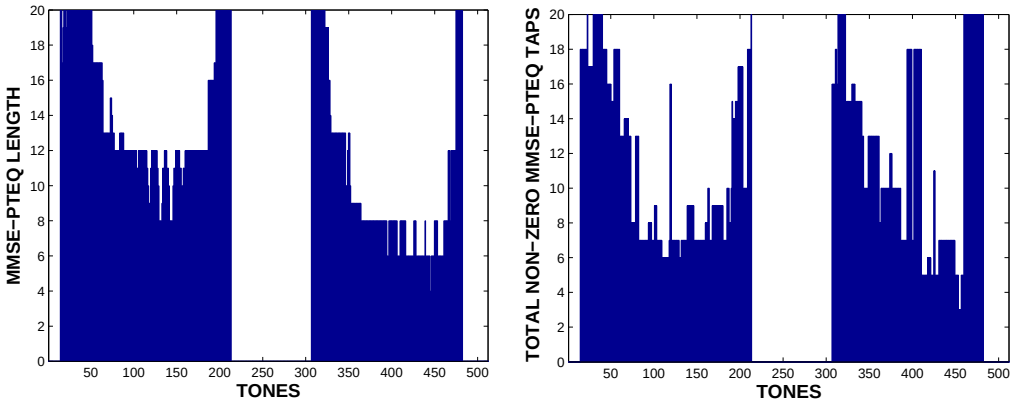

(a) (b)

Figure 4.4: Optimum distribution of number of MMSE-PTEQ taps over tones using (a) the contiguous tap selection based approach (b) the sparse approximation based approach

MMSE-PTEQ filter taps can be reduced to approximately 40% compared to the fixed length non-sparse case without sacrificing performance. Furthermore, we also showed that the sparse approximation based MMSE-PTEQ filter tap allocation approach performs better than the contiguous tap selection based approach. It was also shown that when combined with an transmit power loading algorithm these approaches can further reduce the number of per-tone pulse shaping filter taps needed to achieve the same bit-rate performance.

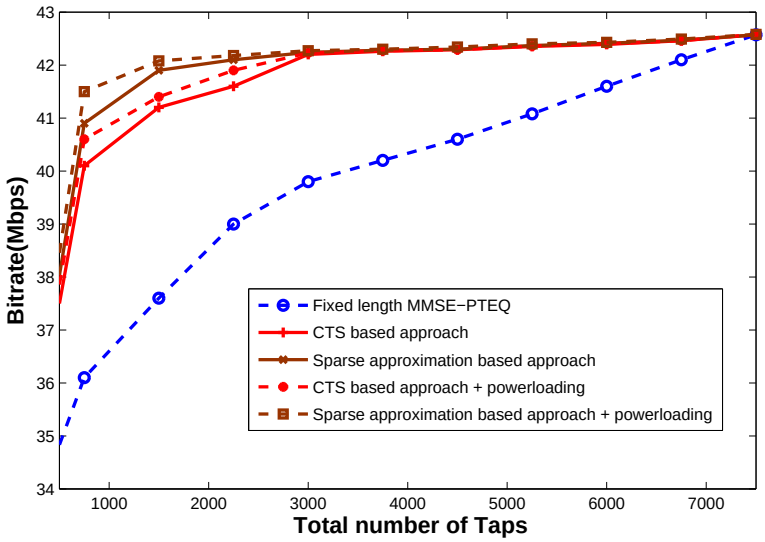

Figure 4.5: Comparison of bit rate versus total number of non-zero MMSE-PTEQ taps for contiguous tap selection based approach, sparse approximation based approach and fixed length MMSE-PTEQ approach with and without transmit power loading

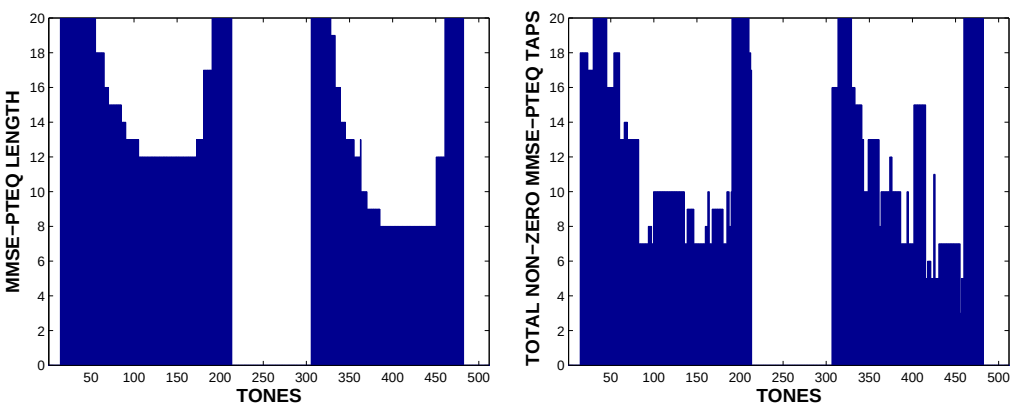

(a) (b)

Figure 4.6: Optimum distribution of number of MMSE-PTEQ taps under transmit power loading over tones using (a) the contiguous tap selection based approach(b) the sparse approximation based approach

Chapter 5

Joint resource allocation in DMT transceivers

5.1 Introduction

In chapter 3, a DMT transmitter with per-tone pulse shaping filter was considered. Under the assumption of long enough cyclic prefix and perfect receiver, efficient resource allocation algorithms to optimally allocate pulse shaping filter taps and transmit power was presented. Then in chapter 4, a DMT receiver with per-tone equalization was considered. It was shown that dispersive channels such as DSL channel has very long CIR, therefore, to ensure there is no ISI and ICI, a very long CP was needed. Therefore, a channel shortening equalizer is needed to ensure the CP is short. Per-tone equalizer combined channel shortening with the frequency domain equalization on each tone by using multitap frequency domain equalization. It was shown in chapter 4 that not every tone needs to be equalized by the equalizer of same order. The tones at the band edges needed longer filters than the tones at the middle of the band. It was also shown that the number of non-zero filter taps can be further reduced by using optimal transmit power allocation along with the MMSE-PTEQ tap allocation. In chapter 4, however, the effect of pulse shaping filter at the transmitter side was not considered. Furthermore, the effect of PSD mask constraint was also neglected.

In this chapter, we will look into combined DMT transceiver structure with per-tone pulse shaping and per-tone equalization. After this point we will refer to this structure as DMT transceiver for the sake of brevity. The non-zero filter taps and transmit power can be allocated more efficiently if the effect of pulse shaping filter and PSD mask constraint is also taken into account. The complexity of

solving optimization problem to jointly allocate resources in DMT transceiver can be very high. Since the constraints are coupled in tones, the optimization problem is non-convex.

The Lagrange multiplier method is often used to convert a constrained optimization problem into a dual unconstrained problem. This method was used in chapter 3 and chapter 4 to reduce the complexity of solving the optimization problem. It was shown that the problem decouples in tone, hence reducing the computational complexity. In this chapter, we will also use the Lagrange multiplier to simplify the optimization problem. We will then investigate contiguous tap selection algorithm, presented in chapter 3 and chapter 4, to further reduce the computational complexity. Additionally, the sparse approximation based resource allocation, presented in chapter 3 and chapter 4, will also be investigated.

This chapter is organized as follows: In section **5.2**, a combined system model of the DMT transceiver employing per-tone pulse shaping filter and per-tone equalizer is presented.

In **section 5.3**, resource allocation problem in DMT transceiver is formulated under PSD mask constraint, and transmitter and receiver filter tap budgets with and without transmit power loading.

In **section 5.4**, resource allocation algorithms to allocate the run-time complexity, i.e., non-zero pulse shaping filter taps and non-zero MMSE-PTEQ taps, under fixed power loading is then presented. The algorithms are based on restricted filter sparsity pattern, which is called contiguous tap selection, and sparse approximation based filter design. These techniques were also presented in chapter 3 and chapter 4.

In **section 5.5**, resource allocation algorithms to jointly allocate the run-time complexity and per-tone transmit power are presented. The technique based on contiguous tap selection and sparse filter design will then be applied to reduce the computational complexity of the resource allocation algorithm.

In **section 5.6**, some simulation results will be presented. Finally conclusions are drawn in section **5.7**.

5.2 System model

The following notation is adopted in the description of the DMT transceiver system. N is the IDFT-size and i denotes the tone index. C_{max} is the maximum pulse shaping filter order, ν is the cyclic prefix length. $\mathbf{x}_l^t$ is the output of the transmitter in time domain, i.e. a vector of length $K = N + C_{max} + \nu$, corresponding to one transmitted symbol at time l. T is the maximum MMSE-PTEQ filter order.

$$\begin{bmatrix} y_{l.s+\nu-T+2} \\ \ddots \\ y_{(l+1).s} \end{bmatrix} = \left[\begin{array}{c|ccc|c} \mathbf{0} & \mathbf{h} & 0 & \dots & \\ & \ddots & \ddots & \ddots & \mathbf{0} \\ & 0 & \dots & \mathbf{h} & \end{array}\right] \begin{bmatrix} \mathbf{x}_{l-l} \\ \mathbf{x}_l \\ \mathbf{x}_{l+1} \end{bmatrix} + \begin{bmatrix} n_{l.s+\nu-T+2} \\ \vdots \\ n_{(l+1).s} \end{bmatrix} \tag{5.1}$$

where,

$$\mathbf{x}_l^t = \underbrace{\begin{bmatrix} \mathbf{0} & \mathbf{I}_\nu \\ \mathbf{I}_N & \\ \mathbf{0}_{C_{max}\times N} & \end{bmatrix}}_{\mathbf{\Phi}} \mathcal{I}_N \mathbf{D}\, \mathbf{x}_l + \underbrace{\sum_{i=0}^{N-1} \begin{bmatrix} -\alpha^{i(\nu+1)}\bar{\mathbf{v}}_i \\ \mathbf{0}_{(N+\nu-C_{max})\times 1} \\ \alpha^i \bar{\mathbf{v}}_i \end{bmatrix} x_{li}}_{\mathbf{a}_l}.$$

$$\mathbf{x}_l^t = \mathbf{\Phi}\mathbf{x}_l + \mathbf{a}_l \tag{5.2}$$

Here, all the quantities are as described in chapter 3. The per-tone transmit pulse shaping filters can be designed as suggested in chapter 3. (5.1) can then be written as

$$\overbrace{\begin{bmatrix} y_{l.s+\nu-T+2} \\ \ddots \\ y_{(l+1).s} \end{bmatrix}}^{\mathbf{y}} = \overbrace{\left[\begin{array}{c|ccc|c} \mathbf{0} & \mathbf{h} & 0 & \dots & \\ & \ddots & \ddots & \ddots & \mathbf{0} \\ & 0 & \dots & \mathbf{h} & \end{array}\right] \begin{bmatrix} \mathbf{\Phi} & \mathbf{0} & \mathbf{0} \\ \mathbf{0} & \mathbf{\Phi} & \mathbf{0} \\ \mathbf{0} & \mathbf{0} & \mathbf{\Phi} \end{bmatrix}}^{\mathbf{H}} \overbrace{\begin{bmatrix} \mathbf{x}_{l-1} \\ \mathbf{x}_l \\ \mathbf{x}_{l+1} \end{bmatrix}}^{\mathbf{x}}$$

$$+ \underbrace{\begin{bmatrix} \mathbf{a}_{l-1} \\ \mathbf{a}_l \\ \mathbf{a}_{l+1} \end{bmatrix} + \begin{bmatrix} n_{l.s+\nu-T+2} \\ \vdots \\ n_{(l+1).s} \end{bmatrix}}_{\mathbf{z}}$$

$$\mathbf{y} = \mathbf{H}\mathbf{x} + \mathbf{z}, \tag{5.3}$$

From chapter 4, we know that the MMSE-PTEQ, $\mathbf{v}_i$ for tone i, can be obtained by minimizing the cost function as follows

$$\min_{\mathbf{v}_i} \quad J(\mathbf{v}_i) = \min_{\mathbf{v}_i} \quad \mathcal{E}\left\{|\mathbf{v}_i \mathbf{F}_i \mathbf{y} - x_{il}|^2\right\}, \tag{5.4}$$

where

$$\mathbf{F}_i = \left[\begin{array}{ccc} \mathbf{I}_{T-1} & |\mathbf{0} & | -\mathbf{I}_{T-1} \\ \hline \mathbf{0} & |\mathcal{F}_N(i,:) & \end{array}\right] \tag{5.5}$$

After few trivial steps it can be written as

$$\min_{\mathbf{v}_i} \quad J(\mathbf{v}_i) = \min_{\mathbf{v}_i} \quad \left\| \underbrace{\begin{bmatrix} \mathbf{S}^{1/2}\mathbf{H}^H\mathbf{F}_i^H \\ \mathbf{R}_z^{1/2}\mathbf{F}_i^H \end{bmatrix}}_{\mathbf{A}_i} \mathbf{v}_i^* - \underbrace{\begin{bmatrix} \mathbf{S}^{1/2}\mathbf{e}_i^H \\ \mathbf{0} \end{bmatrix}}_{\mathbf{b}_i} \right\|_2^2$$

$$= \min_{\mathbf{v}_i} \left\| \mathbf{A}_i\mathbf{v}_i^* - \mathbf{b}_i \right\|_2^2, \tag{5.6}$$

where $\mathbf{E}\{.\}$ is the expectation operation, $\mathbf{S} = \mathcal{E}\{\mathbf{x}\mathbf{x}^H\}$ and $\mathbf{R}_z = \mathcal{E}\{\mathbf{z}\mathbf{z}^H\}$ and $\mathbf{e}_i^H$ is a column vector with 1 at the ith position and 0s elsewhere.

5.3 Problem formulation

In chapter 3 and chapter 4, the motivation for using variably sparse per-tone pulse shaping filter and MMSE-PTEQ was presented. Chapter 3 and chapter 4 formulated and solved the resource allocation problem independent of each other. At the DMT transmitter, the receiver was considered perfect and cyclic prefix was assumed to be long enough to remove ISI and at the DMT receiver, the effect of per-tone pulse shaping filter at the transmitter and the PSD mask constraint was ignored for the sake of simplicity. In this section, we will formulate the joint resource allocation for both DMT transmitter and receiver. Firstly, in section 5.3.2, we will formulate the resource allocation (joint transmit-receive non-zero filter tap allocation) problem under fixed power loading and PSD mask constraint. And secondly, this optimization problem formulation will be extended to include optimal transmit power allocation along with the non-zero filter tap allocation in section 5.3.2.

5.3.1 Resource allocation for a fixed power loading

For given total tap budgets C^t_{budget} and C^r_{budget} for the transmitter and the receiver, we can write the filter tap allocation problem as

$$\max_{\mathbf{C}^t,\mathbf{C}^r} \quad \sum_{i\in\mathcal{I}} R_i$$

$$\text{Subject to} \qquad \sum_{i\in\mathcal{I}}\sum_{j=0}^{C_{max}} C^t_{ij} \le C^t_{budget}$$

$$\sum_{i\in\mathcal{I}}\sum_{p=0}^{T} C^r_{ip} \le C^r_{budget}$$

$$\mathbf{t}_{spec} \le \mathbf{t}_{mask}, \tag{5.7}$$

where $\mathcal{I}$ is the set containing the indices of the used tones, $C_{ij} \in \{0,1\}$. C_{ij} is 1 if the per-tone pulse shaping filter tap is selected and 0 otherwise, C^t_{budget} and C^r_{budget} are the predefined maximum pulse shaping and MMSE-PTEQ filter order respectively. $\mathbf{c}^t_i = [C_{i1}\cdots C_{iC_{max}}]$ is the vector which represents the position of the used per-tone pulse shaping filter taps on i-th tone and is known as sparsity pattern of the resulting per-tone pulse shaping filter, $\mathbf{C}^t$ is a matrix which has $\mathbf{c}^{tT}_i$ as its column, $\mathbf{c}^r_i$ and $\mathbf{C}^r$ can be similarly defined. $\mathbf{t}_{mask}$ is the vector containing $\bar{M}$ sample points of the PSD mask at different frequencies and $\mathbf{t}_{spec}$ is the vector containing the similarly sampled PSD of the transmitter output. R_i is the achieved bit rate for tone i which is given as

$$R_i = F_s \log_2(1 + \frac{SNR_i}{\Gamma}), \tag{5.8}$$

where F_s is the sampling frequency, Γ is the SNR gap, SNR_i is the SNR obtained for tone i, as a function of its equalizer with sparsity pattern $\mathbf{c}_i$, based on (5.4) and can be computed as [2], which is presented in chapter 4. For the sake of convenience, let us rewrite it again as follows

$$\text{SNR}_i = \frac{S_i}{\text{Int}_i + \text{noise}_i}, \tag{5.9}$$

where

$$S_i = \left|(\mathbf{S}^{1/2}\mathbf{H}^H\mathbf{F}^H_i)_{(N+i,:)}\mathbf{v}^*_i\right|^2 \tag{5.10}$$

$$\text{Int}_i = \left\|\mathbf{S}^{1/2}\mathbf{H}^H\mathbf{F}^H_i\mathbf{v}^*_i\right\|^2 - S_i \tag{5.11}$$

$$\text{noise}_i = \left\|\mathbf{R}^{1/2}_z\mathbf{F}^H_i\mathbf{v}^*_i\right\|^2 \tag{5.12}$$

Constraint in (5.7) is coupled in tone and furthermore it is also a combinatorial problem. One possibility to solve (4.6) is to perform an exhaustive search for all the tones over all possible sparsity pattern of the pulse shaping filter and MMSE-PTEQ. This method has a prohibitively high complexity. In order to simplify the (5.7), it can be posed as an unconstrained optimization problem using dual formulation as

$$\min_{\lambda_t,\lambda_r,\gamma}\left\{\max_{\mathbf{C}^t,\mathbf{C}^r} \quad \Psi\right\},$$

where

$$\Psi = \sum_{i\in\mathcal{I}} R_i + \lambda_t\left(C^t_{budget} - \sum_{i\in\mathcal{I}}\sum_{j=0}^{C_{max}} {C_{ij}}^t\right) + \lambda_r\left(C^r_{budget} - \sum_{i\in\mathcal{I}}\sum_{p=0}^{T} {C_{ip}}^r)\right)$$

$$+ \sum_{m=1}^{\bar{M}} \gamma_m\left(t_{mask,m} - t_{spec,m}\right)$$

$$\lambda_t, \lambda_r, \gamma_m \geq 0. \tag{5.13}$$

Here λ_r, λ_t and γ_m are Lagrange multipliers. $C^r_{budget}, C^t_{budget}$ and $t_{mask,m}$ are predefined constants therefore they do not have any impact on the optimization procedure. Hence, these can be removed from the optimization problem (5.13). From (3.11), we know that

$$\begin{aligned} t_{spec,m} &= \sum_{i\in\mathcal{I}} s_i |F_i(e^{j\omega_m})W_i(e^{j\omega_m})|^2 \\ &= \sum_{i\in\mathcal{I}} s_i |F_i(e^{j\omega_m})\hat{\mathbf{e}}^H(e^{j\omega_m})\mathbf{w}_i|^2, \end{aligned} \tag{5.14}$$

where all the quantities are as described in chapter 3. Then the dual problem (5.13) can now be written as

$$\min_{\lambda_t,\lambda_r,\gamma_m} \left\{ \max_{\mathbf{C}^t,\mathbf{C}^r} \quad \Psi \right\},$$

where

$$\Psi = \sum_{i\in\mathcal{I}} R_i - \lambda_t \sum_{i\in\mathcal{I}} \sum_{j=0}^{C_{max}} {C_{ij}}^t - \lambda_r \sum_{i\in\mathcal{I}} \sum_{p=0}^{T} {C_{ip}}^r - \left(\sum_{m=1}^{\bar{M}} \gamma_m \sum_{i\in\mathcal{I}} s_i |F_i(e^{j\omega_m})\hat{\mathbf{e}}^H(e^{j\omega_m})\mathbf{w}_i|^2 \right)$$

$$\lambda_r, \lambda_t, \gamma_m \geq 0. \tag{5.15}$$

Since we are using fixed power loading, (5.15) can be decoupled in tones. This can then be written as

For $i \in \mathcal{I}$

$$\min_{\lambda_r,\lambda_t,\gamma_m} \left\{ \max_{\mathbf{c}_i^t,\mathbf{c}_i^r} \quad \psi_i \right\},$$

where

$$\psi_i = R_i - \lambda \sum_{j=0}^{C_{max}} {C_{ij}}^t - \lambda \sum_{p=0}^{T} {C_{ip}}^r - \sum_{m=1}^{\bar{M}} \gamma_m s_i |F_i(e^{j\omega_m})\hat{\mathbf{e}}^H(e^{j\omega_m})\mathbf{w}_i|^2$$

$$\lambda_r, \lambda_t, \gamma_m \geq 0. \tag{5.16}$$

5.3.2 Joint filter tap and transmit power allocation

For a given total pulse shaping filter tap budget C^t_{budget}, total MMSE-PTEQ tap budget C^r_{budget} and total transmit power budget S_{budget}, we can write the resource

allocation problem as

$$
\begin{aligned}
\underset{\mathbf{C}^t,\mathbf{C}^r,\mathbf{S}}{\text{maximum}} \quad & \sum_{i\in\mathcal{I}} R_i \\
\text{subject to} \quad & \mathbf{t}_{spec} \leq \mathbf{t}_{mask} \\
& \sum_{i\in\mathcal{I}} \sum_{j=0}^{C_{max}} C_{ij}^t \leq C_{budget}^t \\
& \sum_{i\in\mathcal{I}} \sum_{p=0}^{T} C_{ip}^r \leq C_{budget}^r \\
& \sum_{i\in\mathcal{I}} s_i \leq S_{budget} \\
& 0 \leq s_i \leq s_{max,i},
\end{aligned}
\tag{5.17}
$$

where R_i is the bit rate on tone i and can be described as the function of the MMSE-PTEQ and the per-tone transmit power as in (5.8), S_{budget} is the total transmit power budget, $\mathbf{s}$ is the vector containing the transmit power on all the tones, $s_i \in \mathcal{S}$ is the power allocated to tone i, $\mathcal{S}$ is the set containing all the allowed discrete power levels s_i, $s_{max,i}$ is the maximum transmit power allowed on tone i. All the remaining quantities are as defined in section 5.3.1. The primal optimization problem (5.17) is coupled over tones and is a combinatorial problem. It has computational complexity of $\mathcal{O}(\tilde{L}^M 2^{M(C_{max}+1)(T+1)})$, where $\tilde{L}$ is the cardinality of the set $\mathcal{S}$ and gives the number of total discrete power levels and M is the cardinality of set $\mathcal{I}$ and gives the total number of used tones. This is intractable even for moderate number of M, $\tilde{L}$, C_{max} and T. In chapter 3 and chapter 4, it was shown that the problem can be simplified if it formulated as a dual optimization problem, hence reducing the computational complexity. The dual optimization problem can be written as

$$\min_{\gamma,\alpha,\lambda_t,\lambda_r} \left\{ \max_{\mathbf{C}^t,\mathbf{C}^r,\mathbf{S}} (\hat{\Psi}) \right\}$$

where,

$$\hat{\Psi} = \sum_{i\in\mathcal{I}} R_i + \lambda_t \left(C^t_{budget} - \sum_{i\in\mathcal{I}} \sum_{j=0}^{C_{max}} C^t_{ij} \right) + \lambda_r \left(C^r_{budget} \sum_{i\in\mathcal{I}} \sum_{p=0}^{C_{max}} C^r_{ip} \right) +$$

$$\alpha \left(P_{budget} - \sum_{i\in\mathcal{I}} s_i \right) + \sum_{m=1}^{\bar{M}} \gamma_m \left(t_{mask,m} - t_{spec,m} \right)$$

$$\alpha, \gamma_m, \lambda_t, \lambda_r > 0 \tag{5.18}$$

where γ is a vector containing all γ_m's. The last constraint in (5.17) may be excluded from the dual formula since it can be implicitly imposed on the problem. S_{budget}, C^r_{budget}, C^t_{budget} and $t_{mask,m}$ are predefined constants and hence do not influence the optimization problem. Therefore, $\hat{\Psi}$ in the above equation can be written as

$$\hat{\Psi} = \sum_{i\in\mathcal{I}} R_i - \lambda_t \sum_{i\in\mathcal{I}} \sum_{j=0}^{C_{max}} C^t_{ij} - \lambda_r \sum_{i\in\mathcal{I}} \sum_{p=0}^{T} C^r_{ip} - \alpha \sum_{i\in\mathcal{I}} s_i - \sum_{m=1}^{\bar{M}} \gamma_m t_{spec,m} \tag{5.19}$$

By substituting $T_{spec,m}$ from equation (5.14) into equation (5.19) we obtain,

$$\hat{\Psi} = \sum_{i\in\mathcal{I}} R_i - \lambda_t \sum_{i\in\mathcal{I}} \sum_{j=0}^{C_{max}} C^t_{ij} - \lambda_r \sum_{i\in\mathcal{I}} \sum_{p=0}^{T} C^r_{ip} - \alpha \sum_{i\in\mathcal{I}} s_i$$

$$- \sum_{m=1}^{\bar{M}} \gamma_m \sum_{i\in\mathcal{I}} s_i |F_i(e^{j\omega_m}) \hat{\mathbf{e}}^H(e^{j\omega_m}) \mathbf{w}_i|^2 \tag{5.20}$$

The dual optimization problem can then be written as

$$\min_{\gamma,\alpha,\lambda_t,\lambda_r} \left\{ \max_{\mathbf{C}^t,\mathbf{C}^r,\mathbf{S}} (\hat{\Psi}) \right\}$$

where,

$$\hat{\Psi} = \sum_{i\in\mathcal{I}} R_i - \lambda_t \sum_{i\in\mathcal{I}} \sum_{j=0}^{C_{max}} C_{ij}^t - \lambda_r \sum_{i\in\mathcal{I}} \sum_{p=0}^{T} C_{ip}^r - \alpha \sum_{i\in\mathcal{I}} s_i$$

$$- \sum_{m=1}^{\bar{M}} \gamma_m \sum_{i\in\mathcal{I}} s_i |F_i(e^{j\omega_m}) \hat{\mathbf{e}}^H(e^{j\omega_m}) \mathbf{w}_i|^2$$

$$\alpha, \gamma_m, \lambda_t, \lambda_r > 0 \tag{5.21}$$

The computation of MMSE-PTEQ for tone i needs the information about the transmit power in all the other tones as seen in (5.4). Therefore, (5.20) cannot be decoupled in tones. In section 5.5, we will present a simple technique to effectively decouple the problem in tones and hence reduce the computational complexity. Furthermore, (5.20) is combinatorial in $\mathbf{c}_i^r$ and $\mathbf{c}_i^t$. In section 5.5, we will present techniques to reduce the combinatorial complexity based on contiguous tap selection or sparse approximation based filter design.

5.4 Resource allocation for a fixed power loading

Here, we present an alternative approach that is based on restating the constrained optimization problem as an unconstrained dual problem as shown in (5.16). Let us rewrite the equation below for the sake of convenience,

For $i \in \mathcal{I}$

$$\min_{\lambda_r,\lambda_t,\gamma} \left\{ \max_{\mathbf{c}_i^t,\mathbf{c}_i^r} \quad \psi_i \right\},$$

where

$$\psi_i = R_i - \lambda_t \sum_{j=0}^{C_{max}} {C_{ij}}^t - \lambda_r \sum_{p=0}^{T} {C_{ip}}^r - \sum_{m=1}^{\bar{M}} \gamma_m s_i |F_i(e^{j\omega_m}) \hat{\mathbf{e}}^H(e^{j\omega_m}) \mathbf{w}_i|^2$$

$$\lambda_r, \lambda_t, \gamma \geq 0. \tag{5.22}$$

The computational complexity of (5.22) is combinatorial in $\mathbf{c}_i^t$ and $\mathbf{c}_i^r$, i.e., $\mathcal{O}(M2^{(C_{max}+1)(T+1)})$. This complexity can be reduced if we can fix the sparsity pattern of the per-tone filters. In the following section, we present two different approaches to fix the sparsity pattern in order to reduce the computational complexity.

5.4.1 Contiguous tap selection based resource allocation

One way to fix the sparsity pattern of the filters is to restrict the sparsity pattern of the filters such that only contiguous taps can be non-zero. This is known as contiguous tap selection. This reduces the combinatorial search into a linear search over the filter orders. The equation (5.22) can then be written as

$$\text{For} \quad i \in \mathcal{I}$$

$$\min_{\lambda_t,\lambda_r,\gamma} \left\{ \max_{\mathbf{c}_i^t,\mathbf{c}_i^r} \quad \psi_i \right\},$$

where

$$\psi_i = R_i - \lambda_t L_i^t - \lambda_r L_i^r - \sum_{m=1}^{\bar{M}} \gamma_m s_i |F_i(e^{j\omega_m})\hat{\mathbf{e}}^H(e^{j\omega_m})\mathbf{w}_i|^2$$

$$\lambda_t, \lambda_r, \gamma \geq 0, \tag{5.23}$$

where L_i^t and L_i^r are the filter order of the pulse shaping filter and the MMSE-PTEQ for the ith tone respectively.

This per-tone optimization problem can be solved (for fixed Lagrange multipliers) by exhaustively searching over all combinations of L_i^t and L_i^r. For a fixed Lagrange multiplier, the computational complexity then becomes $\mathcal{O}(M(C_{max}+1)(T+1))$. The complexity can be further reduced by fixing the MMSE-PTEQ filter order while optimizing the pulse shaping filter order. And then with the optimized pulse shaping filter order, proceed and optimize MMSE-PTEQ filter order. Therefore, avoiding exhaustive search over all combinations of L_i^t and L_i^r. The computational complexity then becomes $\mathcal{O}(M(C_{max}+T+2))$. The values of Lagrange multipliers can then be updated until all the PSD constraints are met. The Lagrange multipliers, γ_m are updated based on the difference between the PSD mask and the output PSD, i.e.

$$\gamma_m^{t+1} = \gamma_m^t - \mu_m(t_{mask,m} - t_{spec,m}) \tag{5.24}$$

where μ_m is the step size for the update which is always positive. The μ_m can be varied in order to drop the energy at a frequency point quickly if the output spectrum at that frequency exceeds the PSD mask and to cautiously increase it if the output spectrum is under the PSD mask. A typical initialization value for $\gamma = \{\gamma_m\}$ is $\mathbf{0}$ and then $\mu = \{\mu_m\}$ can be initialized with a value generally much larger than 1 as we need to establish a very high value for γ in order to make the $\sum_m \gamma_m P_i |F_i(\omega_m)\mathbf{e}^H(\omega_m)\mathbf{w}_i|^2$ comparable to the value L_i^t and L_i^r.

The Lagrange multipliers λ_t and λ_r can be updated as

$$\lambda_t^{t+1} = \lambda_t^t - \mu_t(C_{budget}^t - \sum_{i \in \mathbf{I}} L_i^t) \tag{5.25}$$

$$\lambda_r^{t+1} = \lambda_r^t - \mu_r(C_{budget}^r - \sum_{i \in \mathbf{I}} L_i^r), \tag{5.26}$$

where μ_t and μ_r are the step sizes. The algorithm stops when the number of taps stops updating. An algorithm description is given in **Alg. 5.1**.

In the following section, we present an alternative approach to fix the sparsity pattern of the filters based on sparse approximation based filter design.

5.4.2 Sparse approximation based filte tap allocation under fixed power loading

Computing sparse per-tone pulse shaping filters

In the previous section, it was shown that if we can fix the sparsity pattern of the per-tone pulse shaping filter and the MMSE-PTEQ, the computational complexity of the optimization problem will reduce significantly. In chapter 3 and chapter 4, it was shown that in order to fix the sparsity pattern, a sparse per-tone pulse shaping filter and a sparse MMSE-PTEQ can be directly computed. For the sake of convenience, let us rewrite the formula to compute sparse per-tone pulse shaping filter and sparse MMSE-PTEQ as follows

$$\min_{\mathbf{w}_i} \quad \mathbf{w}_i^H \mathbf{Q}_i \mathbf{w}_i + \bar{\tau} \left\|\mathbf{w}_i\right\|_1 \quad \text{subject to} \quad W_i(e^{j\omega_i}) = 1, \tag{5.27}$$

$$\boxed{\underset{\mathbf{v}_i}{\text{minimize}} \quad \left\|\mathbf{A}_i \mathbf{v}_i^* - \mathbf{b}_i\right\|_2^2 + \beta \left\|\mathbf{v}_i\right\|_1,} \tag{5.28}$$

Algorithm 5.1 Contiguous tap selection based filter tap allocation

Initialize
repeat
  for tone $i \in \mathcal{I}$ **do**
    Compute $\mathbf{v}_i$ of order $L^r_{i,opt}$
    for Pulse shaping filter order $L^t_i = 1 \cdots C_{max}$ **do**
      compute $\mathbf{w}_i$ of order L^t_i
      $L^t_{i,opt} \Leftarrow \underset{L^t_i}{\text{argmax}} R_i - \lambda L^t_i - \sum_{m=1}^{\bar{M}} \gamma_m s_i |F_i(e^{j\omega_m}) \hat{\mathbf{e}}^H(e^{j\omega_m}) \mathbf{w}_i|^2$
    end for
    for PTEQ filter order $L^r_i = 1 \cdots T$ **do**
      compute $\mathbf{v}_i$ of order L^r_i
      $L^r_{i,opt} \Leftarrow \underset{L^r_i}{\text{argmax}} R_i - \lambda L^r_i$
    end for
  end for
  compute $\mathbf{t}_{spec}$
  for $m = 1 \cdots \bar{M}$ **do**
    $\gamma^{t+1}_m = [\gamma^t_m - \mu_m (t_{mask,m} - t_{spec,m})]^+$
  end for
  $\lambda^{t+1} = \left[\lambda^t - \bar{\mu} \left(C_{budget} - \sum_{i \in \mathcal{I}} (L^t_{i,opt} + L^r_{i,opt})\right)\right]^+$
until (no change in total filter taps)

Sparse approximation based tap allocation under fixed power loading

Since we compute the sparsity pattern $\mathbf{c}^t_i$ and $\mathbf{c}^r_i$ directly using (5.27) and (5.28) and then applying the threshold, there is no need to minimize any objective function. The problem reduces to iteratively computing $\mathbf{w}_i$ and $\mathbf{v}_i$ for different $i \in \mathcal{I}$ and then checking if the PSD mask constraint and the total pulse shaping filter tap constraint and total MMSE-PTEQ tap constraint are met. An algorithm description is given below to iteratively optimize the total number of filter taps needed to fulfill the PSD mask constraint in **Alg. 5.2**. The complexity of the proposed algorithm is then $O(M * \kappa)$ per Lagrange multiplier update, where κ is the cost associated with computing the nearly-sparse filter and then a sparse filter. For large C_{max} and T, the computational complexity of sparse approximation based per-tone pulse shaping filter tap allocation under fixed power is similar to the per-tone exhaustive search on a restricted search space presented in section 5.4.1.

Algorithm 5.2 sparse approximation based filter tap allocation

Initialize
repeat
  for tone $i \in \mathcal{I}$ **do**
    Compute nearly sparse $\mathbf{w}_i$ by solving
    $\min_{\mathbf{w}_i} \quad \mathbf{w}_i^H \mathbf{Q}_i \mathbf{w}_i + \bar{\tau} \left\|\mathbf{w}_i\right\|_1 \quad \text{subject to} \quad W_i(e^{j\omega_i}) = 1$
    apply threshold and obtain the sparsity pattern $\mathbf{c}_i^t$
    Compute sparse $\mathbf{w}_i$ using
    Compute nearly sparse $\mathbf{v}_i$ by solving
    $\min_{\mathbf{v}_i} \quad \left\|\mathbf{A}_i \mathbf{v}_i^* - \mathbf{b}_i\right\|_2^2 + \beta \left\|\mathbf{v}_i\right\|_1$
    apply threshold and obtain sparsity pattern $\mathbf{c}_i^r$
    recompute sparse $\mathbf{v}_i$ by solving
  end for
  compute $\mathbf{t}_{spec}$
  for $m = 1 \cdots \bar{M}$ **do**
    $\gamma_m^{t+1} = \left[\gamma_m^t - \mu_m \left(t_{mask,m} - t_{spec,m}\right)\right]^+$
  end for
  $\lambda^{t+1} = \left[\lambda^t - \bar{\mu} \left(C_{budget} - \sum_{i \in \mathcal{I}} (L_{i,opt}^t + L_{i,opt}^r)\right)\right]^+$
until (no change in total filter taps)

5.5 Joint filter tap and transmit power allocation

For a single-user system without any PSD constraint the optimal transmit power allocation can be calculated by using the water filling procedure [40]. With a PSD constraint this is no longer applicable. In the previous section it was shown how to optimally allocate pulse shaping filter taps if the number of used tones and their transmit powers are known, for a system with PSD constraints. However, the number of used tones can be increased if a lower transmit power at the band edges is used. Therefore, by also allocating the appropriate amount of transmit power for each tone, the total achievable data rate can be maximized for a given total transmit power budget and total filter tap budgets. This then requires a procedure to distribute the available resources (total power and total filter tap budget) optimally over the tones such that the data rate is maximized and the PSD mask constraint is still met. Here, we present an approach that is again based on a dual problem formulation. The unconstrained dual optimization problem can be restated from (5.21). It is rewritten below for the sake of convenience

$$\min_{\gamma,\alpha,\lambda_t,\lambda_r} \left\{ \max_{\mathbf{C}^t,\mathbf{C}^r,\mathbf{S}} (\hat{\Psi}) \right\}$$

where,

$$\hat{\Psi} = \sum_{i\in\mathcal{I}} R_i - \lambda_t \sum_{i\in\mathcal{I}} \sum_{j=0}^{C_{max}} C_{ij}^t - \lambda_r \sum_{i\in\mathcal{I}} \sum_{p=0}^{T} C_{ip}^r - \alpha \sum_{i\in\mathcal{I}} s_i$$

$$- \sum_{m=1}^{\bar{M}} \gamma_m \sum_{i\in\mathcal{I}} s_i |F_i(e^{j\omega_m}) \hat{\mathbf{e}}^H(e^{j\omega_m}) \mathbf{w}_i|^2$$

$$\alpha, \gamma_m, \lambda_t, \lambda_r > 0 \tag{5.29}$$

5.5.1 Contiguous tap selection based joint filter tap and transmit power allocation

Equation 5.29 can be rewritten in the dual form with Lagrange multipliers as

$$\min_{\gamma,\alpha,\lambda_t,\lambda_r} \left\{ \max_{L_i^t,L_i^r,\mathbf{S}} (\hat{\Psi}) \right\}$$

where,

$$\hat{\Psi} = \sum_{i\in\mathcal{I}} R_i - \lambda_t \sum_{i\in\mathcal{I}} L_i^t - \lambda_r \sum_{i\in\mathcal{I}} L_i^r - \alpha \sum_{i\in\mathcal{I}} s_i - \sum_{m=1}^{\bar{M}} \gamma_m \sum_{i\in\mathcal{I}} s_i |F_i(e^{j\omega_m}) \hat{\mathbf{e}}^H(e^{j\omega_m}) \mathbf{w}_i|^2$$

$$\gamma_m, \alpha, \lambda_t, \lambda_r > 0 \tag{5.30}$$

As L_i^t and L_i^r are filter order of the per-tone pulse shaping filter and the MMSE-PTEQ respectively. But (5.30) is still coupled in tones since the computation of the MMSE-PTEQ on tone i requires the transmit power on all the tones to be known. To simplify the problem, we can iteratively update each user's power, as suggested in chapter 4. Perform transmit power allocation and the filter tap allocation in tone i by fixing the transmit power on all the other tones. Then repeat the process for tone $i+1$ with a recently allocated transmit power on tone i. This iterative update decouples (5.30) over tone and hence the per-tone optimization problem now can be written as,

$$\min_{\gamma,\alpha,\lambda_t,\lambda_r} \left\{ \max_{L_i^t, L_i^r, s_i} (\hat{\psi}_i) \right\}$$

where,

$$\hat{\psi}_i = R_i - \lambda_t L_i^t - \lambda_r L_i^r - \alpha s_i - \sum_{m=1}^{\bar{M}} \gamma_m s_i |F_i(e^{j\omega_m}) \hat{\mathbf{e}}^H (e^{j\omega_m}) \mathbf{w}_i|^2$$

$$\gamma, \alpha, \lambda_j > 0 \tag{5.31}$$

where γ is a vector containing all γ_m's. This per-tone optimization problem can be solved (for fixed Lagrange multiplier) by exhaustively searching over all values of s_i (i.e. from -140dBm to P_{max}(-60dBm) in discrete steps) and all filter orders L_i^t and L_i^r. The values of the Lagrange multipliers can then be updated until all the constraints are met. An algorithm description is given below.

The Lagrange multipliers ($\gamma, \alpha, \lambda_t$ and λ_r) are updated based on the difference between the obtained values for the corresponding resources and their target values, i.e.

$$\gamma_j^{t+1} = \lambda_j^t - \mu_m (t_{mask,m} - t_{spec,m})$$

$$\lambda_t^{t+1} = \gamma_t^t - \hat{\mu}_t (C_{budget}^t - \sum_{i \in \mathcal{I}} L_i^t)$$

$$\lambda_r^{t+1} = \gamma_r^t - \hat{\mu}_r (C_{budget}^r - \sum_{i \in \mathcal{I}} L_i^r)$$

$$\alpha_i^{t+1} = \alpha_i^t - \bar{\mu} (S_{budget} - \sum_{i \in \mathcal{I}} s_i)$$

where μ_m, $\hat{\mu}_t$, $\hat{\mu}_r$, and $\bar{\mu}$ are the step sizes for the updates which are always positive.

5.5.2 Sparse approximation based joint filter tap and transmit power allocation

We can rewrite the per-tone optimization problem for the joint per-tone pulse shaping filter tap allocation and power loading given in (5.21) as

$$\hat{\Psi} = \sum_{i \in \mathcal{I}} R_i - \lambda_t \sum_{i \in \mathcal{I}} \sum_{j=0}^{C_{max}} C_{ij}^t - \lambda_t \sum_{i \in \mathcal{I}} \sum_{p=0}^{T} C_{ip}^r - \alpha \sum_{i \in \mathcal{I}} s_i$$
$$- \sum_{m=1}^{\bar{M}} \gamma_m \sum_{i \in \mathcal{I}} s_i |F_i(e^{j\omega_m}) \hat{\mathbf{e}}^H (e^{j\omega_m}) \mathbf{w}_i|^2 \tag{5.32}$$

Algorithm 5.3 Contiguous tap selection based filter tap allocation

Initialize
repeat
  for tone $i \in \mathcal{I}$ **do**
    Compute $\mathbf{v}_i$ of order $L^r_{i,opt}$
    for Pulse shaping filter order $L^t_i = 1 \cdots C_{max}$ **do**
      compute $\mathbf{w}_i$ of order L^t_i
      $L^t_{i,opt} \Leftarrow \underset{L^t_i}{\text{argmax}} R_i - \lambda L^t_i - \sum_{m=1}^{\bar{M}} \gamma_m s_i |F_i(e^{j\omega_m}) \hat{\mathbf{e}}^H(e^{j\omega_m}) \mathbf{w}_i|^2$
    end for
    for PTEQ filter order $L^r_i = 1 \cdots T$ **do**
      compute $\mathbf{v}_i$ of order L^r_i
      $L^r_{i,opt} \Leftarrow \underset{L^r_i}{\text{argmax}} R_i - \lambda L^r_i$
    end for
  end for
  compute $\mathbf{t}_{spec}$
  for $m = 1 \cdots \bar{M}$ **do**
    $\gamma^{t+1}_m = [\gamma^t_m - \mu_m (t_{mask,m} - t_{spec,m})]^+$
  end for
  $\lambda^{t+1} = \left[\lambda^t - \bar{\mu} \left(C_{budget} - \sum_{i \in \mathcal{I}} (L^t_{i,opt} + L^r_{i,opt})\right)\right]^+$
until (no change in total filter taps)

This can be written as

$$\begin{aligned} \hat{\Psi} = \quad & \textstyle\sum_{i \in \mathcal{I}} R_i - \lambda_t \sum_{i \in \mathcal{I}} \|\mathbf{w}_i\|_0 - \lambda_t \sum_{i \in \mathcal{I}} \|\mathbf{v}_i\|_0 - \alpha \sum_{i \in \mathcal{I}} s_i \\ & - \textstyle\sum_{m=1}^{\bar{M}} \gamma_m \sum_{i \in \mathcal{I}} s_i |F_i(e^{j\omega_m}) \hat{\mathbf{e}}^H(e^{j\omega_m}) \mathbf{w}_i|^2 \end{aligned} \tag{5.33}$$

For a given λ_t and λ_r, $\lambda_t \|\mathbf{w}_i\|_0 + \lambda_r \|\mathbf{v}_i\|_0$ is a constant since $\|\mathbf{w}_i\|_0$ and $\|\mathbf{v}_i\|_0$ are fixed while designing. Hence, it can be removed from the optimization problem. By fixing the sparsity pattern using the sparse approximation technique the total computational complexity of sparse approximation based approach is $\mathcal{O}(M\tilde{L} + \kappa)$ per Lagrange multiplier iteration in contrast to $\mathcal{O}(M\tilde{L}(C_{max} + T + 2))$ per Lagrange multiplier iteration in contiguous tap selection based approach discussed in the previous section. For large C_{max} and T, this is a significant reduction in computational complexity. The values of the Lagrange multipliers can then be updated until all the constraints are met. An algorithm description is given in **Alg. 5.2**. The Lagrange multiplier λ_m could be updated using (3.27) and Lagrange multiplier α can be updated based on the difference between the obtained values

for the corresponding resources and their target values, i.e.

$$\alpha_i^{t+1} = \left[\alpha_i^t - \tilde{\mu}(S_{budget} - \sum_{i \in \mathcal{I}} s_i) \right]^+ \tag{5.34}$$

where $\tilde{\mu}$ is a positive step size.

Algorithm 5.4 sparse approximation based filter tap allocation

Initialize
repeat
  for tone $i \in \mathcal{I}$ **do**
    Compute nearly sparse $\mathbf{w}_i$ by solving
    $\min_{\mathbf{w}_i} \quad \mathbf{w}_i^H \mathbf{Q}_i \mathbf{w}_i + \bar{\tau} \left\| \mathbf{w}_i \right\|_1 \quad \text{subject to} \quad W_i(e^{j\omega_i}) = 1$
    apply threshold and obtain the sparsity pattern $\mathbf{c}_i^t$
    Compute sparse $\mathbf{w}_i$ using
    Compute nearly sparse $\mathbf{v}_i$ by solving
    $\min_{\mathbf{v}_i} \quad \left\| \mathbf{A}_i \mathbf{v}_i^* - \mathbf{b}_i \right\|_2^2 + \beta \left\| \mathbf{v}_i \right\|_1$
    apply threshold and obtain sparsity pattern $\mathbf{c}_i^r$
    recompute sparse $\mathbf{v}_i$ by solving
  end for
  compute $\mathbf{t}_{spec}$
  for $m = 1 \cdots \bar{M}$ **do**
    $\gamma_m^{t+1} = \left[\gamma_m^t - \mu_m \left(t_{mask,m} - t_{spec,m} \right) \right]^+$
  end for
  $\lambda^{t+1} = \left[\lambda^t - \bar{\mu} \left(C_{budget} - \sum_{i \in \mathcal{I}} (L_{i,opt}^t + L_{i,opt}^r) \right) \right]^+$
until (no change in total filter taps)

5.6 Simulation results

The channel under consideration here is a 400m twisted pair cable in a bundle of 8 with an interference channel of 400m. In the first scenario, the tones used for transmission are fixed as suggested in [33], i.e., 375 predefined tones, in order to compare with the results in chapter 3. Furthermore, the transmit power for all the tones are assumed to be constant, i.e., -60 dBm/Hz.

5.6.1 Resource allocation for a fixed power loading

In **Figure 5.1**, it can be seen that the allocation of number of taps in the DMT transmitter, i.e., the pulse shaping filter, is same as in the scenario when we

Total filter taps	CTS based approach	SA based approach
5000	9	9
1000	15	13

Table 5.1: Number of outer iterations taken to converge to the solution a fixed transmit power loading

had only transmitter run-time complexity optimization with assumption that the receiver is perfect as described in chapter 3. This is due to the fact that for a fixed number of tones with fixed power loading, the PSD constraint only depends on the pulse shaping filter. Therefore, parameters at the receiver does not affect it. But the MMSE-PTEQ filter tap distribution is affected in order to accommodate the effect of the per-tone pulse shaping at the transmitter. Similar observations can be made in Figure 5.2 for sparse approximation based tap allocation in this scenario. The transmit PSD for this scenario is same as for the scenario when the transmit per-tone pulse shaping filter was optimized without taking the effect of receiver into account. This is illustrated in **Figure 5.3** in the form of transmit PSD in this scenario. It can also be seen that the sparse approximation based approach outperforms the contiguous tap selection based approach. From **Table 5.1**, it can be seen that the sparse approximation based approach converges to the solution faster than the contiguous tap selection approach.

5.6.2 Joint per-tone equalizer tap and transmit power allocation

In the second scenario, now we make all the 428 tones available for the data transmission. The total available power is 11.5 dBm [10]. The tap distribution over tones for both contiguous tap selection based approach and the sparse approximation based approach is now coupled in both transmit pulse shping filter tap budget as well as MMSE-PTEQ filter tap budget. Therefore, the tap distribution in both per-tone pulse shaping based DMT transmitter and the MMSE-PTEQ based DMT receiver vary from the independent optimization problems presented in chapter 3 and chapter 4. This enables joint optimization to perform better than the independent optimization for a given constraint. Since, the joint optimization of the tranceiver filter taps has to consider each others resource constraints implicitly, it always performs better than the blind independent resource allocation. **Table 5.3** and **5.4** presents the achievable bit rate for different combinations of transmit pulse shaping filter budget and MMSE-PTEQ tap budget for joint filter tap and transmit power allocation using contiguous tap selection based approach and sparse approximation based joint filter tap and transmit power allocation respectively. It can be seen that the sparse approximation approach outperforms the contiguous tap based approach.

Total filter taps	CTS based approach	SA based approach
5000	25	21
1000	30	28

Table 5.2: Number of outer iterations taken to converge to the solution for a joint filter tap and transmit power allocation

MMSE-PTEQ taps \ PTPS taps	1000	3000	5000
1000	22.99	24.12	25.8
2000	23.028	34.01	35.6
3000	23.06	39.73	40.1
4000	23.09	41.61	42.08
5000	23.091	42.81	42.9

Table 5.3: Achievable bit rate in Mbps for various combinations of MMSE-PTEQ filter tap and per-tone pulse shaping (PTPS) filter tap constraint using contiguous tap selection based approach and transmit power allocation

From **Table 5.2**, it can be seen that the sparse approximation based approach converges to the solution faster than the contiguous tap selection approach.

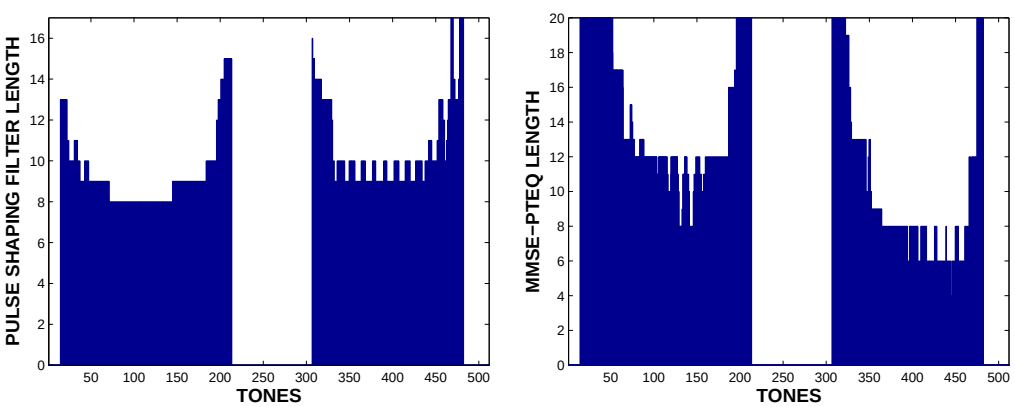

(a) (b)

Figure 5.1: For a fixed transmit power loading, optimum distribution of (a) pulse shaping filter taps (b) MMSE-PTEQ taps, using contiguous tap selection approach

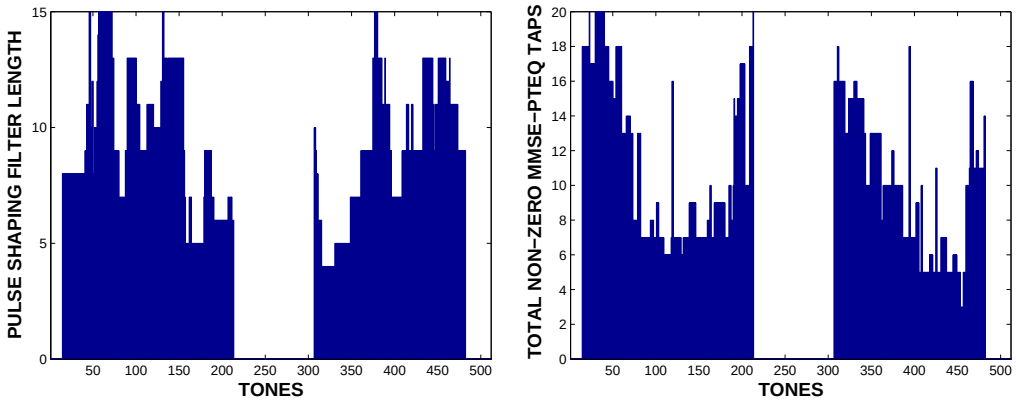

(a) (b)

Figure 5.2: For a fixed transmit power loading optimum distribution of (a) pulse shaping filter taps (b) MMSE-PTEQ taps, using sparse approximation based approach

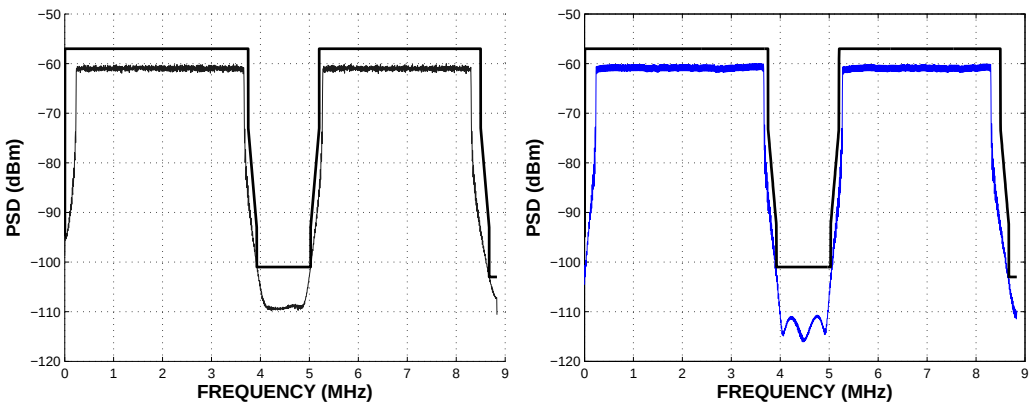

(a) (b)

Figure 5.3: For a fixed transmit power loading, transmit PSD for (a) the contiguous tap selection based approach (b) the sparse approximation based approach

5.7 Conclusion

In this chapter, a per-tone pulse shaping and MMSE-PTEQ based DMT transceiver is considered. It is first shown that the presence of per-tone pulse shaping filter affects the tap allocation in the per-tone based receiver under a

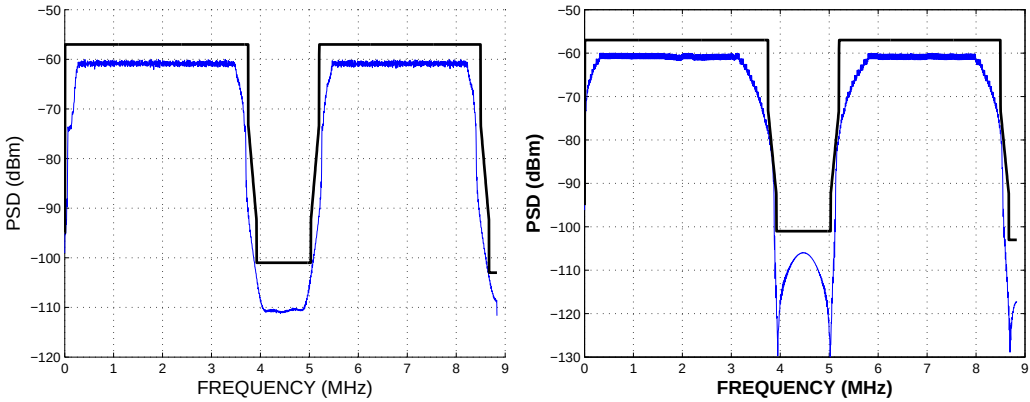

(a) (b)

Figure 5.4: Transmit PSD in the case of joint filter tap and transmit power allocation for the tap budget of 5000 taps each in the DMT transmitter and the DMT receiver using (a) the contiguous tap selection based approach, (b) the sparse approximation based approach

PTPS taps / MMSE-PTEQ taps	1000	3000	5000
1000	24.85	26.7	27.6
2000	24.91	35.88	36.4
3000	24.96	41.03	42.1
4000	25	43.67	44.6
5000	25.01	44.81	45.133

Table 5.4: Achievable bit rate in Mbps for various combinations of MMSE-PTEQ filter tap and per-tone pulse shaping (PTPS) filter tap constraint using sparse approximation based approach and transmit power allocation

constant transmit power loading. It was also shown that the joint filter tap optimization problem in the DMT transceiver could be decoupled in tone by formulating as a dual problem along with a iterative MMSE-PTEQ computation scheme. It can be seen that the achievable bit rate for the same number of taps is lower in the presence of per-tone pulse shaping filter. This is due to the fact that the pulse shaping filter act as a dispersive channel and hence lengthens the output of the transmitter. In our case, we do not increase the overall symbol length, but decrease the effective cyclic prefix to accommodate the extra symbol, therefore better per-tone equalizers are needed to mitigate the effects. Similarly in the case of joint filter tap and transmit power allocation in the DMT transceiver

the effect such as filtering effect at the edge of the bands at the receiver is also taken into account while performing transmit power allocation at the transmitter. This improves the performance of the system for the same number of non-zero filter taps.

Part II

MULTI-USER RESOURCE ALLOCATION

Chapter 6

Resource allocation in crosstalk cancellation

6.1 Introduction

To meet the demand for higher data rates, recent DSL systems use higher frequencies, e.g. up to 30 MHz [142]. At these frequencies, it has been shown that out-of-domain (alien) and in-domain crosstalk between different DSL lines in the same bundle become the dominant source of interference, limiting the performance of the DSL systems.

Crosstalk cancellation is one way to mitigate the effect of crosstalk. Several crosstalk cancellation techniques have been proposed in e.g. [144, 28, 60, 173, 25]. Different techniques may require different levels of transmitter and receiver coordination. In the case of upstream VDSL, only receiver coordination is possible, therefore a successive interference cancellation scheme performs optimally [60, 173]. However, the upstream VDSL channel matrix has a CWDD structure which is due to the fact that the power transmitted on a direct channel is always much larger than the power transmitted on any crosstalk channel by the same transmitter. In [25], under the assumption that the background noise is AWGN, it was shown that the CWDD structure allows a simple linear ZF canceler to perform near optimally. Furthermore, in [27], it was shown that even for simple linear canceler such as linear ZF, the run-time complexity increase with the square of the number of lines. For practical values of number of lines and number of tones, it becomes computationally infeasible. For example, a binder of 8 VDSL lines with 4096 tones and transmitting at a block rate of 4000 blocks per second, the run-time complexity of crosstalk cancellation is larger than 1 billion multiplication per second..

It was shown in [27] that the majority of the crosstalk originates from a small set of crosstalkers on a limited number of tones. Therefore, only a fraction of the original crosstalk cancellation is actually required to cancel most of the crosstalk. To reduce the run-time complexity of the crosstalk cancellation, in [27], a technique to cancel only the strong interferers was introduced. This technique is known as partial crosstalk cancellation.

However, in the case of spatially correlated background noise, e.g., when alien crosstalk is present, a prewhitening operation is needed to whiten the noise [21]. This operation destroys the CWDD structure of the channel matrix. The linear ZF canceler is then found to perform very poorly. In this scenario, an alternative structure that exploits the information provided by the noise correlation matrix should be used. For this purpose, MMSE-based cancelers, both linear and nonlinear, are the natural choices. The linear MMSE canceler is a very simple structure but it significantly outperforms the linear ZF canceler in the presence of spatially correlated noise. However, it is still a suboptimal canceler. MMSE-GDFE is shown to perform optimally under spatially correlated background noise [142]. It is however more complex than the linear canceler.

The MMSE based cancelers also suffer from the run-time complexity issue. To reduce the run-time complexity of the MMSE based cancelers, partial crosstalk cancellation can again be used. One of the advantages of using a linear ZF canceler is that there exists a very simple strategy to perform partial crosstalk cancellation. However, for MMSE-based cancelers there is no obvious strategy that can be followed to realize partial cancellation. Earlier approaches [177, 12] adopt some per-line/per canceler exhaustive search method, which is computationally complex. The complexity of the partial crosstalk cancellation selection schemes increases significantly, if it is combined with optimal spectrum balancing (OSB). In this chapter, we propose algorithms to reduce the complexity of the partial crosstalk cancellation scheme in MMSE based crosstalk cancelers with and without spectrum balancing.

This chapter is organized as follows: In **section 6.2**, the multi-user DSL system with spatially correlated background noise (alien crosstalk) is introduced.

In **section 6.3**, various crosstalk cancelers are presented and their performance in the presence of spatially correlated noise is compared. We show that the MMSE-based cancelers, i.e., the linear MMSE canceler and the MMSE-GDFE, perform significantly better than the linear ZF canceler in this scenario.

In section **6.4**, we first present a scheme to compute the crosstalk canceler coefficients once the lines to be cancelled are chosen.

In **section 6.5**, the partial crosstalk cancellation is formulated as an optimization problem in the case of a fixed power loading, i.e., no spectrum balancing, and in the case of the joint partial crosstalk cancellation and spectrum balancing.

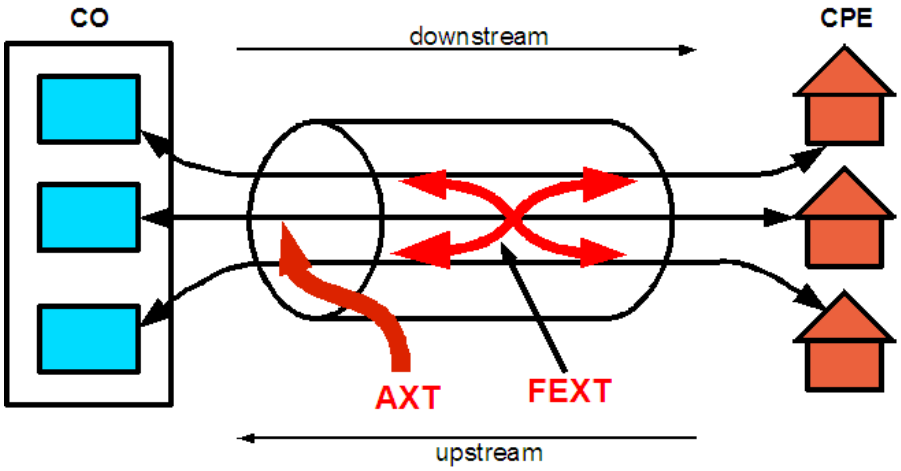

Figure 6.1: A typical VDSL scenario with co-located receivers at the CO (central office) and non co-located transmitters at the CPE (customer-premises equipment) side

In **section 6.6**, efficient algorithms for partial crosstalk cancellation for linear MMSE-based crosstalk cancelers based on selection metrics and sparse canceler design are proposed for scenarios both with and without spectrum balancing.

In **section 6.7**, the algorithms developed for the linear MMSE based partial crosstalk cancellation is then extended to perform partial crosstalk in the nonlinear MMSE crosstalk cancelers.

In **section 6.8**, simulation results are presented. Finally, in **section 6.9** conclusions are drawn.

6.2 System model

In this paper, we consider DMT-based upstream VDSL transmission, where the receivers are co-located as shown in **Fig.** 6.1. The system is first described by

$$\underbrace{\begin{bmatrix} y_k^1 \\ \vdots \\ y_k^N \end{bmatrix}}_{\mathbf{y}_k} = \underbrace{\begin{bmatrix} h_k^{1,1} & \cdots & h_k^{1,N} \\ \vdots & \ddots & \cdots \\ h_k^{N,1} & \cdots & h_k^{N,N} \end{bmatrix}}_{\mathbf{H}_k} \underbrace{\begin{bmatrix} x_k^1 \\ \vdots \\ x_k^N \end{bmatrix}}_{\mathbf{x}_k} + \underbrace{\begin{bmatrix} n_k^1 \\ \vdots \\ n_k^N \end{bmatrix}}_{\mathbf{n}_k}, \tag{6.1}$$

where k is the tone index ($k = 1 \cdots K$), x_k^n and y_k^n are the transmitted and received symbols in line n on tone k and n_k^n is the additive spatially white Gaussian background noise (AWGN) experienced by line n on tone k, such that $E\{\mathbf{n}_k \mathbf{n}_k^H\} = \sigma_k^2 \mathbf{I}_N$, where $\{.\}^H$ denotes the Hermitian transpose operation and $E\{.\}$ denotes the expected value operation. Finally, $h_k^{(n,n)}$ is the direct channel for line n on tone k and $h_k^{(n,m)}$ is the crosstalk channel from line m into line n. Let $E\{\mathbf{x}_k \mathbf{x}_k^H\} = \mathbf{S}_k$. Since the transmitters are not coordinated, $\mathbf{S}_k$ is a diagonal matrix. Furthermore, it is assumed that the transmitters have a fixed transmit spectrum which can not be changed during the data transmission. Here, the channel matrix $\mathbf{H}_k$ is CWDD [25].

In the presence of alien crosstalk, the above model is generalized as

$$\begin{bmatrix} y_k^1 \\ \vdots \\ y_k^N \end{bmatrix} = \begin{bmatrix} h_k^{1,1} & \cdots & h_k^{1,N} \\ \vdots & \ddots & \cdots \\ h_k^{N,1} & \cdots & h_k^{N,N} \end{bmatrix} \begin{bmatrix} x_k^1 \\ \vdots \\ x_k^N \end{bmatrix} + \underbrace{\begin{bmatrix} h_k^{1,axt1} & \cdots & h_k^{1,axtm} \\ \vdots & \ddots & \cdots \\ h_k^{N,axt1} & \cdots & h_k^{N,axtm} \end{bmatrix} \begin{bmatrix} x_k^{axt1} \\ \vdots \\ x_k^{axtm} \end{bmatrix}}_{\text{Alien Crosstalk } (\mathbf{a}_k)} + \begin{bmatrix} n_k^1 \\ \vdots \\ n_k^N \end{bmatrix}. \tag{6.2}$$

In (6.2), $\mathbf{a}_k$ is the vector containing the sum of all the alien crosstalk contributions. Hence, (6.2) can be succinctly written as

$$\begin{aligned} \mathbf{y}_k &= \mathbf{H}_k \mathbf{x}_k + \underbrace{\mathbf{a}_k + \mathbf{n}_k}_{\mathbf{z}_k} \\ &= \mathbf{H}_k \mathbf{x}_k + \mathbf{z}_k \end{aligned} \tag{6.3}$$

Even though the individual alien crosstalk channels are not known at the receiver, it is assumed that the total noise correlation matrix $\mathbf{R}_{kz} = E\{\mathbf{z}_k \mathbf{z}_k^H\}$ is known or can be estimated. Generally, the alien crosstalk is spatially correlated therefore the correlation matrix $\mathbf{R}_{kz}$ is not a diagonal matrix.

6.3 MMSE-based crosstalk cancellation

The upstream VDSL scenario with receiver coordination and no transmitter coordination corresponds to the multiple access channel (MAC) in information theory. The capacity of this MAC in the AWGN case can be written as [21]

$$b = \sum_k \log_2 |\mathbf{I}_N + \sigma_k^{-2} \mathbf{H}_k \mathbf{S}_k \mathbf{H}_k^H| \tag{6.4}$$

In [25], it was shown that due to the CWDD structure of the channel matrix $\mathbf{H}_k$, a simple linear ZF canceler can be used to obtain near-optimal capacity approaching performance.

In the case of alien crosstalk, the background noise is spatially correlated. The capacity formula then includes a prewhitening operation and can be written as [21]

$$\tilde{b} = \sum_k \log_2 |\mathbf{I}_N + \underbrace{(\mathbf{R}_{kz}^{-1/2} \mathbf{H}_k)}_{\tilde{\mathbf{H}}_k} \mathbf{S}_k (\mathbf{R}_{kz}^{-1/2} \mathbf{H}_k)^H|, \tag{6.5}$$

where $\tilde{\mathbf{H}}_k$ is the equivalent channel matrix after prewhitening. This equivalent channel matrix is no longer CWDD and hence a linear ZF canceler no longer provides near-optimal performance. We, therefore, consider MMSE-based cancelers which take the noise correlation matrix into account explicitly.

6.3.1 Linear MMSE canceler

The linear MMSE canceler output can be written as [163]

$$\hat{\mathbf{x}}_k = decision\left(\mathbf{W}_k \mathbf{y}_k\right), \tag{6.6}$$

where

$$\mathbf{W}_k = \mathbf{S}_k \mathbf{H}_k^H (\mathbf{H}_k \mathbf{S}_k \mathbf{H}_k^H + \mathbf{R}_{kz})^{-1} \tag{6.7}$$

is the $N \times N$ linear MMSE canceler matrix. Unlike the linear ZF canceler, the linear MMSE canceler takes the noise correlation matrix into account. This enables the linear MMSE canceler to cancel the alien crosstalk much more efficiently than the linear ZF canceler. In a high SNR AWGN scenario, the linear MMSE canceler approaches the linear ZF canceler.

6.3.2 Nonlinear MMSE canceler

The linear MMSE canceler in general performs suboptimally. A non-linear MMSE canceler such as the MMSE-GDFE [142, 60, 173, 162] and the MMSE-VBLAST [170] achieves optimal performance by feeding back the already detected symbols to remove the corresponding interference.

MMSE-GDFE

$$\mathbf{W}_{k,f} = (\mathbf{Q}_k)^{-1}(\mathbf{G}_k)^{-H}\mathbf{H}_k^H \tag{6.8}$$

where $\mathbf{Q}_k$ is a diagonal matrix and $\mathbf{G}^k$ is a monic lower triangular matrix. Here $\mathbf{Q}_k$ and $\mathbf{G}_k$ can be obtained from the Cholesky factorization of

$$(\bar{\mathbf{R}}_k)^{-1} = ((\mathbf{S}_k)^{-1} + \mathbf{H}_k^H(\mathbf{R}_{kz})^{-1}\mathbf{H}_k) \tag{6.9}$$

i.e.

$$(\bar{\mathbf{R}}_k)^{-1} = \mathbf{G}_k\mathbf{Q}_k\mathbf{G}_k^H. \tag{6.10}$$

The lower triangular structure of $\mathbf{G}^k$ defines a detection order (line 1 is detected first, line N is detected last). When different lines have different priorities, the highest priority line should be detected last [153]. In [60, 173], it was shown that the MMSE-GDFE performs optimally in the spatially correlated noise scenario.

6.3.3 Performance comparison

Fig. 6.2 plots a direct channel characteristic for a 1200m line and also shows the in-domain crosstalk from 6 other lines ranging from 600m to 1100m with increments of 100m, as simulated using the analytical channel model given in [52]. The dashed line gives an example of a typical alien crosstalk characteristic.

In the absence of alien crosstalk, it can be seen from **Fig.** 6.3(a) that the performance (i.e. total bit rate summed over 7 lines) of the linear ZF canceler, the linear MMSE canceler and the MMSE-GDFE are similar. As can be seen from **Fig.** 6.3(b), as soon as alien crosstalk is introduced the performance decreases for the linear cancelers. The performance of the linear ZF canceler is extremely poor whereas the linear MMSE canceler still provides relatively good performance. The best performance is given by the MMSE-GDFE. This is our motivation for using the MMSE-based cancelers. Even though the performance of the linear MMSE canceler is lower compared to the MMSE-GDFE, it has a lower complexity and hence represents an attractive intermediate solution. Even for the linear MMSE canceler, however, the complexity of full crosstalk cancellation is still $\mathcal{O}(N^2)$ [27], hence for a large number of lines the crosstalk cancellation becomes computationally heavy. This provides the motivation for developing partial crosstalk cancellation algorithms.

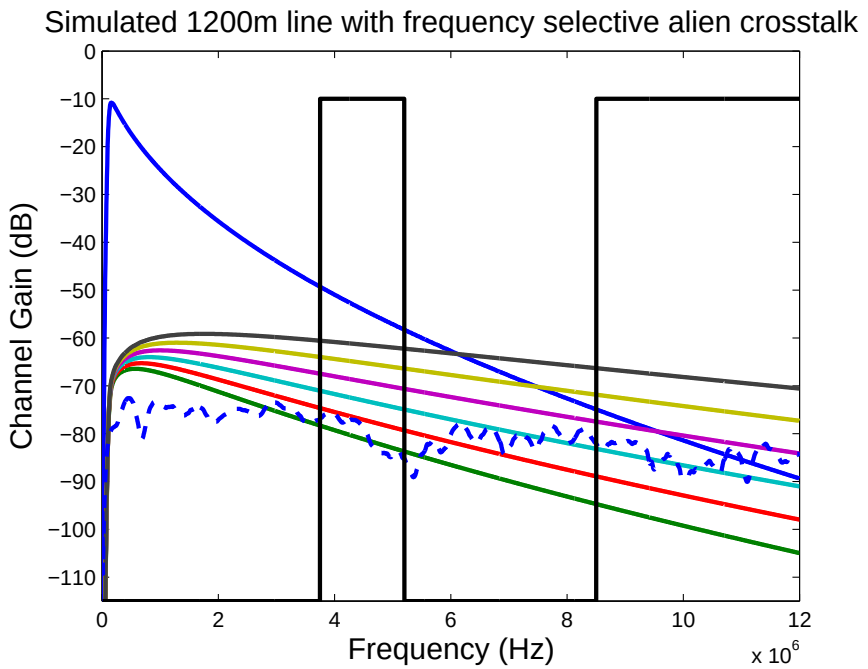

Figure 6.2: Channel characteristics for a 1200m line with 6 in-domain crosstalkers ranging from 600m to 1100m and an alien-crosstalker (dashed line). The solid black rectangular line represents the transmit band for upstream VDSL.

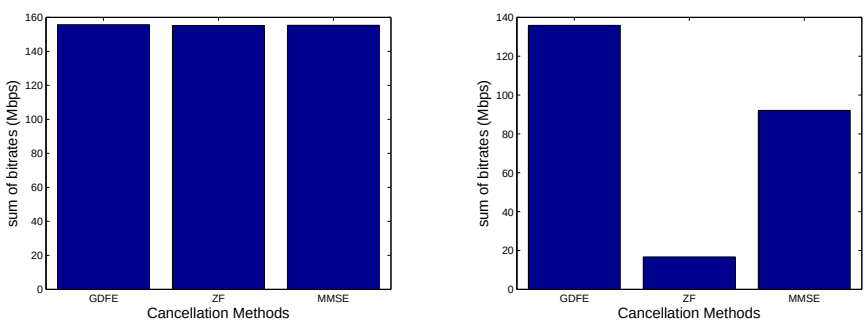

Figure 6.3: Comparison of the total bit rate achieved with the linear ZF canceler and MMSE-based cancelers when alien crosstalk is (a) not present (b) present.

6.4 MMSE-based resource allocation

In [27], a simple partial crosstalk cancellation scheme for the linear ZF canceler was presented, which exploits the spatial and frequency selectivity of the crosstalk. Only strong crosstalkers are canceled which reduces complexity significantly without any dramatic performance degradation. For the MMSE-based cancelers, however, there is no obvious strategy that can be followed to realize partial cancellation. Before delving into different schemes to select the crosstalkers to be canceled, we first establish how the partial crosstalk canceler coefficients can be computed once the lines have been selected that are used for the cancellation.

6.4.1 Computation of linear MMSE partial crosstalk canceler coefficients

Let us assume that there are N lines, therefore there are $N-1$ in-domain crosstalkers to be canceled for each individual line. Let $p_{k,n}$ be the number of observed lines, i.e., used by the crosstalk canceler, to detect the signal in line n on tone k, where $p_{k,n} = N-1$ corresponds to full crosstalk cancellation and $p_{k,n} = 0$ corresponds to no crosstalk cancellation i.e. single-user detection (SUD). Let $\mathcal{M}_n^k$ be the set of indices of all the observed lines including the index of line n, i.e.,

$$\mathcal{M}_k^n \triangleq \{m_{k,n}(1) \cdots m_{k,n}(p_{k,n}+1)\}. \tag{6.11}$$

Similarly, let $\underline{\mathcal{M}}_k^n$ be the set of indices of the unobserved lines, i.e., lines that are not used to detect the signal in line n on tone k, i.e.,

$$\underline{\mathcal{M}}_k^n \triangleq \mathcal{N} \backslash \mathcal{M}_k^n, \tag{6.12}$$

where $\mathcal{N}$ is a set containing all indices $1 \cdots N$. Let $\overline{\mathbf{H}}_k^n$ be the channel matrix containing the channels corresponding to the observed lines, i.e.,

$$\overline{\mathbf{H}}_k^n \triangleq \left[[\mathbf{H}_k]_{rows\mathcal{M}_k^n, cols\mathcal{M}_k^n} \right], \tag{6.13}$$

and $\underline{\mathbf{H}}_k^n$ be the matrix containing all the crosstalk channels from the unobserved lines into the observed lines, i.e.,

$$\underline{\mathbf{H}}_k^n \triangleq \left[[\mathbf{H}_k]_{rows\mathcal{M}_k^n, cols\underline{\mathcal{M}}_k^n} \right]. \tag{6.14}$$

Similarly $\overline{\mathbf{R}}_k^n$ is defined as the noise correlation matrix of the observed lines, i.e.,

$$\overline{\mathbf{R}}_k^n \triangleq \mathbf{R}_{kz}^n + \underline{\mathbf{H}}_k^n \underline{\mathbf{S}}_k^n \underline{\mathbf{H}}_k^{nH} \tag{6.15}$$

where $\underline{\mathbf{S}}_k^n$ is the diagonal matrix containing powers transmitted on the unobserved lines and $\mathbf{R}_{kz}^n$ is the background noise correlation matrix for the observed lines.

Now the linear MMSE partial crosstalk cancellation can be written as

$$\hat{x}_k^n = decision\left(\overline{\mathbf{w}}_k^n \left[\mathbf{y}_k\right]_{rows\mathcal{M}_k^n}\right), \tag{6.16}$$

where the partial cancellation coefficient vector $\overline{\mathbf{w}}_k^n$ can be calculated using (6.7) and (6.15) as

$$\overline{\mathbf{w}}_k^n \triangleq \overline{\mathbf{e}}_q^H \left(\mathbf{S}_k^n \overline{\mathbf{H}}_k^{nH} \left(\overline{\mathbf{H}}_k^n \mathbf{S}_k^n \overline{\mathbf{H}}_k^{nH} + \overline{\mathbf{R}}_k^n\right)^{-1}\right), \tag{6.17}$$

where $\overline{\mathbf{e}}_q \triangleq \left[\mathbf{I}_{p_{k,n}+1}\right]_{col\,q}$ represents the q-th column of the identity matrix of size $p_{k,n}+1$. Here, q is the position of line n in the set $\mathcal{M}_k^n$ and $\mathbf{S}_k^n$ is the diagonal matrix containing the powers transmitted on the observed lines.

6.4.2 Computation of MMSE-GDFE partial crosstalk canceler coefficients

Let $\mathcal{W}_k^n$ be the set of indices of all the observed lines by the feedforward section to detect the signal in line n on tone k, including line n, and let $\underline{\mathcal{W}}_k^n$ be the set of indices of the unobserved lines not used by the feedforward section. Similarly, let $\mathcal{B}_k^n$ be the set of indices of all the observed lines used by the feedback section to detect the signal in line n on tone k and let $\underline{\mathcal{B}}_k^n$ be the set of indices of the unobserved lines not used by the feedback section. The channel matrix corresponding to the observed lines in the feedforward section can be written as

$$\overline{\mathbf{H}}_{k,ff}^n \triangleq \left[\left[\mathbf{H}_k\right]_{rows\mathcal{W}_k^n, cols(\mathcal{W}_k^n \setminus \mathcal{B}_k^n)}\right]. \tag{6.18}$$

The crosstalk channel matrix corresponding to the unobserved lines can then be written as

$$\underline{\mathbf{H}}_{k,ff}^n \triangleq \left[\left[\mathbf{H}_k\right]_{rows\mathcal{W}_k^n, cols\underline{\mathcal{W}}_k^n \setminus \mathcal{B}_k^n}\right]. \tag{6.19}$$

Similarly $\overline{\mathbf{R}}_{k,ff}^n$ is defined as the noise correlation matrix of the observed lines, i.e.,

$$\overline{\mathbf{R}}_{k,ff}^n \triangleq \mathbf{R}_{kz,ff}^n + \underline{\mathbf{H}}_{k,ff}^n \underline{\mathbf{S}}_{k,ff}^n \underline{\mathbf{H}}_{k,ff}^{nH} \tag{6.20}$$

where $\underline{\mathbf{S}}_{k,ff}^n$ is the diagonal matrix containing powers transmitted on the unobserved lines and $\mathbf{R}_{kz,ff}^n$ is a background noise correlation matrix for the observed lines. The MMSE feedforward filter coefficient can then be computed as

$$\mathbf{w}_{ff,k}^n = \mathbf{e}_q^H \left(\mathbf{S}_{k,ff}^n \overline{\mathbf{H}}_{k,ff}^{nH} (\overline{\mathbf{H}}_{k,ff}^n \mathbf{S}_{k,ff}^n \overline{\mathbf{H}}_{k,ff}^{nH} + \overline{\mathbf{R}}_{k,ff}^n)^{-1}\right), \tag{6.21}$$

where $\mathbf{e}_q$ is the $q-th$ column of the identity matrix whose size is defined by the cardinality of $\mathcal{W}_k^n$. Here q is the position of the line n in the set $\mathcal{W}_k^n$ and $\mathbf{S}_{k,ff}^n$

is the diagonal matrix containing the power of the observed lines used by the feedforward section. With

$$\overline{\mathbf{h}}_{k,fb}^{n} \triangleq \left[[\mathbf{H}_k]_{row\, n, cols \mathcal{B}_k^n} \right]^T, \tag{6.22}$$

the feedback coefficient vector in line n on tone k can be written as

$$\mathbf{w}_{fb,k}^{n} = \mathbf{w}_{ff,k}^{n} \overline{\mathbf{h}}_{k,fb}^{n}. \tag{6.23}$$

Now the output of the MMSE-GDFE partial crosstalk canceler can be written as

$$\hat{x}_k^n = decision \left(\mathbf{w}_{ff,k}^{n} \mathbf{y}_{ff,k}^{n} - \mathbf{w}_{fb,k}^{n} \mathbf{x}_{fb,k}^{n} \right), \tag{6.24}$$

where $\mathbf{x}_{fb,k}^{n}$ is a vector containing the detected symbols from all the observed lines used by the feedback section.

6.5 Problem formulation

6.5.1 Partial crosstalk cancellation with a fixed power loading

The partial crosstalk cancellation problem amounts to maximizing the total bitrate summed over all lines when using only C_{tot} cancellation taps, i.e., non-zero elements in the canceler matrices. This comes down to the following maximization problem,

$$\begin{aligned} &\max_{\mathbf{c}} \sum_{k=1}^{K} \sum_{n=1}^{N} \tilde{b}_k^n \\ &\text{s.t} \sum_{k=1}^{K} \sum_{n=1}^{N} \sum_{\substack{m=1 \\ n \neq m}}^{\tilde{N}} c_k^{n,m} \leq C_{tot}, \end{aligned} \tag{6.25}$$

where $\mathbf{c} = [\mathbf{c}_1, \mathbf{c}_2, ..., \mathbf{c}_K]$, $[\mathbf{c}_k]_{n,m} = c_k^{n,m} \in \{0, 1\}$.

- For the linear MMSE, $\tilde{N} = N$ therefore $\mathbf{c}_k$ is an $N \times N$ matrix containing the cancellation tap configurations $c_k^{n,m}$ on tone k. Here $c_k^{n,m} = 1$ indicates that a cancellation tap has been assigned to position (n, m), i.e., that line m is used for the detection of line n the tone k ($m \in \mathcal{M}_k^n$). Similarly, $c_k^{n,m} = 0$ indicates a cancellation tap has not been assigned to position (n, m) ($m \in \underline{\mathcal{M}}_k^n$). Finally, $\tilde{b}_k^n$ is the bit rate of line n on tone k given as

$$\tilde{b}_k^n \triangleq \log_2 \left(1 + \frac{1}{\Gamma} \frac{\left| \overline{\mathbf{h}}_k^n(q) \right|^2 s_k^n(q)}{\hat{n}} \right), \tag{6.26}$$

where Γ is the SNR gap, $\overline{\mathbf{h}}_k^n = \overline{\mathbf{w}}_k^n \overline{\mathbf{H}}_k^n$, $\overline{\mathbf{h}}_k^n(i)$ represents the i-th element of vector $\overline{\mathbf{h}}_k^n$, $\hat{n} = \sum_{i \neq q} \left|\overline{\mathbf{h}}_k^n(i)\right|^2 s_k^n(i) + Tr(\overline{\mathbf{w}}_k^n \overline{\mathbf{R}}_k^n \overline{\mathbf{w}}_k^{nH})$, $Tr(\mathbf{X})$ takes the trace of the matrix $\mathbf{X}$ and $s_n^k(i)$ represents the i-th diagonal element of $\mathbf{S}_k^n$.

- For the MMSE-GDFE, the maximum feedback filter length is equal to N therefore the $\tilde{N} = 2N$. Hence $\mathbf{c}_k$ is a $N \times 2N$ matrix, where the N added columns account for the tap allocation in the feedback section. Due to the triangular structure of the feedback section the maximum number of non-zero elements in $\mathbf{c}_k$ is $N^2 + \frac{N(N-1)}{2}$. If $m \leq N$ then $c_k^{n,m} = 1$ indicates that a cancellation tap has been assigned to the feedforward section in position (n, m) $(m \in \mathcal{W}_k^n)$ and when $m > N$ it indicates that a cancellation tap has been assigned to the feedback section in position $(n, m-N)$ $(m \in \mathcal{B}_k^n)$. The bitrate of line n on tone k is given by

$$\tilde{b}_n^k \triangleq \log_2 \left(1 + \frac{1}{\Gamma} \frac{\left|\overline{\mathbf{h}}_k^n(q)\right|^2 s_k^n(q)}{\tilde{n}}\right), \tag{6.27}$$

where $\tilde{n} = \sum_{i \neq q} \left|\overline{\mathbf{h}}_k^n(i)\right|^2 s_k^n(i) + Tr(\overline{\mathbf{w}}_{f,k}^n \overline{\mathbf{R}}_k^n \overline{\mathbf{w}}_{f,k}^{nH}) - Tr(\mathbf{w}_{fb,k}^n \underline{\mathrm{S}}_{k,bb}^n \mathbf{w}_{fb,k}^{nH})$, $\underline{\mathrm{S}}_{k,bb}^n$ is the diagonal matrix containing powers transmitted on the observed fedback lines, $\overline{\mathbf{h}}_k^n = \overline{\mathbf{w}}_{f,k}^n \overline{\mathbf{H}}_k^n$, $\overline{\mathbf{h}}_k^n(i)$ represents the i-th element of vector $\overline{\mathbf{h}}_k^n$ and $s_n^k(i)$ represents the i-th diagonal element of $\underline{\mathrm{S}}_{k,ff}^n$.

The global optimum for (6.25) can be found by exhaustively searching over all possible cancellation tap configurations. However, the constraint is coupled over tones, which results in an exponential complexity in the number of tones. The overall complexity is then $\mathcal{O}(2^{KN(N-1)})$ for the linear MMSE canceler and $\mathcal{O}(2^{K\frac{3}{2}N(N-1)})$ for the MMSE-GDFE, which is generally intractable. This complexity can be made linear in K by using a dual decomposition approach. To achieve this, the constraint in the optimization problem is moved into the objective with the help of a Lagrange multiplier λ. This can then be written as

$$\min_{\lambda} \left(\max_{\mathbf{c}} \left(\sum_{k=1}^{K} \sum_{n=1}^{N} \tilde{b}_k^n + \lambda (C^{tot} - \sum_{k=1}^{K} \sum_{n=1}^{N} \sum_{\substack{m=1 \\ m \neq n}}^{\tilde{N}} c_k^{n,m}) \right) \right)$$

$$\text{subject to } \lambda \geq 0 \qquad n = 1 \cdots N \tag{6.28}$$

In [174], for multicarrier systems with a sufficiently large number of tones, the duality gap was shown to be zero for this type of optimization problems. For a given λ, the optimization problem is decoupled over tones hence it can be solved

for each tone separately. The per-tone optimization can then be written as

$$\text{For } k = 1 \cdots K$$

$$\max_{\mathbf{c}_k} \sum_{n=1}^{N} \tilde{b}_k^n - \sum_{n=1}^{N} \sum_{\substack{m=1 \\ m \neq n}}^{\tilde{N}} \lambda c_k^{n,m}.$$

(6.29)

The maximization of (6.29) can be performed by an exhaustive search over all possible $\mathbf{c}_k$'s. Additionally, the constraint can be enforced by tuning λ. An algorithm to efficiently tune the Lagrange multiplier is given in [77]. An exhaustive search of the partial crosstalk canceler configuration still has a complexity of $\eta K \mathcal{O}(2^{N(N-1)})$ for the linear MMSE canceler and $\eta K \mathcal{O}(2^{\frac{3}{2}N(N-1)})$ for the MMSE-GDFE, where η is the number of iterations required for the tuning of λ. However, this complexity can be further reduced based on two properties, namely line independence and line selection [77]:

Line independence

For each line, a crosstalk cancellation configuration has to be decided on. However, from (6.26) and (6.27), it can be seen that when it is decided to observe line m for the detection of line n, this obviously only affects the performance of line n. Hence, (6.29) can be further decoupled over lines, leading to

$$\text{For } k = 1 \cdots K$$

$$\text{For } n = 1 \cdots N$$

$$\max_{\mathbf{c}_k(n,:)} \tilde{b}_k^n - \sum_{m=1}^{\tilde{N}} \lambda c_k^{n,m}.$$

(6.30)

This reduces the complexity from $\eta K \mathcal{O}(2^{N(N-1)})$ to $\eta K N \mathcal{O}(2^{(N-1)})$ for the linear MMSE canceler and from $\eta K \mathcal{O}(2^{\frac{3}{2}N(N-1)})$ to $\eta K N \mathcal{O}(2^{\frac{3}{2}(N-1)})$ for the MMSE-GDFE.

Line selection

For the linear MMSE canceler, each line n it has to be decided whether or not $N-1$ other lines are observed. Hence, there are 2^{N-1} possible crosstalk cancellation

configurations for each line. Similarly, for the MMSE-GDFE there are $2^{(N-1+l)}$ possible crosstalk cancellation configurations for each line, where l is the number of previously decoded lines, i.e., $l = 1 \cdots (N-1)$. If $\bar{q}$ cancellation taps are available then these should be allocated such that the effectively canceled interference is maximized. For a line n if we can define a metric, $\mathcal{I}^{n,k}$ such that the $N-1$ cancellation taps for the linear MMSE canceler or $(N-1+l)$ cancellation taps for the MMSE-GDFE can be ordered, then $\bar{q}$ lines can be selected that have the largest values for this metric. In this fashion the number of possible crosstalk configurations reduces from 2^{N-1} to $N-1$ for the linear MMSE canceler and from $2^{(N-1+l)}$ to $(N-1+l)$ for the MMSE-GDFE, and so the overall complexity becomes $\eta K N(N-1)$ for the linear MMSE canceler and $\eta K \frac{3}{2} N(N-1)$ for the MMSE-GDFE. Hence the optimization problem can be written as

$$\begin{aligned} &\text{For } k = 1 \cdots K \\ &\text{For } n = 1 \cdots N \\ &\max_{\mathbf{c}_k(n,:)} \tilde{b}_k^n(\bar{q}) - \lambda \bar{q} \end{aligned} \tag{6.31}$$

where $\tilde{b}_n^k(\bar{q})$ is the bit rate when $\bar{q}$ lines are observed and selected based on the selection metric $\mathcal{I}_k^n$.

6.5.2 Joint partial crosstalk cancellation and spectrum balancing

The partial crosstalk cancellation problem amounts to maximizing the total bitrate summed over all lines when using only C_{tot} cancellation taps, i.e., non-zero elements in the canceler matrices. This comes down to the following maximization problem,

$$\begin{aligned} &\max_{\mathbf{c},\mathbf{s}} \sum_{k=1}^{K} \sum_{n=1}^{N} \tilde{b}_k^n \\ &\text{subject to } \sum_{k=1}^{K} \sum_{n=1}^{N} \sum_{\substack{m=1 \\ n \neq m}}^{\tilde{N}} c_k^{n,m} \leq C_{tot} \\ &\sum_{k=1}^{K} s_k^n \leq S^{n,tot} \\ &0 \leq s_k^n \leq s_k^{n,max}, \end{aligned} \tag{6.32}$$

where $\mathbf{c} = [\mathbf{c}_1, \mathbf{c}_2, ..., \mathbf{c}_K]$, $[\mathbf{c}_k]_{n,m} = c_k^{n,m} \in \{0, 1\}$, $S^{n,tot}$ is the total power of line n and $s_k^{n,max}$ is the maximum allowed transmit power by line n on tone k. Let $\mathcal{S}$ be the set containing power levels with cardinality $\tilde{L}$.

The joint resource allocation problem (6.32) is a non-convex constrained optimization problem. Finding the global optimum for (6.32) requires an exhaustive search over all the possible solutions. The problem is coupled over tones and the users, this results in exponential complexity in number of tones and number of users. Therefore, the computational complexity is $\mathcal{O}(\tilde{L}2^{N-1})^{KN}$ for the linear MMSE canceler and $\mathcal{O}(\tilde{L}2^{N-1})^{K\frac{3}{2}N}$ for the MMSE-GDFE, which is generally intractable. This complexity can be made linear in tone by using a dual decomposition approach. To achieve this, the constraint in the optimization problem is moved into the objective with the help of Lagrange multipliers. This can then be written as

$$\min_{\lambda,\gamma} \left(\max_{\mathbf{c},\mathbf{s}} \left(\sum_{k=1}^{K} \sum_{n=1}^{N} \tilde{b}_k^n + \lambda \left(C^{tot} - \sum_{k=1}^{K} \sum_{n=1}^{N} \sum_{\substack{m=1 \\ m \neq n}}^{\tilde{N}} c_k^{n,m} \right) + \sum_{n=1}^{N} \gamma_n \left(S^{n,tot} - \sum_{k=1}^{K} s_k^n \right) \right) \right)$$

$$\text{subject to } \lambda, \gamma_n \geq 0 \tag{6.33}$$

For multicarrier systems with a sufficiently large number of tones, the duality gap was shown to be zero [174]. For a given λ, the optimization problem is decoupled over tones hence it can be solved for each tone separately. The per-tone optimization can then be written as

$$\text{For } k = 1 \cdots K$$

$$\max_{\mathbf{c}_k,\mathbf{s}_k} \sum_{n=1}^{N} \tilde{b}_k^n - \sum_{n=1}^{N} \sum_{\substack{m=1 \\ m \neq n}}^{\tilde{N}} \lambda c_k^{n,m} - \sum_{n=1}^{N} \gamma_n s_k^n$$

$$\begin{aligned} \text{subject to} \quad & \lambda \geq 0 \quad m = 1 \cdots \tilde{N} \\ & \gamma_n \geq 0 \quad n = 1 \cdots N \end{aligned} \tag{6.34}$$

The maximization of (6.34) can be performed by an exhaustive search over all possible combinations of $\mathbf{c}_k$'s and $\mathbf{s}_k$'s. Additionally, the constraint can be enforced by tuning λ and γ_n. An algorithm to efficiently tune the Lagrange multiplier is given in [77]. An exhaustive search of the partial crosstalk canceler configuration still has a complexity of $K\mathcal{O}((\tilde{L}2^(N-1))^N)$ for the linear MMSE canceler and $K\mathcal{O}((\tilde{L}2^(N-1))^{\frac{3}{2}N})$ for the MMSE-GDFE for each iteration to update the Lagrange multipliers λ and γ_n. This is still very high computational complexity and intractable for practical values of $\tilde{L}$ and N. In section 6.6.2, we will present various techniques to reduce the complexity.

6.6 Resource allocation in MMSE based crosstalk canceler

6.6.1 Partial cancellation with a fixed power loading

In [27], it was shown that the interferers can be ordered based on their crosstalk power as selection metric, i.e.,

$$\mathcal{I}_{k,zf}^{n} = |h_k^{n,m}|^2 s_k^m. \tag{6.35}$$

The interferers are then ordered in descending order with respect to the selection metric. And then a simple exhaustive search over all the ordered interferer was performed to allocate the crosstalk cancellation tap based on the defined cost function. The algorithm is presented in Alg. 6.1.

Algorithm 6.1 Partial crosstalk canceler in Zero- Forcing canceler

initialize $\tilde{b}_k^n(\bar{q})$, λ^0
while $C \neq C_{tot}$ **do**
  for tone $k = 1 \cdots K$ **do**
    for line $n = 1 \cdots N$ **do**
      compute metric $\mathcal{I}_{k,zf}^{n}$
      order the interferers based on $\mathcal{I}_{k,zf}^{n}$ and the combination is stored in $\mathcal{M}_k^n$
      for number of crosstalkers to be cancelled $\bar{q} = 1 \cdots N-1$ **do**
        compute $\mathbf{w}_{k,ZF}^{n}$ for $\bar{q}$ interferers with indices in $m(\bar{q}) \in \mathcal{M}_k^n$
        $\bar{q}_{k,opt}^{n} = \underset{\bar{q}}{\operatorname{argmax}}\ \tilde{b}_k^n(\bar{q}) - \lambda^t \bar{q}$
      end for
    end for
  end for
  compute $C = \sum_k \sum_n \bar{q}_{k,opt}^{n}$
  update $\lambda^{t+1} = [\lambda^t + \mu(C - C_{tot})]^+$
end while

For the ZF canceler, the metric ($\mathcal{I}_{k,ZF}^{n}$), could be easily defined based only on the crosstalk power [27]. However, in the presence of spatially correlated background noise, the metric cannot be defined so easily for the MMSE-based cancelers. In the next section, we address the issue of defining a suitable metric for the linear MMSE canceler and for the MMSE-GDFE.

Selection metric for linear MMSE partial crosstalk cancelers

For the linear MMSE canceler, a first option is to use the metric used in the case of the ZF canceler based only on the in-domain crosstalk power and the information about the spatially correlated background noise is ignored. So the strategy is to cancel the strongest in-domain crosstalker first. This first metric can be written as

$$\mathcal{I}_{k,1}^{n} = |h_k^{n,m}|^2 s_k^m, \quad \text{where } m = 1 \cdots N \quad m \neq n. \tag{6.36}$$

The interferers are then ordered in descending order with respect to the the selection metric $\mathcal{I}_{k,1}^{n}$. Then the indices are stored in $\mathcal{M}_k^n$. This is a good strategy when the alien crosstalk is white/nearly white or very small. However, if the background noise is spatially correlated and strong then this metric may not provide good results. In such a scenario, instead of the in-domain crosstalk information, the spatial correlation of the background noise can be used as a selection metric. This second metric can thus be defined as

$$\mathcal{I}_{k,2}^{n} = r_k^{n,m}, \quad \text{where } m = 1 \cdots N \quad m \neq n \tag{6.37}$$

where $r_k^{i,j}$ is the entry in the ith row and the jth column in the noise correlation matrix $\mathbf{R}_k$ on tone k. The interferers are ordered in descending order with respect to the slection metric $\mathcal{I}_{k,2}^{n}$ and the indices are stored in $\mathcal{M}_k^n$. If the alien crosstalk is much stronger than the in-domain crosstalk then this metric provides a good cancellation order. In the scenario, where both the in-domain crosstalk and the alien crosstalk are large, a metric can be defined that combines the available information about the in-domain crosstalk power and the background noise correlation. For line n, the total information provided by the background noise correlation can be written empirically as follows

$$n_{k,emp}^{n,m} \triangleq \underbrace{r_k^{n,n}\tilde{r}_k^{n,m}}_{I} \underbrace{\left(\frac{r_k^{m,m}}{|h_k^{m,m}|^2 s_k^m}\right)}_{II}, \tag{6.38}$$

where $\tilde{r}_k^{n,m}$ is the entry in the nth row and the mth column in the noise correlation matrix $\mathbf{R}_k$ after normalization. Part I of (6.38) yields the amount of alien crosstalk that can be canceled if line m is selected. Part II accounts for the fact that the effective alien crosstalk that can be canceled also depends on the SINR of line m. The third metric is then defined as

$$\mathcal{I}_3^{n,k} = n_{k,emp}^{n,m} + |h_k^{n,m}|^2 s_k^m, \tag{6.39}$$

where $m = 1 \cdots N$

$m \neq n$

The interferers are ordered in descending order with respect to the slection metric $\mathcal{I}_{k,3}^n$ and the indices are stored in $\mathcal{M}_k^n$. The performance achieved with $\mathcal{I}_{k,3}^n$ is found to be close to the performance achieved with the optimum tap selection scheme, i.e., obtained with an exhaustive search (see section 6.8).

Selection metric based partial cancellation tap selection

For $k = 1 \cdots K$

For $n = 1 \cdots N$

$$\max_{\mathbf{c}_k(n,:)} \tilde{b}_k^n(\bar{q}) - \lambda \bar{q} \tag{6.40}$$

The complexity of choosing $\bar{q}$ now reduces from the combinatorial complexity to linear complexity.

In (6.40), increasing the λ increases the penalty for increasing the equalizer length. Hence, the value of λ is quite important in obtaining the optimal solution. There are many ways to update the value of λ such as the bisection method, the gradient descent method etc. [29] [152]. In [152], the update of λ is based on the difference between the total available system resources and the used system resources for the current value of λ. For our problem this can be written as,

$$\lambda^{t+1} = \lambda^t - \mu(C_{\text{budget}} - \sum_{i \in \mathcal{I}} \sum_{j=1}^{T} c_{ij}) \tag{6.41}$$

where λ^c is the value of λ at cth iteration, μ is a scaling factor, whose value can be changed in order to obtain a faster convergence to the solution. For simplicity, in our simulations μ is taken as a fixed arbitrary value close to zero.

A simple algorithm description is provided as Alg. 6.2. In the presented algorithm, a search over the equalizer length for a particular tone and for a fixed λ is terminated when either the maximum number of taps that can be allocated is reached or when the cost function for a particular equalizer length is lower than that for the previous length.

Algorithm 6.2 Selection metric based partial MMSE crosstalk cancellation tap selection

initialize $\tilde{b}_k^n(\bar{q})$, λ^0
while $C \neq C_{tot}$ **do**
  for tone $k = 1 \cdots K$ **do**
    for line $n = 1 \cdots N$ **do**
      compute metric $\mathcal{I}_{k,3}^n$
      order the interferers based on $\mathcal{I}_{k,3}^n$ and the combination is stored in $\mathcal{M}_k^n$
      for number of crosstalkers to be cancelled $\bar{q} = 1 \cdots N-1$ **do**
        compute $\mathbf{w}_{k,MMSE}^n$ for $\bar{q}$ interferers with indices in $m(\bar{q}) \in \mathcal{M}_k^n$
        $\bar{q}_{k,opt}^n = \underset{\bar{q}}{\text{argmax}}\ \tilde{b}_k^n(\bar{q}) - \lambda^t \bar{q}$
      end for
    end for
  end for
  compute $C = \sum_k \sum_n \bar{q}_{k,opt}^n$
  update $\lambda^{t+1} = [\lambda^t + \mu(C - C_{tot})]^+$
end while

Sparse approximation based partial cancellation

From the previous section, it is clear that if the order of the crosstalk cancellation taps can be fixed, then the computational complexity of the partial crosstalk cancellation can be reduced. In the previous section, we needed to perform per-tone exhaustive search over crosstalk canceler coefficients of the given line n. In order to avoid the per-tone exhaustive search, the non-zero crosstalk canceler coefficient can be determined by using sparse approximation based linear MMSE crosstalk canceler design. In the following section, we will present a sparse linear MMSE crosstalk canceler design procedure.

Sparse linear MMSE crosstalk canceler design

Let us rewrite the linear MMSE design criteria as follows

$$\mathbf{w}_{k,MMSE}^n = \underset{\mathbf{w}_k^k}{\text{argmin}} \quad \mathcal{E}\left\{|\mathbf{w}_k^n(\mathbf{H}_k^n\mathbf{x}_k + \mathbf{z}_k) - \mathbf{x}_{\mathbf{k}}^{\mathbf{n},\mathbf{n}}|^2\right\} \tag{6.42}$$

After few trivial manipulations, we can write (6.42) as follows

$$\mathbf{w}_{k,MMSE}^{n} = \underset{\mathbf{w}_k^k}{\operatorname{argmin}} \left\| \underbrace{\begin{bmatrix} \mathbf{S}_k^{1/2} \\ \mathbf{R}_{z,k}^{1/2} \end{bmatrix}}_{\mathbf{A}_k} \mathbf{w}_k^{nH} - \underbrace{\begin{bmatrix} \mathbf{S}_k^{1/2} e_n \\ \mathbf{0} \end{bmatrix}}_{\mathbf{b}_k} \right\|_2^2$$

$$\mathbf{w}_{k,MMSE}^{n} = \underset{\mathbf{w}_k^k}{\operatorname{argmin}} \quad \left\| \mathbf{A}_k \mathbf{w}_k^{nH} - \mathbf{b}_k \right\|_2^2 \tag{6.43}$$

In order to find a better way to control the sparsity pattern, let us write the problem of designing a linear MMSE crosstalk canceler in (6.43) as a sparse approximation problem [150, 151, 49] as

$$\boxed{\tilde{\mathbf{w}}_{k,MMSE}^{n} = \underset{\tilde{\mathbf{w}}_k^n}{\operatorname{argmin}} \quad \left\| \mathbf{A}_k \tilde{\mathbf{w}}_k^{nH} - \mathbf{b}_k \right\|_2^2 + \gamma \left\| \tilde{\mathbf{w}}_k^n \right\|_0} \tag{6.44}$$

where $\|.\|_0$ is a ℓ_0 quasi-norm of the vector in the argument; it just counts the number of non-zero elements of the vector in the argument. γ controls the trade off between the sparsity and the quadratic term. Problem (6.44) is however known to be a NP hard in general [150].

To simplify (6.44), the non-convex ℓ_0 quasi-norm is often replaced by the convex ℓ_1 norm [150, 151, 49]. This can be written as

$$\boxed{\bar{\mathbf{w}}_{k,MMSE}^{n} = \underset{\bar{\mathbf{w}}_k^n}{\operatorname{argmin}} \quad \left\| \mathbf{A}_k \bar{\mathbf{w}}_k^{nH} - \mathbf{b} \right\|_2^2 + \tilde{\gamma} \left\| \bar{\mathbf{w}}_k^n \right\|_1}, \tag{6.45}$$

where $\tilde{\gamma}$ controls the trade off between the sparsity and the quadratic term. (6.45) is a convex problem and can be solved using any generic solver in polynomial time [24]. If the underlying system admits a sparse solution, it has been shown that solving (6.45) is equivalent to solving (6.44) [151, 49]. In our case, the underlying system does not necessarily admit sparse solution, therefore we can not obtain a sparse linear MMSE crosstalk canceler by just solving (6.45). One way to obtain a sparse linear MMSE crosstalk canceler is to adopt a two steps procedure. Firstly, we use (6.45), for a given $\tilde{\gamma}$, to obtain a nearly-sparse linear MMSE crosstalk canceler and then force the coefficients below a certain threshold level ζ to zero and obtain the sparsity pattern $\mathbf{c}_k^n$. Secondly, we use the sparsity pattern obtained after applying the threshold and we compute the linear MMSE crosstalk canceler using (6.17).

It is clear that the choice of the trade off parameter $\tilde{\gamma}$ and ζ is important for the algorithm to work properly. An efficient update rule for these parameter is based on the difference between the total available system resources and the used system resources for the current value of $\tilde{\gamma}$. This can be written as

$$\tilde{\gamma}^{t+1} = \left[\tilde{\gamma}^{t} - \mu(C_{\text{budget}} - \sum_{i \in \mathcal{I}} \|\mathbf{v}_i\|_0) \right]^{+} \tag{6.46}$$

where $\tilde{\gamma}^{c}$ is the value of $\tilde{\gamma}$ at c-th iteration, μ is a scaling factor, and [a]+ is max(0,a). For simplicity, in our simulations μ is taken as a fixed arbitrary value close to zero. Furthermore, we can penalize the equalizers with low approximation error. This criteria can also be incorporated in (6.46) and can be rewritten as

$$\tilde{\gamma}^{t+1} = \left[\tilde{\gamma}^{t} - \mu(C_{\text{budget}} - \sum_{i \in \mathcal{I}} \left\|\bar{\mathbf{w}}^{n}_{k,MMSE}\right\|_0)\varepsilon_i^{-1} \right]^{+}, \tag{6.47}$$

where ε_i.

The threshold level can be fixed to a constant level and the coefficients smaller than the threshold value can be set to zero. But we can also update threshold level to speed up the convergence. It is obvious that if the threshold level is set to a higher value, the probability of a sparser equalizer becomes higher. The update formula for the threshold level can be written as

$$\zeta^{t+1} = \left[\zeta^{t} - \sigma(C_{\text{budget}} - \sum_{i \in \mathcal{I}} \left\|\bar{\mathbf{w}}^{n}_{k,MMSE}\right\|_0)\varepsilon_i^{-1} \right]^{+}, \tag{6.48}$$

where σ is an arbitrarily small scaling factor.

Sparse approximation based partial cancellation

Based on previous section, we are now ready to describe the full sparse approximation based partial crosstalk cancellation scheme.

Since the sparsity pattern $\mathbf{c}_k^n$ is obtained directly gives the number and the position of crosstalkers to be canceled, we do not need to compute any objective function. The indices of the interferers cancelled can then be stored in $\mathcal{M}_k^n$ and the linear MMSE canceler can be computed using (6.17).

Eventhough the crosstalk canceler has to be computed twice, for large N, it has similar complexity to the selection metric based crosstalk canceler coefficient selection algorithm presented in the section above. The algorithm to implement this is presented in **Alg. 6.3**.

Algorithm 6.3 Sparse approximation based MMSE-based partial crosstalk canceler selection

initialize $\tilde{b}_k^n(\bar{q})$, λ^0
while $C \neq C_{tot}$ **do**
  for tone $k = 1 \cdots K$ **do**
    for line $n = 1 \cdots N$ **do**
      compute nearly sparse $\bar{\mathbf{w}}_k^n$ with (6.45)
      apply threshold ζ on $\bar{\mathbf{w}}_k^n$ to obtain $\mathbf{c}_k^n$
      compute the sparse $\mathbf{w}_{k,MMSE}^n$ using (6.17)
    end for
  end for
  compute $C = \sum_k \sum_n \bar{c}_n^k$
  update $\gamma^{t+1} = \gamma^t + \mu(C_{budget} - C)$
  update $\zeta^{t+1} = \zeta^t + \sigma(C_{budget} - C)$
end while

6.6.2 Joint partial crosstalk cancellation and spectrum balancing in MMSE-based DMT receiver

In the previous section, the linear MMSE crosstalk canceler tap allocation in the case of a fixed power loading was presented. In order to avoid severe crosstalk, different line can vary power transmitted on a certain tone such that the crosstalk presented by the line is reduced without significantly reducing its own performance. This is known as spectrum balancing.

Here we present an approach based on joint crosstalk canceler tap selection and spectrum balancing problem formulation given in (6.34). For the sake of convenience, let us restate the problem formulation again

$$\text{For } k = 1 \cdots K$$

$$\max_{\mathbf{c}_k, \mathbf{s}_k} \sum_{n=1}^{N} \tilde{b}_k^n - \sum_{n=1}^{N} \sum_{\substack{m=1 \\ m \neq n}}^{\tilde{N}} \lambda_n c_k^{n,m} - \sum_{n=1}^{N} \gamma_n s_k^n$$

$$\text{subject to} \quad \lambda_m \geq 0 \quad m = 1 \cdots \tilde{N}$$

$$\gamma_n \geq 0 \quad n = 1 \cdots N. \tag{6.49}$$

In the case of a fixed power loading scheme, the problem decoupled over lines. But computation of linear MMSE crosstalk canceler relies on the information of the power transmitted by other line as seen in (6.7).

$\mathbf{S}_k$ contains the power transmitted by all the lines, therefore changing power transmitted on one line changes crosstalk caused by that line and hence the linear MMSE coefficients of all the other lines. Therefore, the solution of (6.49) requires search over all combinations of power for all the lines. This is can be reduced by iteratively updating power of each line fixing the power of all the other lines. Hence, the the problem is decoupled in lines. This can be written as

$$\begin{aligned}
&\text{For } k = 1 \cdots K \\
&\text{For } n = 1 \cdots N \\
&\text{For } s_k^n = 0 \cdots s_k^{n,max} \\
&\max_{\mathbf{c}_k, \mathbf{s}_k} \quad \tilde{b}_k^n - \sum_{\substack{m=1 \\ m \neq n}}^{\tilde{N}} \lambda c_k^{n,m} - \gamma_n s_k^n \\
&\quad \text{subject to} \quad \lambda \geq 0 \\
&\qquad\qquad\quad \gamma_n \geq 0 \quad n = 1 \cdots N.
\end{aligned} \tag{6.50}$$

This problem still has combinatorial complexity since the sparsity pattern $\mathbf{c}_i$ is combinatorial. In order to further reduce the complexity, if we can restrict the search space for the canceler tap selection. In the following sections, we present techniques to further reduce the complexity of the canceler coefficient selection and spectrum balancing.

Selection metric based joint partial canceler and power allocation

The complexity of (6.50) can be further reduced if we can restrict the search space of the canceler taps. For a given transmit power for user n, this can be achieved by using the selection metric based approach described in section 6.6.1. The combinatorial search space of the crosstalk canceler tap selection then reduces to the linear search space based on the selection metric, $\mathcal{I}_{k,3}^n$. Therefore, the problem now reduces to per-tone per-user exhaustive search over all the crosstalk canceler

and transmit power. This can be written as follows

$$\begin{aligned}
&\text{For } k = 1 \cdots K \\
&\text{For } n = 1 \cdots N \\
&\text{For } s_k^n = 0 \cdots s_k^{n,max} \\
&\text{For } q_k^n = 1 \cdots N - 1 \\
&\max_{\mathbf{c}_k, \mathbf{s}_k} \quad \tilde{b}_k^n - \lambda q_k^n - \gamma_n s_k^n \\
&\quad \text{subject to} \quad \lambda \geq 0 \\
&\qquad\qquad\qquad \gamma_n \geq 0 \quad n = 1 \cdots N, .
\end{aligned} \tag{6.51}$$

where λ and γ_n are Lagrange multipliers and can be updated as

$$\lambda^{t+1} = \lambda^t + \mu(C_{budget} - \sum_{i \in \mathcal{I}} \sum_{n=1}^{N} q_k^n) \tag{6.52}$$

$$\gamma_n^{t+1} = \gamma_n^t + \tilde{\mu}^n(S_{budget} - \sum_{k=1}^{K} s_k^n) \tag{6.53}$$

The algorithm to implement this scheme is given in **Alg. 6.4**.

Even though the overall computational complexity is reduced to $\mathcal{O}(\tilde{L}NK)$, the exhaustive search over all the ordered canceler taps has to be performed for each power level. Furthermore, we need to compute new linear MMSE coefficient for each change in power. To reduce this complexity we can use sparse approximation based linear MMSE crosstalk canceler design as proposed in section 6.6.1. This will be described in detail in the following section.

Sparse approximation based joint partial canceler and power allocation

Based on the sparse linear MMSE crosstalk canceler design in section (6.6.1), we are now ready to describe the full sparse approximation based joint partial crosstalk cancellation and spectrum balancing. From definition, we can see that $\|\mathbf{w}_k^n\|_0 = \sum_{j=1}^{N} C_{ij}$ therefore we can also write (4.8) as

$$\max_{\mathbf{v}_i} \quad b_k^n - \lambda \|\mathbf{w}_k^n\|_0 - \gamma s_k^n, \tag{6.54}$$

Now for each discrete power level, we can compute sparse $\mathbf{w}_k^n$ using method described above. This results in solving (4.16) and (4.15) once for each power

Algorithm 6.4 Selection metric based joint MMSE-based partial crosstalk canceler and spectrum balancing

initialize $\tilde{b}_k^n(\bar{q})$, $\mathbf{s}_k$, λ^0, γ_n^0, $s_{k,opt}^n$
while $C \neq C_{tot}$ **do**
  for tone $k = 1 \cdots K$ **do**
    for line $n = 1 \cdots N$ **do**
      for transmit power $s_k^n = 0 \cdots s_k^{n,max}$ **do**
        compute metric $\mathcal{I}_{k,3}^n$
        update the nth entry of vector $\mathbf{s}_k$ as $\mathbf{s}_k[n] = s_k^n$
        for the number of interferers to be cancelled $\bar{q}_k^n = 1 \cdots N-1$ **do**
          compute $\mathbf{w}_{k,MMSE}^n$ using (6.17) and updated s_k^n and $\bar{q}_k^n$
          $[\bar{q}_k^n, s_{k,opt}^n] = \underset{\bar{q}_k^n}{\operatorname{argmax}}\ \tilde{b}_k^n(\bar{q}_k^n) - \lambda^t \bar{q}_k^n$
        end for
      end for
    end for
  end for
  compute $C = \sum_{k=1}^{K} \sum_{n=1}^{N} \bar{q}_k^n$
  compute $S = \sum_{k=1}^{K} \bar{s}_k^n$
  update $\lambda^{t+1} = \lambda^t + \mu(C - C_{budget})$
  update $\gamma_n^{t+1} = \gamma_n^t + \mu(S - S^{n,tot})$ for all $n = 1 \cdots N$
end while

level. Even though the equalizer coefficient needs to be computed twice, for a large N it has similar computational complexity to the contiguous tap selection based approach of [105], which requires solving (4.15) N times for each power level. The computational complexity can be further reduced by solving (4.16) only once for the initial power level and then using same sparsity pattern for all the other power levels. For a fixed $\|\mathbf{w}_k^n\|_0$ and λ, the $\lambda \|\mathbf{w}_k^n\|_0$ does not affect the optimization procedure. Therefore, we can write (6.54) as

$$\max_{\mathbf{v}_i} \quad b_i - \gamma s_i, \tag{6.55}$$

Furthermore the Lagrange multiplier γ, which enforces the power constraint also has to be updated. The Lagrange multiplier only depends on the difference between the current total power and the total power budget and hence can be written as

$$\gamma^{t+1} = \left[\gamma^t - \eta (S_{\text{tot}} - \sum_{i \in \mathcal{I}} s_i) \right]^+, \tag{6.56}$$

where η is an arbitrarily small scaling factor.

An algorithm to allocate the resources, i.e. number of equalizer taps and the power, for given resource constraints is given in **Alg.** 6.5.

Algorithm 6.5 Sparse approximation based joint MMSE-based partial crosstalk canceler selection and spectrum balancing

initialize $\tilde{b}_k^n(\bar{q})$, λ^0
while $C \neq C_{tot}$ **do**
  for tone $k = 1 \cdots K$ **do**
    for line $n = 1 \cdots N$ **do**
      compute nearly sparse $\mathbf{w}_k^n$
      apply threshold $zeta$ and obtain the indices of the interferers to be cancelled store in $\mathcal{M}_k^n$
      for transmit powers $s_k^n = 0 \cdots s_k^{n,max}$ **do**
        compute sparse $\mathbf{w}_{k,MMSE}^n$ using $\mathcal{M}_k^n$
        $\bar{s}_n^k = \underset{s_i}{\text{argmax}}\ b_i - \gamma s_i$
      end for
    end for
  end for
  compute $C = \sum_k \sum_n \bar{c}_n^k$
  update $\lambda^{t+1} = \lambda^t + \mu(C - C_{tot})$
end while

6.7 Partial crosstalk cancellation in MMSE-GDFE

6.7.1 Partial crosstalk cancellation in MMSE-GDFE under a fixed power loading

Selection metric for MMSE-GDFE partial crosstalk cancelers

In the MMSE-GDFE, in addition to a selection metric for the feedforward path we also need a selection metric for the feedback path. If the detection order is fixed, only already decoded lines can be used in the feedback. The feedforward path in the MMSE-GDFE is basically a linear MMSE canceler. Therefore the selection metric for the feedforward section can also be given by (6.39). The feedback section in the MMSE-GDFE can only cancel the in-domain interference from the already decoded lines, hence the selection metric for the feedback section can be given as (6.36). Combining these selection metrics, the final selection metric for the MMSE-GDFE can be written as

$$\mathcal{I}_4^{n,k} = \{\mathcal{I}_3^{n,k}, |h_{(n,g)}^k|^2 s_g^k\}, \quad \text{for } g = 1 \cdots l \qquad (6.57)$$

$$g \neq n,$$

where g represents previously detected lines. The interferers are ordered with respect to $\mathcal{I}_{k,4}^n$ and stored in $\mathcal{M}_k^n$. The performance achieved with $\mathcal{I}_4^{n,k}$ is found to be close to the performance achieved with the optimum tap selection scheme, i.e., obtained with an exhaustive search (see section 6.8).

Selection metric based crosstalk canceler selection

$$\text{For } k = 1 \cdots K$$

$$\text{For } n = 1 \cdots N$$

$$\max_{\mathbf{c}_k(n,:)} \tilde{b}_k^n(\bar{q}) - \lambda \bar{q} \qquad (6.58)$$

The complexity of choosing $\bar{q}$ now reduces from the combinatorial complexity to linear complexity.

In (6.58), increasing the λ increases the penalty for increasing the equalizer length. Hence the value of λ is quite important in obtaining the optimal solution. There are many ways to update the value of λ such as the bisection method, the gradient descent method etc. [29] [152]. In [152], the update of λ is based on the difference between the total available system resources and the used system resources for the current value of λ. For our problem this can be written as,

$$\lambda^{t+1} = \lambda^t - \mu(C_{\text{budget}} - \sum_{k=1}^{K} \sum_{n=1}^{N} c_k^n) \qquad (6.59)$$

where λ^c is the value of λ at cth iteration, μ is a scaling factor, whose value can be changed in order to obtain a faster convergence to the solution. For simplicity, in our simulations μ is taken as a fixed arbitrary value close to zero. For further details of the algorithm we refer to [152].

Algorithm 6.6 Selection metric based partial MMSE-GDFE crosstalk cancellation tap selection

initialize $\tilde{b}_k^n(\bar{q})$, λ^0
while $C \neq C_{tot}$ **do**
  for tone $k = 1 \cdots K$ **do**
    for line $n = 1 \cdots N$ **do**
      compute metric $\mathcal{I}_{k,4}^n$
      order the interferers based on $\mathcal{I}_{k,3}^n$ and the combination is stored in $\mathcal{M}_k^n$
      for number of crosstalkers to be cancelled $\bar{q} = 1 \cdots N-1$ **do**
        compute $\mathbf{w}_{k,MMSE}^n$ for $\bar{q}$ interferers with indices in $m(\bar{q}) \in \mathcal{M}_k^n$
        $\bar{q}_{k,opt}^n = \underset{\bar{q}}{\text{argmax}}\ \tilde{b}_k^n(\bar{q}) - \lambda^t \bar{q}$
      end for
    end for
  end for
  compute $C = \sum_k \sum_n \bar{q}_{k,opt}^n$
  update $\lambda^{t+1} = [\lambda^t + \mu(C - C_{tot})]^+$
end while

6.7.2 Joint partial crosstalk cancellation and spectrum balancing in MMSE-based DMT receiver

Selection metric based joint partial canceler and power allocation

$$\begin{aligned}
&\text{For } k = 1 \cdots K \\
&\text{For } n = 1 \cdots N \\
&\text{For } s_k^n = 0 \cdots s_k^{n,max} \\
&\text{For } q_k^n = 1 \cdots N-1 \\
&\max_{\mathbf{c}_k, \mathbf{s}_k} \quad \tilde{b}_k^n - \lambda_n q_k^n - \gamma_n s_k^n \\
&\quad \text{subject to} \quad \lambda_m \geq 0 \quad m = 1 \cdots \tilde{N} \\
&\qquad\qquad\qquad\ \ \gamma_n \geq 0 \quad n = 1 \cdots N.
\end{aligned} \tag{6.60}$$

The complexity of choosing $\bar{q}$ now reduces from the combinatorial complexity to linear complexity.

In (6.60), increasing the λ increases the penalty for increasing the equalizer length. Hence the value of λ is quite important in obtaining the optimal solution. There

are many ways to update the value of λ such as the bisection method, the gradient descent method etc. [29] [152]. In [152], the update of λ is based on the difference between the total available system resources and the used system resources for the current value of λ. For our problem this can be written as,

$$\lambda^{t+1} = \lambda^t - \mu(C_{\text{budget}} - \sum_{k=1}^{K}\sum_{n=1}^{N} c_{ij}) \tag{6.61}$$

where λ^c is the value of λ at cth iteration, μ is a scaling factor, whose value can be changed in order to obtain a faster convergence to the solution. For simplicity, in our simulations μ is taken as a fixed arbitrary value close to zero. For further details of the algorithm we refer to [152].

Algorithm 6.7 Selection metric based joint partial MMSE-GDFE crosstalk cancellation tap selection and spectrum balancing

initialize $\tilde{b}_k^n(\bar{q})$, $\mathbf{s}_k$, λ^0, γ_n^0, $s_{k,opt}^n$
while $C \neq C_{tot}$ **do**
  for tone $k = 1 \cdots K$ **do**
    for line $n = 1 \cdots N$ **do**
      for transmit power $s_k^n = 0 \cdots s_k^{n,max}$ **do**
        compute metric $\mathcal{I}_{k,4}^n$
        update the nth entry of vector $\mathbf{s}_k$ as $\mathbf{s}_k[n] = s_k^n$
        for the number of interferers to be cancelled $\bar{q}_k^n = 1 \cdots N-1$ **do**
          compute $\mathbf{w}_{k,MMSE}^n$ using (6.17) and updated s_k^n and $\bar{q}_k^n$
          $[\bar{q}_k^n, s_{k,opt}^n] = \underset{\bar{q}_k^n}{\text{argmax}}\ \tilde{b}_k^n(\bar{q}_k^n) - \lambda^t \bar{q}_k^n$
        end for
      end for
    end for
  end for
  compute $C = \sum_{k=1}^{K}\sum_{n=1}^{N} \bar{q}_k^n$
  compute $S = \sum_{k=1}^{K} \bar{s}_k^n$
  update $\lambda^{t+1} = \lambda^t + \mu(C - C_{budget})$
  update $\gamma_n^{t+1} = \gamma_n^t + \mu(S - S^{n,tot})$ for all $n = 1 \cdots N$
end while

6.8 Simulation results

Simulations were run for a scenario with 7 lines ranging from 600m to 1200m in 100m increments and an alien crosstalk line of 500m. The direct channels, the crosstalk channels and the alien crosstalk channel are generated using the

Table 6.1: Simulation Parameters

Number of DMT tones	4096
Tone width	4.3125 kHz
symbol rate	4 kHz
Coding gain	3 dB
Noise margin	6 dB
Symbol error probability	$< 10^{-7}$
Transmit PSD	Flat (-60 dBm/Hz)
FDD band plan	998
Cable type	0.5 mm

analytical and semi-analytical model in [52]. The simulation parameters are summarized in **Table** 6.1.

The maximum number of taps that can be allocated to the linear MMSE canceler is $N \times (N-1) \times$ number of used tones. Here $N = 7$ and the number of used tones is 1147 hence the C_{tot}^{max} is 48174. With the additional lower triangular feedback section the C_{tot}^{max} in the case of MMSE-GDFE is 72261.

In the first scenario, we consider a fixed power loading linear MMSE based crosstalk cancellation scheme. In **Figure 6.4**, we compare various crosstalk canceler selection schemes based on selection metric given in (6.36), (6.37) and (6.39) and the exhaustive search over all the canceler taps. The result demonstrates that the selection metric which takes both in-domain crosstalk and the background noise information into account perform close to the performance of the exhaustive search based approach. From **Figure** 6.3 (b), it was shown that linear ZF canceler performs poorly in the presence of spatially correlated background noise, therefore the performance is not compared.

In **Figure** 6.5, we then compare the selection metric based approach to the sparse approximation based approach presented in section 6.6.1, for a fixed power loading scenario. It can be seen that the sparse approximation based approach also performs close to the exhaustive search based approach.

In the joint spectrum balancing and partial crosstalk cancellation scenario, it can be seen that the achievable bitrate increase at both no crosstalk cancellation and full crosstalk cancellation scenario. This due to the fact that the by reducing the power transmitted in the shorter line the crosstalk longer lines is reduced. Furthermore, the lower SNR on the shorter line also help to cancel alien crosstalk in the longer loop more effectively.

In **Figure 6.6**, we compare the performance of the selection metric based approach and sparse approximation based approach combined with the spectrum balancing. This is then compared with the iterative spectrum balancing (ISB) approach with

partial crosstalk cancellation. This is a suboptimal algorithm but it was shown to perform very close to optimal spectrum balancing in [153] with much reduced computational complexity. It can be seen that the the selection metric based joint partial crosstalk cancellation and spectrum balancing performs close to the ISB. Similarly we can see that sparse approximation based joint partial crosstalk cancellation and spectrum balancing also performs close to the performance of ISB and selection metric based approach but it has much lower computational complexity that the selection metric based approach.

In the next scenario, a MMSE-GDFE based crosstalk canceler was considered. In **Figure 6.7**, it can be seen that the full crosstalk cancellation using MMSE-GDFE requires higher number of canceler taps but achieves higher bitrate. In **Figure 6.7**, we then compare the exhaustive search based partial crosstalk canceler selection with the selection metric based crosstalk canceler selection for a fixed power loading. It is seen that the selection metric based crosstalk canceler tap selection performs close to the exhaustive search based approach. In **Figure 6.8**, we compare the selection metric based method and exhaustive search based approach for joint partial crosstalk cancellation and spectrum balancing. It can be seen that the selection metric based partial crosstalk cancellation scheme performs close to the exhaustive search based approach.

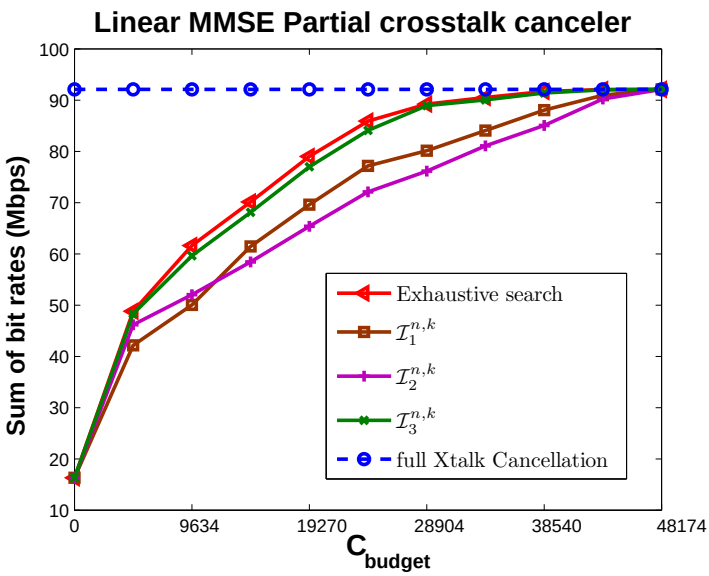

Figure 6.4: Performance comparison of the different metrics for partial cancellation using a linear MMSE canceler

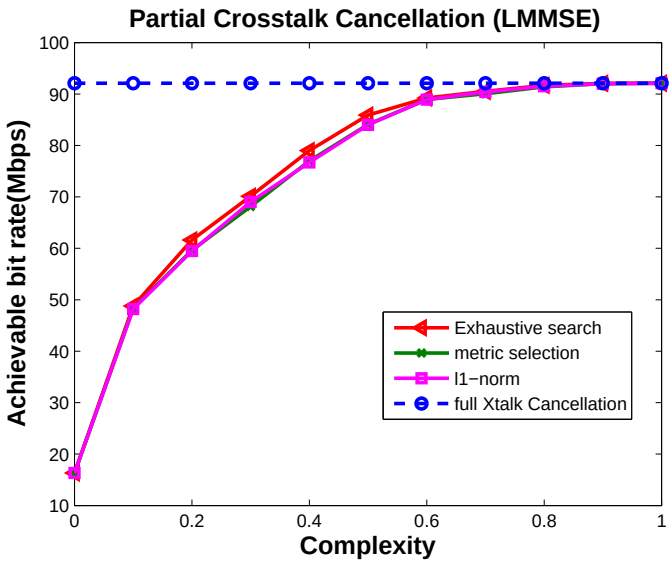

Figure 6.5: Performance comparison of the different metrics for partial cancellation using a linear MMSE canceler

6.9 Conclusion

In this chapter, we have considered crosstalk cancellation in upstream VDSL, where receivers are co-located, in the presence of spatially correlated background noise such as alien crosstalk . It is shown that the MMSE based crosstalk canceler perform significantly better than a linear ZF based canceler in this scenario. It is shown full crosstalk cancellation scheme has a run-time complexity of $\mathcal{O}(N^2)$, therefore for a large number of lines the run-time complexity might be prohibitive. Previously, it had been shown that, for a system with only AWGN background noise and linear ZF canceler, the run-time complexity might be reduced by selectively canceling only few significant crosstalker on each tone. This is known as partial crosstalk cancellation. In this chapter, this technique was extended to include MMSE-based crosstalk cancelers.

It is shown that in the case of linear MMSE crosstalk canceler and a fixed power loading, the combinatorial search over all the crosstalkers can be reduce to linear search by ordering the interferers based on some selection metric. Similarly the crosstalk canceler selection can be simplified by directly designing sparse linear MMSE crosstalk cancelers. These methods are shown to achieve performance close to the exhaustive search based crosstalk canceler selection. Furthermore, it is shown that the achievable rate increases if spectrum balancing is performed

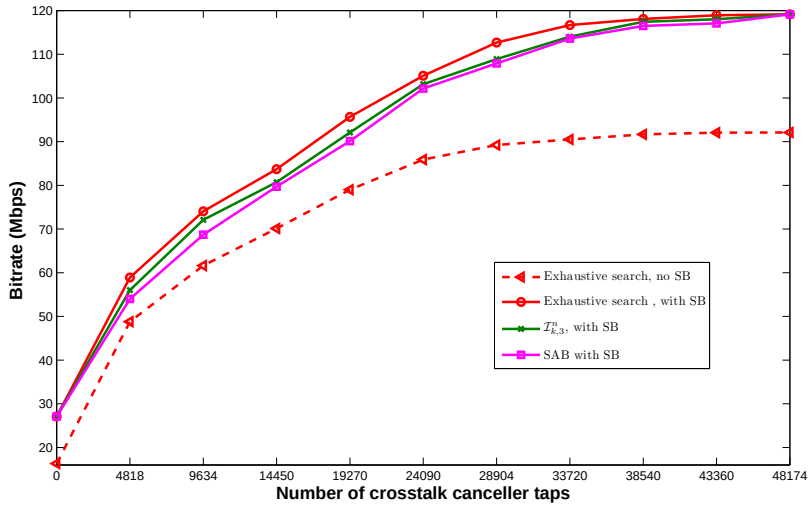

Figure 6.6: Performance comparison of the different metrics for partial cancellation using a linear MMSE canceler

alongside crosstalk cancellation. In order to reduce the overall complexity of the joint partial cancellation and spectrum balancing on linear MMSE based systems, the selection metric based approach was used alongside iterative spectrum balancing. It was shown that the sparse approximation based partial crosstalk cancellation further reduces the overall search complexity. These methods are shown to achieve performance close to the performance of exhaustive search based approach.

The selection metric based approach is then simply extended to accommodate MMSE-GDFE based crosstalk cancellation scheme. It is shown that the MMSE-GDFE based crosstalk cancellation achieve higher data rate but at higher run-time complexity. The selection metric based approach then used to reduce the overall complexity of partial crosstalk canceler tap selection. It was shown that selection metric based crosstalk cancellation selection approaches the performance of exhaustive search based approach. Furthermore, the approach is then extended to perform partial crosstalk cancellation with spectrum balancing. It is shown that selection metric based approach alongside ISB performs very close to exhaustive search based crosstalk cancellation scheme with ISB.

It was also shown that for the same number of crosstalk cancelers MMSE-GDFE based crosstalk cancellation outperforms linear MMSE based crosstalk cancellation.

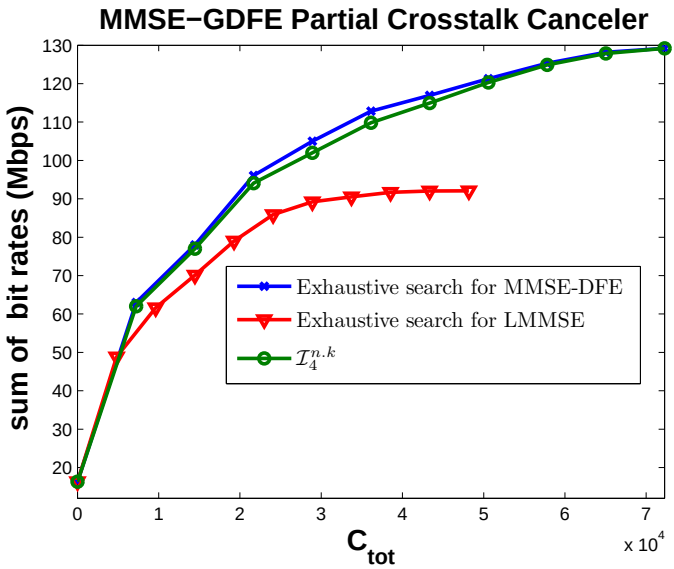

Figure 6.7: Comparison between the optimum linear MMSE partial cancellation and the MMSE-GDFE partial cancellation

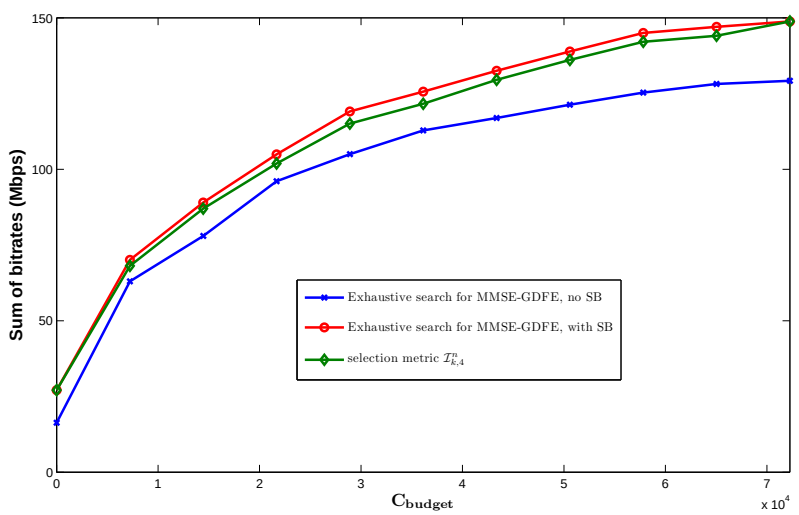

Figure 6.8: Comparison between the optimum linear MMSE partial cancellation and the MMSE-GDFE partial cancellation

Chapter 7

Conclusions and Future Works

7.1 Conclusions

In this chapter we will highlight the main conclusions and list some suggestions for the future works.

7.1.1 Conclusions

The channel impairments such as ISI, crosstalks have a large impact on the achievable bit rate of the DMT system. Furthermore, achievable bit rate is reduced by nulling certain carriers at the band edges in order to comply with the PSD constraint. In order to combat these effects, several signal processing techniques have been proposed. However, the use of sophisticated signal processing techniques increases the run-time complexity. In some cases, the prohibitive computational complexity renders the signal processing algorithm impractical. The DSL channel is a slowly time-varying channel. This provides us with the opportunity to optimize the signal processing algorithm used to mitigate various non-ideal effect in the DMT transceiver. This dissertation focuses on reducing the run-time complexity of various signal processing blocks used in the DMT transceiver by exploiting various characteristics of the DSL channel in both single-user and the multi-user scenario. The main goals of this thesis are

- to design low complexity resource allocation algorithms with near optimal performance in the single-user DSL scenario
- to design low complexity resource allocation algorithm without compromising the performance in the multi-user DSL scenario

This dissertation was broadly divided into two parts: **Part I** focused on various run-time complexity reduction techniques in the single-user DSL scenario. Specific scenario of per-tone pulse shaping DMT transmitter and per-tone equalization based DMT receivers has been considered. In **Part II**, we investigated the resource allocation algorithms in the multi-user DSL scenario in the presence of alien crosstalk.

In **chapter 2**, we provided introduction to various aspects of a DSL system. All the important building blocks of a DSL transceiver were explained. A brief overview of the different modulation schemes considered for the DSL system was introduced and the motivation for using the multicarrier modulation was then presented. A mathematical model of a DMT based system was also introduced and DMT transmitter and receiver structures were then described. Various techniques to increase the capacity of the DMT system, such as bit loading and power loading was also discussed in detail. various channel impairments present in DSL system were then presented. In the end, techniques such as time domain equalization and per-tone based equalization to mitigate the effect of channel impairments were introduced. The effect of crosstalk in the case of multi-user DSL scenario was discussed and then a simple multi-user channel modelling technique was also presented. Various techniques to optimize the transmission in this scenario was also discussed in order to either avoid the crosstalk or cancel it. At the end, various receiver structures that are generally used to cancel the effect of crosstalk were presented.

In **chapter 3**, it was shown that the use of per-tone pulse shaping reduces the number of virtual carriers on the band edges, thus increasing the achievable bit rate of the DMT system. Furthermore, it was also shown that using a constant length non-sparse pulse shaping filter on every tone unnecessarily increases the run-time complexity of the system. Thereby motivating the use of variably sparse pulse shaping filter on each tone. But the constrained optimization problem to optimally allocate the non-zero per-tone pulse shaping filter was shown to be coupled over tones. Furthermore, computation of a sparse per-tone pulse shaping filter was also shown to be a combinatorial problem. We showed that a dual problem formulation leads to an unconstrained optimization problem that is decoupled over tones, but the sparse filter design problem still remains a combinatorial problem. In order to reduce this combinatorial complexity of filter design, some simple techniques were presented. Firstly, the restriction in sparsity pattern of the filter allowing only contiguous taps to be non-zero was shown to reduce the combinatorial complexity to a linear search in filter order. Thereby reducing the the overall complexity of the filter tap selection problem. But the restriction in sparsity pattern of the pulse shaping filter may not be the best approach, since the best sparsity pattern may not lie in the restricted sparsity set. Secondly, it was shown that a sparse approximation based approach with convex relaxation allows design of sparse pulse shaping filter without imposing any restriction on the sparsity pattern of the

pulse shaping filter with similar complexity as the linear search over the filter order. Furthermore, the techniques were also extended to jointly allocate pulse shaping filter taps and the transmit power. It was shown that these techniques reduce the run-time complexity significantly without affecting the performance significantly. Furthermore, it was shown that when combined with an transmit power loading algorithm these approaches can further reduce the number of per-tone pulse shaping filter taps needed to achieve the same bit-rate performance.

In **chapter 4**, we showed that the use of MMSE-PTEQ increases the achievable bit rate of the DMT system. Furthermore, it was also shown that using a constant length non-sparse MMSE-PTEQ filter on every tone unnecessarily increases the run-time complexity of the DMT system. Therefore, using variably sparse PTEQ filter on each tone reduces the run-time complexity without affecting the performance significantly. The constrained optimization problem to allocate the non-zero MMSE-PTEQ tap was shown to be coupled in tone. For a constant transmit power To this end, we have proposed efficient resource allocation algorithms to distribute the available resources (total transmit power budget and total MMSE-PTEQ filter tap budget) over tones in a DMT receiver with per-tone equalization. We have shown that a dual problem formulation leads to an unconstrained optimization problem that is decoupled over tones but due to the combinatorial nature of the filter tap allocation the resulting optimization problem is still NP hard. Two approaches were proposed to further simplify the problem. First, by restricting only contiguous PTEQ taps to be non-zero hence the combinatorial search in the sparsity pattern is reduced to the linear search in filter order. Second, by using sparse approximation technique to design the PTEQ filter. Using convex relaxation of the sparsity constraints, the sparse filter design problem can be written as convex problem and solved efficiently. Furthermore, the techniques were also extended to jointly allocate PTEQ filter taps and the transmit power. A VDSL simulation demonstrated that under a fixed power loading, the number of PTEQ filter taps can be reduced significantly compared to the fixed length non-sparse case without sacrificing performance. Furthermore, it was also shown that the sparse approximation based PTEQ filter tap allocation approach performs better than the contiguous tap selection based approach. When combined with an transmit power loading algorithm these approaches can further reduce the number of per-tone pulse shaping filter taps needed to achieve the same bit-rate performance.

In **chapter 5**, a per-tone pulse shaping and per-tone equalizer based DMT transceiver is considered. It is first shown that the presence of per-tone pulse shaping filter affects the tap allocation in the per-tone based receiver under a constant transmit power loading. It was shown that the joint filter tap optimization problem in the DMT transceiver could be decoupled in tone by formulating as a dual problem along with a iterative MMSE-PTEQ computation scheme. It can be seen that the achievable rate for the same number of taps is

lower in the presence of per-tone pulse shaping filter. This is due to the fact that the pulse shaping filter act as a dispersive channel and hence lengthens the output of the transmitter. In our case, we do not increase the overall symbol length, but decrease the effective cyclic prefix to accommodate the extra symbol, therefore better per-tone equalizers are needed to mitigate the effects. Similarly in the case of joint filter tap and transmit power allocation in the DMT transceiver, it can be seen that since the signal-to noise ratio at the output receiver is fed back to the transmitter, the effect such as filtering effect at the edge of the bands at the receiver is also taken into account while performing transmit power allocation at the transmitter side. This improves the performance of the system for the same number of non-zero filter taps.

In **chapter 6**, we have considered crosstalk cancellation in upstream VDSL, where receivers are co-located, in the presence of spatially correlated background noise such as alien crosstalk . It is shown that the MMSE based crosstalk canceler perform significantly better than a linear ZF based canceler in this scenario. It is shown full crosstalk cancellation scheme has a run-time complexity of $\mathcal{O}(N^2)$, therefore for a large number of lines the run-time complexity might be prohibitive. Previously, it had been shown that, for a system with only AWGN background noise and linear ZF canceler, the run-time complexity might be reduced by selectively canceling only few significant crosstalker on each tone. This is known as partial crosstalk cancellation. In this chapter, this technique was extended to include MMSE-based crosstalk cancelers. It is shown that in the case of linear MMSE crosstalk canceler and constant powerloading, the combinatorial search over all the crosstalkers can be reduce to linear search by ordering the interferers based on some selection metric. Similarly the crosstalk canceler selection can be simplified by directly designing sparse linear MMSE crosstalk cancelers. These methods are shown to achieve performance close to the exhaustive search based crosstalk canceler selection. Furthermore, it is shown that the achievable rate increases if spectrum balancing is performed alongside crosstalk cancellation. In order to reduce the overall complexity of the joint partial cancellation and spectrum balancing on linear MMSE based systems, the selection metric based approach was used alongside iterative spectrum balancing. It was shown that the sparse approximation based partial crosstalk cancellation further reduces the overall search complexity. These methods are shown to achieve performance close to the performance of exhaustive search based approach.The selection metric based approach is then simply extended to accommodate MMSE-GDFE based crosstalk cancellation scheme. It is shown that the MMSE-GDFE based crosstalk cancellation achieve higher data rate but at higher run-time complexity. The selection metric based approach then used to reduce the overall complexity of partial crosstalk canceler tap selection. It was shown that selection metric based crosstalk cancellation selection approaches the performance of exhaustive search based approach. Furthermore, the approach is then extended to perform partial crosstalk cancellation with spectrum balancing. It is shown that selection metric

based approach alongside ISB performs very close to exhaustive search based crosstalk cancellation scheme with ISB. It was also shown that for the same number of crosstalk cancelers MMSE-GDFE based crosstalk cancellation outperforms linear MMSE based crosstalk cancellation.

7.2 Future Work

Initialization complexity reduction

In this dissertation, the main focus was to reduce the run-time complexity of the signal processing blocks. But number of filter taps to be initialized is still quite high. Therefore, better and efficient initialization schemes are desired. In [2], initialization complexity reduction based on tone grouping is presented, but it is not really applicable to the sparse filters. Therefore, efficient filter coefficient initialization schemes for variably sparse filters needs to be investigated in depth..

Effect of channel estimation error

In this dissertation, in the case of multi-user DSL scenario, the crosstalk channels and the noise covariance are assumed to be perfectly known. But, practical estimation techniques have inherent estimation errors. The MMSE based cancelers rely on accurate estimation of crosstalk channels and the noise autocorrelation. Therefore, it is important to investigate the effect of such errors in the performance of the DSL system. Furthermore, more reliable channel and noise correlation estimation techniques need to be investigated.

Efficient computation of MMSE canceler coefficients

In the case of multi-user DSL it is shown that in a vectored DSL lines, whenever the transmit power of a line changes or a line joins or leaves of vectored group, the full MMSE coefficients have to be recomputed. This adds a lot of computational complexity. In order to reduce this computational complexity, a simplified MMSE canceler computation scheme is needed. Since the noise covariance changes with respect to which lines are taken into account, a simple matrix inversion lemma based recursive update is not possible.

Dynamic crosslayer partial crosstalk cancellation

In this dissertation, We optimized the resources only with respect to achievable bitrate. But it has been shown in [88] that this can be extended to include crosslayer objectives, which are more related to user experience, QoS and are more meaningful to the end users.

Stability of the DSL system

In this dissertation, the lines in vectored DSL was considered to be static, i.e., it remains in the vectored line for ever. But in practice, the lines continuously join and leave the vectored DSL system. This may create instability in the DSL system. Therefore, the impact of the dynamical entry and exit if the lines in a DSL system has to be analyzed, And the impact in the initialization as well as run-time complexity of the MMSE based cancelers has to be investigated.

Partial crosstalk precoding

In this dissertation, we have only investigated upstream VDSL scenario. The receiver was assumed to be co-located. Similar approach may be possible in the downstream scenario, where all the transmitters are co-located. A optimum precoding structure in the presence of AWGN background noise was presented in [26]. It might be interesting to extend this idea in the presence of spatially correlated background noise.

Bibliography

[1] K. Van Acker. *Equalization and echo cancellation for DMT-based DSL modems*. PhD Thesis, Department of Electrical Engineering, Katholieke Universiteit Leuven, Belgium, Jan 2001.

[2] K. Van Acker, G. Leus, M. Moonen, O. Van de Wiel, and T. Pollet. Per tone equalization for DMT-based systems. *Communications, IEEE Transactions on*, 49:109–119, January 2001.

[3] A.N. Akansu, P. Duhamel, Lin Xueming, and M. de Courville. Orthogonal transmultiplexers in communication: a review. *Signal Processing, IEEE Transactions on*, 46(4):979 –995, April 1998.

[4] A.N. Akansu and L. Xueming. A comparative performance evaluation of dmt (ofdm) and dwmt (dsbmt) based dsl communications systems for single and multitone interference. In *Acoustics, Speech and Signal Processing, 1998. Proceedings of the 1998 IEEE International Conference on*, volume 6, pages 3269 –3272, May 1998.

[5] N. Al-Dhahir and J.M. Cioffi. Fast computation of channel-estimate based equalizers in packet data transmission. *Signal Processing, IEEE Transactions on*, 43(11):2462 –2473, November 1995.

[6] N. Al-Dhahir and J.M. Cioffi. Efficient computation of the delay-optimized finite length mmse-dfe. *Signal Processing, IEEE Transactions on*, 44(5):1288 –1292, May 1996.

[7] N. Al-Dhahir and J.M. Cioffi. Efficiently computed reduced-parameter input-aided mmse equalizers for ml detection: a unified approach. *Information Theory, IEEE Transactions on*, 42(3):903 –915, May 1996.

[8] N. Al-Dhahir and J.M. Cioffi. Optimum finite-length equalization for multicarrier transceivers. *Communications, IEEE Transactions on*, 44:56–64, 1996.

[9] N. Al-Dhahir and J.M. Cioffi. A bandwidth-optimized reduced-complexity equalized multicarrier transceiver. *Communications, IEEE Transactions on*, 45(8):948 –956, August 1997.

[10] ANSI. Interface between networks and customer installations: very-high speed digital subscriber lines (VDSL). *ANSI T1E1.4/2002-031R2*, 2002.

[11] ANSI. Spectrum management for loop transmission systems. *ANSI T1.417, Issue 2*, 2003.

[12] S. Ariyavisitakul and L.J. Greenstein. Reduced-complexity equalization techniques for broadband wireless channels. *Selected Areas in Communications, IEEE Journal on*, 15(1):5 –15, January 1997.

[13] E. Baccarelli, A. Fasano, and M. Biagi. Novel efficient bit-loading algorithms for peak-energy-limited adsl-type multicarrier systems. *Signal Processing, IEEE Transactions on*, 50(5):1237 –1247, May 2002.

[14] R. Baldemair. Suppression of narrow frequency bands in multicarrier transmission systems. *in Proc. European Signal Processing Conf. EUSIPCO 2000, Tampere, Finland*, pages 553–556, Sept. 2000.

[15] M. Barton, L. Chang, and T.R. Hsing. Performance study of high-speed asymmetric digital subscriber lines technology. *Communications, IEEE Transactions on*, 44(2):156 –157, February 1996.

[16] A.G. Bell. Improvement in telegraphy. Letters Patent No. 174,465, 7 March 1876. Application filed on 14 February 1876.

[17] J. Bingham and M. Mallory. RFI egress supression for SDMT. *ANSI Contribution T1E1.4/96-085*, 1996.

[18] J.A.C. Bingham. Multicarrier modulation for data transmission: An idea whose time has come. *Communications Magazine, IEEE*, 28:5–14, May 1990.

[19] John A. C. Bingham. *ADSL, VDSL, and multicarrier modulation.* John Wiley & Sons, Hoboken, NJ, USA, 2000.

[20] P. Biyani, A. Mahadevan, P. Duvaut, and S. Singh. Cooperative mimo for alien noise cancellation in upstream vdsl. In *Acoustics, Speech and Signal Processing, 2009. ICASSP 2009. IEEE International Conference on*, pages 2645 –2648, 2009.

[21] R.S. Blum. Mimo capacity with interference. *Selected Areas in Communications, IEEE Journal on*, 21(5):793 – 801, 2003.

[22] H. Bolcskei, P. Duhamel, and R. Hleiss. Design of pulse shaping ofdm/oqam systems for high data-rate transmission over wireless channels. In *Communications, 1999. ICC '99. 1999 IEEE International Conference on*, 1999.

[23] B. Borna and T.N. Davidson. Efficient filter bank design for filtered multitone modulation. In *Communications, 2004 IEEE International Conference on*, volume 1, pages 38 – 42, 2004.

[24] S. Boyd and L. Vandenberghe. *Convex Optimization*. Cambridge University Press, New York, NY, USA, 2004.

[25] R. Cendrillon, G. Ginis, E. Van den Bogaert, and M. Moonen. A near-optimal linear crosstalk canceler for upstream VDSL. *Signal Processing, IEEE Transactions on*, 54(8):3136 –3146, 2006.

[26] R. Cendrillon, G. Ginis, E. Van den Bogaert, and M. Moonen. A near-optimal linear crosstalk precoder for downstream VDSL. *Communications, IEEE Transactions on*, 55(5):860 –863, May 2007.

[27] R. Cendrillon, M. Moonen, G. Ginis, K. Van Acker, T. Bostoen, and P. Vandaele. Partial crosstalk cancellation for upstream vdsl. *Applied Signal Processing, EURASIP Journal on*, 2004(10):1520–1535, 2004.

[28] R. Cendrillon, M. Moonen, R. Suciu, and G. Ginis. Simplified power allocation and tx/rx structure for mimo-dsl. In *Global Telecommunications Conference, 2003. GLOBECOM '03. IEEE*, volume 4, pages 1842 – 1846 vol.4, 2003.

[29] R. Cendrillon, M. Moonen, J. Verlinden, T. Bostoen, and W. Yu. Optimal multi-user spectrum management for digital subscriber lines. In *Proc. IEEE ICC*, Paris, France, 2004.

[30] R. Cendrillon, Wei Yu, M. Moonen, J. Verlinden, and T. Bostoen. Optimal multiuser spectrum balancing for digital subscriber lines. *Communications, IEEE Transactions on*, 54(5):922 – 933, May 2006.

[31] R. Chang. Synthesis of band-limited orthogonal signals for multichannel data transmission. *Bell System Tech., Journal*, 45:1775 –1796, 1966.

[32] R. Chang and R. Gibby. A theoretical study of performance of an orthogonal multiplexing data transmission scheme. *Communication Technology, IEEE Transactions on*, 16(4):529 –540, 1968.

[33] C-Y. Chen and S-M. Phoong. Per tone shaping filters for DMT transmitters. *Acoustics, Speech, and Signal Processing, 2004. Proceedings. (ICASSP '04). IEEE International Conference on*, 4:iv–1061–4 vol.4, 17-21 May 2004.

[34] G. Cherubini, E. Eleftheriou, and S. Ölçer. Filtered multitone modulation for very high-speed digital subscriber lines. *Selected Areas in Communications, IEEE Journal on*, 20(5):1016 –1028, June 2002.

[35] G. Cherubini, E. Eleftheriou, S. Ölçer, and J.M. Cioffi. Filter bank modulation techniques for very high speed digital subscriber lines. *Communications Magazine, IEEE*, 38(5):98 –104, May 2000.

[36] J.S. Chow, J.C. Tu, and J.M. Cioffi. A discrete multitone transceiver system for hdsl applications. *Selected Areas in Communications, IEEE Journal on*, 9(6):895 –908, August 1991.

[37] P.S. Chow, J.M. Cioffi, and J.A.C. Bingham. A practical discrete multitone transceiver loading algorithm for data transmission over spectrally shaped channels. *Communications, IEEE Transactions on*, 43(234):773 –775, 1995.

[38] P.S. Chow, J.C. Tu, and J.M. Cioffi. Performance evaluation of a multichannel transceiver system for adsl and vhdsl services. *Selected Areas in Communications, IEEE Journal on*, 9(6):909 –919, August 1991.

[39] J. Cioffi, W. Yu, G. Ginis, Zheng S, F. Sjoberg, and R. Nilsson. Robust VDSL in the presence of bridged taps. Tech. Rep. NT-039, ITU-SG15, Nashville, Tennessee, November 1999.

[40] J. M. Cioffi. *Advanced digital communication, class reader, EE379C*. Stanford University, 2005.

[41] J.M. Cioffi. A multicarrier primer. *T1E1.4 contribution number 91-157*, 1991.

[42] J.M. Cioffi and M. Mohseni. Dynamic spectrum management- A methodology for providing significantly higher broadband capacity to the users. *Teletronikk*, 4, 2004.

[43] J.M. Cioffi, V. Oksman, J. J. Werner, T. Pollet, P.M.P. Spruyt, J.S. Chow, and K.S. Jacobsen. Very-high-speed digital subscriber lines. *Communications Magazine, IEEE*, 37(4):72 –79, April 1999.

[44] J.M. Cioffi, P. Silverman, and T. Starr. *Understanding Digital subscriber line technology*. Prentice Hall, first edition, 1999.

[45] J. Cook. Wideband impulsive noise survey of the access network. *BT Technol. Journal*, 11:155 –162, 1993.

[46] J.W. Cook, R.H. Kirkby, M.G. Booth, K.T. Foster, D.E.A. Clarke, and G. Young. The noise and crosstalk environment for ADSL and VDSL systems. *Communications Magazine, IEEE*, 37(5):73 –78, May 1999.

[47] G. Cuypers, K. Vanbleu, G. Ysebaert, and M. Moonen. Egress reduction by intra-symbol windowing in DMT-based transmitters. In *Acoustics, Speech, and Signal Processing, 2003. Proceedings. (ICASSP '03). 2003 IEEE International Conference on*, volume 4, pages IV – 532–5 vol.4, 2003.

[48] G. Cuypers, K. Vanbleu, G. Ysebaert, M. Moonen, and P. Vandaele. Combining raised cosine windowing and per tone equalization for RFI mitigation in dmt receivers. In *Communications, 2003. ICC '03. IEEE International Conference on*, volume 4, pages 2852 – 2856 vol.4, May 2003.

[49] D. L. Donoho, M. Elad, and V. N. Temlyakov. Stable recovery of sparse overcomplete representations in the presence of noise. 52:6–18, January 2006.

[50] M. Ergen. *Mobile Broadband: Including WiMAX and LTE*. Springer Science + Business Media LLC., Spring Street, NY, USA, 2009.

[51] ETSI. Transmission and multiplexing(TM); access transmission systems on metallic access cables; very high speed digital subscriber line(VDSL);part 2: Transceiver specification. *ETSI Std. TS 101 270-2, V.0.1.0 (2000-03)*, March 2000.

[52] ETSI. Transmission and multiplexing(TM); access transmission systems on metallic access cables; very high speed digital subscriber line(VDSL);part 1:functional requirements. *ETSI Std. TS 101 270-1, Rev. V.1.3.1*, 2003.

[53] R. Fano. A theory of impulse noise in telephone networks. *Communications, IEEE Transactions on*, 25(6):577 – 588, June 1977.

[54] B. Farhang-Boroujeny and L. Lekun. Cosine modulated multitone for very high-speed digital subscriber lines. In *Acoustics, Speech, and Signal Processing, 2005. Proceedings. (ICASSP '05). IEEE International Conference on*, volume 3, pages iii/345 – iii/348, 2005.

[55] R.F.H. Fischer and J.B. Huber. Comparison of precoding schemes for digital subscriber lines. *Communications, IEEE Transactions on*, 45(3):334 –343, March 1997.

[56] G. Foschini. Crosstalk in outside plant cable systems. *Bell System Tech. Journal*, 50:2421 –2448, 1971.

[57] A. Gibbs and R. Addie. The covariance of near end crosstalk and its application to pcm system engineering in multipair cable. *Communications, IEEE Transactions on*, 27(2):469 – 477, February 1979.

[58] G. Ginis and J.M. Cioffi. On the relation between v-blast and the gdfe. *Communications Letters, IEEE*, 5(9):364 –366, September 2001.

[59] G. Ginis and J.M. Cioffi. Vectored-DMT: a FEXT canceling modulation scheme for coordinating users. In *Communications, 2001. ICC 2001. IEEE International Conference on*, volume 1, pages 305 –309 vol.1, June 2001.

[60] G. Ginis and J.M. Cioffi. Vectored transmission for digital subscriber line systems. *Selected Areas in Communications, IEEE Journal on*, 20(5):1085 –1104, June 2002.

[61] G. Ginis and C.-N. Peng. Alien crosstalk cancellation for multipair digital subscriber line systems. *Applied Signal Processing, EURASIP Journal on*, 2006:12, 2006.

[62] P. Golden, H. Dedieu, and K.S. Jacobsen. *Implementation and Applications of DSL Technology*. Auerbach Publication, FL, USA, 2000.

[63] P. Golden, H. Dedieu, and K.S. Jacobsen. *Fundamentals of DSL Technology*. Auerbach Publication, FL, USA, 2006.

[64] W. Goralski. xDSL loop qualification and testing. *Communications Magazine, IEEE*, 37(5):79 –83, May 1999.

[65] M. Grant and S. Boyd. Graph implementations for nonsmooth convex programs. In V. Blondel, S. Boyd, and H. Kimura, editors, *Recent Advances in Learning and Control*, Lecture Notes in Control and Information Sciences, pages 95–110. Springer-Verlag Limited, 2008. `http://stanford.edu/~boyd/graph-dcp.html`.

[66] M. Grant and S. Boyd. CVX: Matlab software for disciplined convex programming, version 1.21. `http://cvxr.com/cvx`, October 2010.

[67] F.H. Gregorio, J.L. Figueroa, and J.E. Cousseau. Impulsive noise reduction in dsl using a nonlinear TEQ. In *Circuits and Systems, 2004. ISCAS '04. Proceedings of the 2004 International Symposium on*, volume 3, pages III – 353–6 Vol.3, May 2004.

[68] H. Harashima and H. Miyakawa. Matched-transmission technique for channels with intersymbol interference. *Communications, IEEE Transactions on*, 20(4):774 – 780, August 1972.

[69] J. Heiskala and J. Terry. *OFDM Wireless LANs: A Theoritical and Practical Guide*. Sams Publishing, Indianapolis, USA, 2002.

[70] W. Henkel and T. Kessler. A wideband impulse noise survey in the German telephone network: statistical description and modeling. *AEÜ*, 48:277 –288, 1994.

[71] B. Hirosaki. An analysis of automatic equalizers for orthogonally multiplexed qam systems. *Communications, IEEE Transactions on*, 28(1):73 – 83, January 1980.

[72] B. Hirosaki, S. Hasegawa, and A. Sabato. Advanced groupband data modem using orthogonally multiplexed qam technique. *Communications, IEEE Transactions on*, 34(6):587 – 592, June 1986.

[73] H. Hrasnica, A. Haidine, and R. Lehnert. *Broadband Powerline Communications: Network Design*. John Wiley & Sons, West Sussex, England, 2004.

[74] Dai Huaiyu and H.V. Poor. Crosstalk mitigation in DMT VDSL with impulse noise. *Circuits and Systems I: Fundamental Theory and Applications, IEEE Transactions on*, 48(10):1205 –1213, October 2001.

[75] Gi-Hong Im and J.-J. Werner. Bandwidth-efficient digital transmission over unshielded twisted-pair wiring. *Selected Areas in Communications, IEEE Journal on*, 13(9):1643 –1655, December 1995.

[76] H.-H. Im and J.-J. Werner. Bandwidth-efficient digital transmission up to 155 mb/s over unshielded twisted pair wiring. In *Communications, 1993. ICC 93. Geneva. Technical Program, Conference Record, IEEE International Conference on*, volume 3, pages 1797 –1803 vol.3, May 1993.

[77] M. Moonen J. Verlinden J. Vangorp, P. Tsiaflakis and G. Ysebaert. A dual decomposition aprroach to partial crosstalk cancellation in a multiuser dmt-xdsl environment. *Applied Signal Processing, EURASIP Journal on*, 2004(10):1520–1535, 2004.

[78] ITU-T Rec J.222.1. Third-generation transmission systems for interactive cable television services IP cable modems: Physical layer specification, 2007.

[79] K.S. Jacobsen. Methods of upstream power backoff on very high speed digital subscriber lines. *Communications Magazine, IEEE*, 39(3):210 –216, March 2001.

[80] G.D. Forney Jr. and M.V. Eyuboglu. Combined equalization and coding using precoding. *Communications Magazine, IEEE*, 29(12):25 –34, December 1991.

[81] I. Kalet. The multitone channel. *Communications, IEEE Transactions on*, 37(2):119 –124, February 1989.

[82] I. Kalet and S. Shamai. On the capacity of a twisted-wire pair: Gaussian model. *Communications, IEEE Transactions on*, 38(3):379 –383, March 1990.

[83] K.J. Kerpez and A.M. Gottlieb. The error performance of digital subscriber lines in the presence of impulse noise. *Communications, IEEE Transactions on*, 43(5):1902 –1905, May 1995.

[84] K.J. Kerpez and K. Sistanizadeh. High bit rate asymmetric digital communications over telephone loops. *Communications, IEEE Transactions on*, 43(6):2038 –2049, June 1995.

[85] W. Kozek and A.F. Molisch. Nonorthogonal pulseshapes for multicarrier communications in doubly dispersive channels. *Selected Areas in Communications, IEEE Journal on*, 16(8):1579–1589, Oct 1998.

[86] E.A. Lee and D.G. Messerschnitt. *Digital Communication*. Kluwer Academic Publisher, second edition, 1994.

[87] A. Leke and J.M. Cioffi. A maximum rate loading algorithm for discrete multitone modulation systems. In *Global Telecommunications Conference, 1997. GLOBECOM '97., IEEE*, volume 3, pages 1514 –1518, November 1997.

[88] B. Li, P. Tsiaflakis, M. Moonen, J. Maes, and M. Guenach. Dynamic resource allocation based partial crosstalk cancellation in dsl networks. In *GLOBECOM 2010, 2010 IEEE Global Telecommunications Conference*, pages 1 –5, dec. 2010.

[89] Y.-P. Lin and S.-M. Phoong. Window designs for DFT-based multicarrier systems. *IEEE Trans. on Signal Processing*, 53:1015–1024, March 2005.

[90] J. Maes, M. Guenach, and M. Peeters. Statistical mimo channel model for gain quantification of dsl crosstalk mitigation techniques. In *Communications, 2009. ICC '09. IEEE International Conference on*, pages 1 –5, 2009.

[91] T. Magesacher. *Common-Mode Aided Wireline Communications*. PhD Thesis, Department of Information Technology, Lund University, Sweden, ISBN 91-7167-041-6, ISRN LUTEDX/TEIT-06/1037-SE, September 2006.

[92] T. Magesacher. Optimal intra-symbol transmit windowing for multicarrier modulation. *in Proc. Intl. Symp. on Communications, Control and Signal Processing ISCCSP 2006, Marrakech, Morocco*, March 2006.

[93] T. Magesacher, P. Ödling, and P. O. Börjesson. Optimal intersymbol transmit windowing for multicarrier modulation. *in Proc. Nordic Signal Processing Symp. NORSIG 2006*, June 2006.

[94] A. Mahadevan, J. Pons, and P. Duvaut. Performance and design of an impulse noise detector for OFDM systems with Reed-Solomon erasure-decoding. In *Global Telecommunications Conference, 2008. IEEE GLOBECOM 2008. IEEE*, 30 2008.

[95] K. W. Martin. Small side-lobe filter design for multitone data-communication applications. *Circuits and Systems II: Analog and Digital Signal Processing, IEEE Transactions on [see also Circuits and Systems II: Express Briefs, IEEE Transactions on]*, 45(8):1155–1161, Aug 1998.

[96] R.K. Martin, K. Vanbleu, Ming Ding, G. Ysebaert, M. Milosevic, B.L. Evans, M. Moonen, and C.R. Johnson. Implementation complexity and communication performance tradeoffs in discrete multitone modulation equalizers. *Signal Processing, IEEE Transactions on*, 54(8):3216 –3230, 2006.

[97] R.K. Martin, K. Vanbleu, Ming Ding, G. Ysebaert, M. Milosevic, B.L. Evans, M. Moonen, and C.R. Johnson Jr. Unification and evaluation of equalization structures and design algorithms for discrete multitone modulation systems. *Signal Processing, IEEE Transactions on*, 53(10):3880 – 3894, 2005.

[98] R.K. Martin, G. Ysebaert, and K. Vanbleu. Bit error rate minimizing channel shortening equalizers for cyclic prefixed systems. *Signal Processing, IEEE Transactions on*, 55(6):2605 –2616, 2007.

[99] D.G. Mestdagh, M.R. Isaksson, and P. Odling. Zipper VDSL: A solution for robust duplex communication over telephone lines. *Communications Magazine, IEEE*, 38(5):90 –96, May 2000.

[100] A. F. Molisch. *Wideband wireless digital communications*. Prentice Hall PTR, Upper Saddle River, NJ, USA, 2000.

[101] J. Nocedal and S. Wright. *Numerical Optimization*. Springer verlag, 2006.

[102] M. Ouzzif, D. Toumpakaris, J. Cioffi, and A. Zeddam. Comparison of QAM-VDSL and DMT-VDSL in an impulse noise environment. In *Global Telecommunications Conference, 2003. GLOBECOM '03. IEEE*, volume 4, pages 2141 – 2145 vol.4, 2003.

[103] S Braet P Spruyt, P Reusens. Performance of improved DMT transceiver for VDSL. *Tech. Report T1E1.4/96-104, ANSI*, 1996.

[104] K. Pahlavan and J.L. Holsinger. Voice-band data communication modems-a historical review: 1919-1988. *Communications Magazine, IEEE*, 26(1):16 –27, January 1988.

[105] P. K. Pandey and M. Moonen. Resource allocation in ADSL variable length per-tone equalizers. *Signal Processing, IEEE Transactions on*, 56:2161–2164, May 2008.

[106] P. K. Pandey, M. Moonen, and L. Deneire. Joint transmit power and filter tap allocation in DMT transmitters with per-tone pulse shaping. In *Proc. IEEE Global Communications Conference (GLOBECOM 08)*., New Orleans, LA, USA, November 2008.

[107] P. K. Pandey, M. Moonen, and L. Deneire. Resource allocation in DMT transmitters with per-tone pulse shaping. In *Proc. IEEE International Conference on Acoustics, Speech and Signal Processing*, Las Vegas, Nevada, USA, 2008.

[108] P. K. Pandey, M. Moonen, and L. Deneire. MMSE-based partial crosstalk cancellation for upstream VDSL. In *Proc. IEEE International Conference on Communications (ICC '10)*, Cape Town, South Africa, May 2010.

[109] P. K. Pandey, M. Moonen, and L. Deneire. Joint transmit power and filter tap allocation in DMT transceivers. *Submitted*, 2011.

[110] P. K. Pandey, M. Moonen, and L. Deneire. MMSE-based partial crosstalk cancellation for upstream VDSL. 2011.

[111] P. K. Pandey, M. Moonen, and L. Deneire. Sparse approximation based partial cancellation in upstream VDSL. *Submitted*, 2011.

[112] P. K. Pandey, M. Moonen, and L. Deneire. Sparse approximation based resource allocation in DMT receivers with per-tone equalization. *Submitted*, 2011.

[113] P. K. Pandey, M. Moonen, and L. Deneire. Sparse approximation based resource allocation in DMT transmitters with per-tone pulse shaping. *submitted.....*, 2011.

[114] White Paper. Broadband technology overview. WP6321 ed. Corning, June 2005. http://www.corning.com.

[115] White Paper. VDSL2, The ideal access technology for delivering video services (Revision 2). Aware Inc., 2006. http://www.aware.com.

[116] White Paper. Optical Access. International Engineering Consortium (IEC), 2007. http://www.iec.org.

[117] Z. Papir and A. Simmonds. Competing for throughput in the local loop. *Communications Magazine, IEEE*, 37(5):61 –66, May 1999.

[118] A. Peled and A. Ruiz. Frequency domain data transmission using reduced computational complexity algorithms. In *Acoustics, Speech, and Signal Processing, IEEE International Conference on ICASSP '80.*, volume 5, pages 964 – 967, April 1980.

[119] T. Pollet, M. Peeters, M. Moonen, and L. Vandendorpe. Equalization for dmt based broadband modems. *Communications Magazine, IEEE*, 38(5):106 –113, May 2000.

[120] J.G. Proakis. *Digital Communications*. McGraw-Hill, New York, NY, USA, third edition, 1995.

[121] R. Ramaswami, K.N. Sivarajan, and G.H. Sasaki. *Optical Networks: A practical perspective*. Morgan Kaufman Publishers, Burlington, MA, USA, third edition, 2010.

[122] Bell Communications Research. NYNEX loop performance survey: Report of results. *Loop survey report, Bellcore*, 1986.

[123] W. Rhee, J.C. Chuang, and L.J. Cimini Jr. Performance comparison of OFDM and multitone with polyphase filterbank for wireless communications. *Vehicular Technology Conference, 1998. VTC 98. 48th IEEE*, 2:768–772 vol.2, 18-21 May 1998.

[124] D. Roddy. *Satellite Communications*. The Mcgraw Hill Companies Inc., NY, USA, fourth edition, 2006.

[125] A. Ruiz, J.M. Cioffi, and S. Kasturia. Discrete multiple tone modulation with coset coding for the spectrally shaped channel. *Communications, IEEE Transactions on*, 40(6):1012 –1029, June 1992.

[126] C. Salema. *Microwave Radio Links: From Theory to Design*. John Wiley & Sons, Hoboken, NJ, USA, 2002.

[127] B. Saltzberg. Performance of an efficient parallel data transmission system. *Communication Technology, IEEE Transactions on*, 15(6):805 –811, 1967.

[128] B.R. Saltzberg. Comparison of single-carrier and multitone digital modulation for adsl applications. *Communications Magazine, IEEE*, 36(11):114 –121, November 1998.

[129] J. Salz. Optimum mean-square decision feedback equalization. *Bell System Tech. Journal*, 52(9):1341 –1373, 1973.

[130] L. Sandstrom, K. Schneider, L. Joiner, and A. Wilson. Spatial correlation of alien crosstalk in MIMO DSL systems. *Communications, IEEE Transactions on*, 57(8):2269 –2271, 2009.

[131] S. Schelstraete. Defining upstream power backoff for VDSL. *Selected Areas in Communications, IEEE Journal on*, 20(5):1064 –1074, June 2002.

[132] A. Sendonaris, V.V. Veeravalli, and B. Aazhang. Joint signaling strategies for approaching the capacity of twisted-pair channels. *Communications, IEEE Transactions on*, 46(5):673 –685, May 1998.

[133] C. Shannon. A mathematical theory of communication. *Bell System Techn. Journal*, 27(5):379–423, 623–656, July and October 1948.

[134] The Samuel Morse Historic Site. http://www.lgny.org/history/morse.html.

[135] F. Sjoberg. *A VDSL tutorial*. Research report, Institutionen för Systemteknik, Avdelningen för Signalbehandling, Lulea tekniska Universitet, Sweden, ISSN 1402-1528, ISRN LTU-FR-00/02-SE, 2000.

[136] F. Sjoberg, M. Isaksson, R. Nilsson, P. Odling, S.K. Wilson, and P.O. Borjesson. Zipper: a duplex method for VDSL based on DMT. *Communications, IEEE Transactions on*, 47(8):1245 –1252, August 1999.

[137] F. Sjoberg, R. Nilsson, P.O. Borjesson, P. Odling, B. Wiese, and J.A.C. Bingham. Digital RFI suppression in DMT-based VDSL systems. *Circuits and Systems I: Regular Papers, IEEE Transactions on*, 51(11):2300 – 2312, 2004.

[138] F. Sjoberg, R. Nilsson, M. Isaksson, P. Odling, and P.O. Borjesson. Asynchronous zipper [subscriber line duplex method]. In *Communications, 1999. ICC '99. 1999 IEEE International Conference on*, 1999.

[139] N. Sloane and A. Wyner. *Claude E. Shannon(Collected Papers)*. 1993.

[140] Kee Bong Song, Seong Taek Chung, G. Ginis, and J.M. Cioffi. Dynamic spectrum management for next-generation DSL systems. *Communications Magazine, IEEE*, 40(10):101 – 109, October 2002.

[141] M. Sorbara, P. Duvaut, F. Shmulyian, S. Singh, and A. Mahadevan. Construction of a dsl-mimo channel model for evaluation of fext cancellation systems in vdsl2. In *Sarnoff Symposium, 2007 IEEE*, 30 2007.

[142] T. Starr, M. Sorbara, J.M. Cioffi, and P. Silverman. *DSL Advances*. Pearson Education, 2002.

[143] R. Stolle. Electromagnetic coupling of twisted pair cables. *Selected Areas in Communications, IEEE Journal on*, 20(5):883 –892, June 2002.

[144] G. Taubock and W. Henkel. Mimo systems in the subscriber line network. In *Fifth International OFDM Workshop, Hamburg, Germany*, pages 18.1 – 18.3, 2000.

[145] Lucent Technologies. Impact of bridged taps on VDSL performance. Tech. Rep. NT-091, ITU-SG15/Q4, Nashville, Tennessee, November 1999.

[146] W. Tiejun, J.G. Proakis, and J.R. Zeidler. Analysis of per-channel equalized filtered multitone modulations over time-varying fading channels. In *Personal, Indoor and Mobile Radio Communications, 2006 IEEE 17th International Symposium on*, pages 1–5, 2006.

[147] A. Tkacenko, P.P. Vaidyanathan, and T.Q. Nguyen. On the eigenfilter design method and its applications: a tutorial. *Circuits and Systems II: Analog and Digital Signal Processing, IEEE Transactions on [see also Circuits and Systems II: Express Briefs, IEEE Transactions on]*, 50(9):497–517, Sept. 2003.

[148] M. Tomlinson. New automatic equaliser employing modulo arithmetic. *Electronics Letters*, 7(5):138 –139, 25 1971.

[149] D. Toumpakaris, Wei Yu, J.M. Cioffi, D. Gardan, and M. Ouzzif. A simple byte-erasure method for improved impulse immunity in DSL. In *Communications, 2003. ICC '03. IEEE International Conference on*, volume 4, pages 2426 – 2430 vol.4, May 2003.

[150] J. A. Tropp. Just relax: Convex programming methods for subset selection and sparse approximation. *ICES Report 04-04*, pages 1–39, February 2004.

[151] J. A. Tropp. Just relax: Convex programming methods for identifying sparse signals in noise. 52:1030–1050, March 2006.

[152] P. Tsiaflakis, J. Vangorp, M. Moonen, J. Verlinden, and K. Van Acker. An efficient search algorithm for the lagrange multipliers of optimal spectrum balancing in multi-user xDSL systems. In *Proc. IEEE International Conference on Acoustics, Speech and Signal Processing*, Toulouse, France, May 2006.

[153] P. Tsiaflakis, J. Vangorp, J. Verlinden, and M. Moonen. Multiple access channel optimal spectrum balancing for upstream DSL transmission. *Communications Letters, IEEE*, 11(4):398 –300, 2007.

[154] A. Vahlin and N. Holte. Optimal finite duration pulses for OFDM. *Communications, IEEE Transactions on*, 44(1):10–14, Jan 1996.

[155] L. van der Perre, S. Thoen, P. Vandenameele, B. Gyselinckx, and M. Engels. Adaptive loading strategy for a high speed ofdm-based wlan. In *Global Telecommunications Conference, 1998. GLOBECOM 98. The Bridge to Global Integration. IEEE*, 1998.

[156] K. Vanbleu, G. Ysebaert, G. Cuypers, and M. Moonen. On time-domain and frequency-domain mmse-based teq design for dmt transmission. *Signal Processing, IEEE Transactions on*, 53(8):3311 – 3324, 2005.

[157] K. Vanbleu, G. Ysebaert, G. Cuypers, and M. Moonen. Adaptive bit rate maximizing time-domain equalizer design for dmt-based systems. *Signal Processing, IEEE Transactions on*, 54(2):483 – 498, 2006.

[158] K. Vanbleu, G. Ysebaert, G. Cuypers, M. Moonen, and K. Van Acker. Bitrate-maximizing time-domain equalizer design for dmt-based systems. *Communications, IEEE Transactions on*, 52(6):871 – 876, 2004.

[159] K. Vanbleu, G. Ysebaert, M. Moonen, and P. Vandaele. Combined equalization and alien crosstalk cancellation in ADSL receivers. In *European Signal Processing Conference 2002 (EUSIPCO 2002)*, pages 1–4, Toulouse, France, 2002.

[160] J. Vangorp, M. Moonen, M. Guenach, and M. Peeters. Downstream power backoff in CO/RT-deployed xDSL networks. *Communications, IEEE Transactions on*, 58(2):453 –456, 2010.

[161] F. Vanier. World broadband statistics: Short report, Q3 2010. Point Topic Ltd., December 2010. http://www.point-topic.com.

[162] M.K. Varanasi. Decision feedback multiuser detection: a systematic approach. *Information Theory, IEEE Transactions on*, 45(1):219 –240, January 1999.

[163] Sergio Verdu. *Multiuser Detection*. Cambridge University Press, New York, NY, USA, 1st edition, 1998.

[164] I. Wahibi, M. Ouzzif, J. Le Masson, and S. Saoudi. Stationary interference cancellation in upstream coordinated dsl using a turbo-MMSE receiver. *Digital Multimedia Broadcasting, International Journal of*, 2008:8, 2008.

[165] A. Wang, J. J. Werner, and S. Kallel. Effect of bridged taps on channel capacity at VDSL frequencies. In *Communications, 1999. ICC '99. 1999 IEEE International Conference on*, 1999.

[166] S. Weinstein and P. Ebert. Data transmission by frequency-division multiplexing using the discrete fourier transform. *Communication Technology, IEEE Transactions on*, 19(5):628 –634, 1971.

[167] J.-J. Werner. The HDSL environment [high bit rate digital subscriber line]. *Selected Areas in Communications, IEEE Journal on*, 9(6):785 –800, August 1991.

[168] J.-J. Werner. Tutorial on carrierless am/pm-Part I: Fundamentals and digital CAP transmitter. *ANSI X3T9.5 TP/PMD*, June 1992.

[169] B. Wiese and K.S. Jacobsen. Use of the reference noise method bounds the performance loss due to upstream power backoff. *Selected Areas in Communications, IEEE Journal on*, 20(5):1075 –1084, June 2002.

[170] P.W. Wolniansky, G.J. Foschini, G.D. Golden, and R.A. Valenzuela. V-blast: an architecture for realizing very high data rates over the rich-scattering wireless channel. In *Signals, Systems, and Electronics, 1998. ISSSE 98. 1998 URSI International Symposium on*, 1998.

[171] A. M. Wyglinski, P. Kabal, and F. Labeau. Variable-length subcarrier equalizers for multicarrier systems. In *Proc. IEEE Vehicular Technology Conference*, Los Angeles, California, USA, 2004.

[172] A.M. Wyglinski, M. Cudnoch, F. Labeau, and P. Kabal. Tap loading of subcarrier equalizers for wireless multicarrier transceivers. *Vehicular Technology, IEEE Transactions on*, 57(1):393 –403, 2008.

[173] Wei Yu and J.M. Cioffi. Multiuser detection for vector multiple access channels using generalized decision feedback equalization. In *Signal Processing Proceedings, 2000. WCCC-ICSP 2000. 5th International Conference on*, 2000.

[174] Wei Yu and R. Lui. Dual methods for nonconvex spectrum optimization of multicarrier systems. *Communications, IEEE Transactions on*, 54(7):1310 –1322, 2006.

[175] Chaohuang Zeng and J.M. Cioffi. Crosstalk cancellation in ADSL systems. In *Global Telecommunications Conference, 2001. GLOBECOM '01. IEEE*, 2001.

[176] W. Zhendao and G.B. Giannakis. Wireless multicarrier communications. *Signal Processing Magazine, IEEE*, 17(3):29 –48, May 2000.

[177] Lin Zhiwei, A.B. Premkumar, and A.S. Madhukumar. Matching pursuit-based tap selection technique for uwb channel equalization. *Communications Letters, IEEE*, 9(9):835 – 837, September 2005.

Publication List

Journals

1. P.K. Pandey , M. Moonen , "Resource allocation in ADSL variable length per-tone equalizers", *IEEE Trans. on Signal Processing*, vol. 56, no. 5, May 2008, pp. 2161-2164

2. P.K. Pandey, M. Moonen, and L. Deneire, "MMSE-based partial crosstalk cancellation for upstream VDSL", *Signal Processing*, Submitted in April 2011

3. P.K. Pandey, M. Moonen, and L. Deneire, "Sparse approximation based resource allocation in DMT transmitters with per-tone pulse shaping", *Signal Processing*, Submitted in April 2011

4. P.K. Pandey, M. Moonen, and L. Deneire, "Sparse approximation based resource allocation in DMT receiver with per-tone equalization", *Signal Processing*, Submitted in April 2011

5. P.K. Pandey, M. Moonen, and L. Deneire, "MMSE-based partial crosstalk cancellation for upstream VDSL", *Signal Processing*, Submitted in April 2011

6. P.K. Pandey, M. Moonen, and L. Deneire, "Joint MMSE-based partial crosstalk cancellation and spectrum balancing for upstream VDSL", to be submitted

7. P.K. Pandey, M. Moonen, and L. Deneire, "Sparse approximation based linear MMSE partial crosstalk cancellation and spectrum balancing for upstream VDSL", to be submitted

Conferences

1. P.K. Pandey, M. Moonen, and L. Deneire, "Resource allocation in DMT transmitters with per-tone pulse shaping", *in Proc. of the International*

Conference on Acoustics, Speech, and Signal Processing (ICASSP), Las Vegas, USA, Mar. 2008

2. P.K. Pandey, M. Moonen, and L. Deneire, "Joint transmit power and filter tap allocation in DMT transmitters with per-tone pulse shaping", *in Proc. of the Global Communications Conference (GLOBECOM)*, New orleans, USA, Nov. 2008

3. P.K. Pandey, M. Moonen, and L. Deneire, "MMSE-based partial crosstalk cancellation for Upstream VDSL", *in Proc. of the IEEE International Conference on Communications (IEEE-ICC)*, Cape Town, South Africa, May 2010

Internal report

1. P.K. Pandey, M. Moonen, and L. Deneire, "Resource allocation in DMT transmitters with per-tone pulse shaping", *Internal Report 08-225, ESAT-SISTA, K.U.Leuven (Leuven, Belgium)*, 2008., Lirias number: 242631

Poster

1. P.K. Pandey, M. Moonen, and L. Deneire, "MMSE-based partial crosstalk cancellation for upstream VDSL", *Poster presentation, Bell Labs Colloquium*, Antwerp, Belgium, October 20 2009

Curriculum Vitae



Prabin Kumar Pandey was born in Nepal, in 1978. He received his B.E. in Electrical and Electronics Engineering (Distinction) from Kathmandu University, Nepal in 2001 and M.Sc. in Communication Engineering from RWTH Aachen University, Aachen, Germany in 2005. From October 2005 to August 2006, he was a predoctoral student at the Department of Electrical Engineering under the supervision of Prof. Marc Moonen. Since September 2006, he has been pursuing Ph.D under the supervision of Prof. Marc Moonen and Prof. Luc Deneire at the Department of Electrical Engineering, K.U. Leuven, Belgium.

From 2006 to 2009, he was a Marie Curie Fellow involved in the EST-SIGNAL project (Early Stage Training in Signal processing). Since 2009 he is a Research Assistant with K.U.Leuven. In 2009, he was visiting scholar at CAS group TU Delft, Delft, The Netherlands under the supervision of Prof. Geert Leus. In 2010, he was awarded a travel grant by research Foundation Flanders (FWO), Belgium to attend ICC 2010 in Cape town, South Africa. His research interest includes digital signal processing and optimization of digital communication systems.

Arenberg Doctoral School of Science, Engineering & Technology
Faculty of Engineering
Department of Electrical Engineering
Research group ESAT-SCD: SISTA/COSIC/DOCARCH
Kasteelpark Arenberg 10, B-3301 Leuven

KATHOLIEKE UNIVERSITEIT LEUVEN

ASSOCIATIE K.U.LEUVEN